行政院國家科學委員會專題研究計畫 期末報告

LNAPL 多相抽除法對 BTEX 移除效能提升之探討

計 畫 類 別 ：個別型
計 畫 編 號 ：NSC 101-2221-E-009-135-
執 行 期 間 ：101 年 08 月 01 日至 102 年 07 月 31 日
執 行 單 位 ：國立交通大學土木工程學系（所）

計 畫 主 持 人：單信瑜

計畫參與人員：碩士班研究生-兼任助理人員：吳志清
碩士班研究生-兼任助理人員：曹書銘
博士班研究生-兼任助理人員：江潤翰

報 告 附 件 ：出席國際會議研究心得報告及發表論文

公 開 資 訊 ：本計畫可公開查詢

中 華 民 國 102 年 10 月 13 日

中文摘要：油品污染場址之整治中，若該場址地下水位面上有浮油的存在，則首要工作即為浮油回收(Free product recovery)以移除污染源 (Source removal)。浮油回收的模擬在過去使用的程式僅考慮雙相流或三相流，僅將 LNAPL 視為單一液體。換言之，雖然汽油、柴油、飛機燃料油都是混合物，但在模擬中都僅視為單一流體，賦予單一性質，其密度、黏滯性、介面張力等都個別僅以一個參數計算。實際上，油品污染場址的整體控制或整治效果，其核心還是地下水中的 BTEX。油品中除了 BTEX 與 MTBE 幾種有危害性成分以外，其他的成分毒性甚小、溶解度低且較易被生物降解，對地下環境的影響較小。本研究將利用 TMVOC 軟體模擬近年來油品污染整治場址常用之多相抽除法(Multi-phase Extraction, MPE)，因 TMVOC 中的 LNAPL 相可分別將油品中的各種成分包括 BTEX 與 MTBE 精確地模擬，故可藉以更深入瞭解在多相抽除過程中，除了浮油回收以外，BTEX 與 MTBE 從非飽和層與浮油中移除的狀況，以及在浮油回收過程中對 BTEX 與 MTBE 溶解至地下水抑制的效率與回收效率。透過不同回收井間距與負壓之配置，以及將地下水位同時洩降納入，藉 BTEX 回收與溶解至地下水中的總量找出提升 MPE 之方式。

本研究以大型儲油槽汽油洩漏在砂質土層造成的污染作為研究對象，以數值模擬軟體 TMVOC 探討多相抽除法在該場址中，佈井位置、孔隙率、井底壓力此三變數對整治效率的影響。模擬結果顯示佈井於洩漏點下游 10 m 處整治效率最佳，由此點向上游或下游佈井效率將降低，距離此點越遠效率越差。大孔隙率之場址整治效率較高。井底壓力與大氣壓力的壓差和整治效率有正相關性，但非成正比，加大負壓對回收速率的影響在整治前期較為明顯，整治後期影響降低。

中文關鍵詞：輕質非水相液體、浮油回收、多相抽除、TMVOC、BTEX

英文摘要：In remediation of LNAPL contaminated sites, free product recovery is the major tool for source removal when there is a LNAPL layer on top of the groundwater table. In the past, the modeling of free product recovery consider LNAPL phase as a single fluid without discriminating its components including BTEX and MTBE. However, the dissolution and control of BTEX and MTBE are the most critical issue of an LNAPL contaminated site, all other components of LNAPL are less toxic, less soluble in water, and easily biodegraded. The objective of this proposed research is to use TMVOC, which can take the multiple

component of LNAPL especially BTEX and MTBE into account, to simulate the multi-phase extraction and assess the relative effectiveness of free product recovery and soil vapor extraction to control the release rate into groundwater and recovery rate of BTEX and MTBE. The removal of BTEX under various layouts and vacuum of MPE wells, as well as incorporating groundwater pumping, will be evaluated for determination of best scheme for enhancement of remediation effectiveness.

In this study, numerical simulations had been performed with TMVOC, in order to assess the influence of well location, well bottom pressure and porosity on the efficiency of MPE. A hypothesized aquifer of sandy soil had been assumed to receive gasoline from oil spill from tank farms and thus to be remediated with MPE. The results of simulation show that the extraction well placed 10 m downstream from spill point gives the best efficiency. Efficiency decreases as the extraction well was located away from that particular point, either upstream or downstream. Furthermore, the aquifer of which a higher porosity has been assumed shows a better efficiency than one with lower porosity. In addition, the efficiency of extraction exhibits a positive correlation with the difference between well bottom pressure and atmospheric pressure. Nevertheless, the benefit of high negative pressure is obvious only in the earlier few months after which the benefit decreases with time.

英文關鍵詞： LNAPL, free product recovery, multi-phase extraction, TMVOC, BTEX

行政院國家科學委員會補助專題研究計畫 □期中進度報告 ■期末報告

LNAPL 多相抽除法對 BTEX 移除效能提升之探討

計畫類別：■個別型計畫　□整合型計畫
計畫編號：NSC 101-2221-E-009 -135 -
執行期間：　101 年 8 月 1 日至 102 年 7 月 31 日

執行機構及系所：交通大學土木工程系

計畫主持人：單信瑜
共同主持人：
計畫參與人員：江潤翰、吳志清、曹書銘

本計畫除繳交成果報告外，另含下列出國報告，共 1 份：
□移地研究心得報告
■出席國際學術會議心得報告
□國際合作研究計畫國外研究報告

處理方式：除列管計畫及下列情形者外，得立即公開查詢
□涉及專利或其他智慧財產權，□一年□二年後可公開查詢

中　華　民　國　102　年　10　月　15　日

摘要

油品污染場址之整治中，若該場址地下水位面上有浮油的存在，則首要工作即為浮油回收(Free product recovery)以移除污染源 (Source removal)。浮油回收的模擬在過去使用的程式僅考慮雙相流或三相流，僅將 LNAPL 視為單一液體。換言之，雖然汽油、柴油、飛機燃料油都是混合物，但在模擬中都僅視為單一流體，賦予單一性質，其密度、黏滯性、介面張力等都個別僅以一個參數計算。實際上，油品污染場址的整體控制或整治效果，其核心還是地下水中的 BTEX。油品中除了 BTEX 與 MTBE 幾種有危害性成分以外，其他的成分毒性甚小、溶解度低且較易被生物降解，對地下環境的影響較小。本研究將利用 TMVOC 軟體模擬近年來油品污染整治場址常用之多相抽除法(Multi-phase Extraction, MPE)，因 TMVOC 中的 LNAPL 相可分別將油品中的各種成分包括 BTEX 與 MTBE 精確地模擬，故可藉以更深入瞭解在多相抽除過程中，除了浮油回收以外，BTEX 與 MTBE 從非飽和層與浮油中移除的狀況，以及在浮油回收過程中對 BTEX 與 MTBE 溶解至地下水抑制的效率與回收效率。透過不同回收井間距與負壓之配置，以及將地下水位同時洩降納入，藉 BTEX 回收與溶解至地下水中的總量找出提升 MPE 之方式。

本研究以大型儲油槽汽油洩漏在砂質土層造成的污染作為研究對象，以數值模擬軟體 TMVOC 探討多相抽除法在該場址中，佈井位置、孔隙率、井底壓力此三變數對整治效率的影響。模擬結果顯示佈井於洩漏點下游 10 m 處整治效率最佳，由此點向上游或下游佈井效率將降低，距離此點越遠效率越差。大孔隙率之場址整治效率較高。井底壓力與大氣壓力的壓差和整治效率有正相關性，但非成正比，加大負壓對回收速率的影響在整治前期較為明顯，整治後期影響降低。

關鍵詞：輕質非水相液體、浮油回收、多相抽除、TMVOC、BTEX

計畫名稱：Assessment of Removal Rate Enhancement of BTEX by Multi-Phase Extraction of LNAPLs

ABSTRACT

In remediation of LNAPL contaminated sites, free product recovery is the major tool for source removal when there is a LNAPL layer on top of the groundwater table. In the past, the modeling of free product recovery consider LNAPL phase as a single fluid without discriminating its components including BTEX and MTBE. However, the dissolution and control of BTEX and MTBE are the most critical issue of an LNAPL contaminated site, all other components of LNAPL are less toxic, less soluble in water, and easily biodegraded. The objective of this proposed research is to use TMVOC, which can take the multiple component of LNAPL especially BTEX and MTBE into account, to simulate the multi-phase extraction and assess the relative effectiveness of free product recovery and soil vapor extraction to control the release rate into groundwater and recovery rate of BTEX and MTBE. The removal of BTEX under various layouts and vacuum of MPE wells, as well as incorporating groundwater pumping, will be evaluated for determination of best scheme for enhancement of remediation effectiveness.

In this study, numerical simulations had been performed with TMVOC, in order to assess the influence of well location, well bottom pressure and porosity on the efficiency of MPE. A hypothesized aquifer of sandy soil had been assumed to receive gasoline from oil spill from tank farms and thus to be remediated with MPE. The results of simulation show that the extraction well placed 10 m downstream from spill point gives the best efficiency. Efficiency decreases as the extraction well was located away from that particular point, either upstream or downstream. Furthermore, the aquifer of which a higher porosity has been assumed shows a better efficiency than one with lower porosity. In addition, the efficiency of extraction exhibits a positive correlation with the difference between well bottom pressure and atmospheric pressure.

Nevertheless, the benefit of high negative pressure is obvious only in the earlier few months after which the benefit decreases with time.

Keywords: LNAPL, free product recovery, multi-phase extraction, TMVOC, BTEX

一、前言

1.1 國內加油站與儲槽數量概況

各類油品從製造到銷售會經過一連串的儲存和運輸過程，每一個過程中都有洩漏的可能，其中油槽與附屬管線的洩漏則是主要的油品污染來源。尤其是數量龐大的加油站地下儲油槽及管線埋設於地下，易使油槽或管線系統受氧化腐蝕、外力破壞或其他原因造成洩漏污染。

由於地下儲油槽及管線埋設於地下，易使油槽或管線受氧化腐蝕、外力破壞或其它原因造成洩漏污染，而地下儲油槽洩漏的機率與其埋設的年代有正比例的關係，根據美國賓州環境資源部的研究，埋設 10 年以上的儲油槽有 46%會發生洩漏，而埋設 15 年以上者，其洩漏機率更高達 71%。地面上及地下儲槽，依據美國賓州之統計，地下儲油槽系統產生的洩漏，儲槽本身之洩漏佔 49%，管路之洩漏佔 39%，其他兩者皆洩漏者佔 12%，亦隨著儲槽埋設時間之增加而增加。國內加油站漏油大部分在油管部分，原因有施工不當造成土木結構之鋼筋與油管或油槽連接、包覆不良使金屬外漏與土壤直接接觸、及加油機漏電與接觸不良導致電蝕。

設置時間 10 年以上的加油站和超過一百公秉的大型儲槽是發生滲漏的高危險群。環保署預估至少有一成的儲槽和加油站有滲漏的情況。90 年與 91 年間，環保署更利用「地下水潛在污染源調查計畫」針對 191 座加油站，與「全國 10 年以上加油站及大型儲槽潛在污染源調查計畫」針對選定的 400 座加油站，進行潛在污染的調查工作。根據前者的結果來看，在調查的 191 座的加油站中有 19 座有滲漏的情況，並已經造成土壤和地下水的污染；在調查的 21 座儲槽中也有 6 座有同樣的情況。依據環保署「地下水潛在污染源調查計畫」，各縣市各年度石化儲槽污染調查場處及座數，91 年度調查 21 場處 1,402 座大型儲槽，92 年度調查 172 場處 2,171 座大型儲槽，合計已完成 193 場處 3,573 座大型儲槽污染潛勢調查工作(行政院環保署，2001)。

1.2 加油站地下儲槽與管線滲漏之主要污染物

石油碳氫化合物為混合物，含有各種化學物質對人體也都有一定程度的危害性，但是衡量這些物質對於人體與環境的危害輕重程度與行政管理上的務實考量，所以目前一般所公認石油碳氫化合物中的主要污染物有兩大類，一為 BTEX，另一為 MTBE(甲基第三丁基醚)。此外，為了易於掌握石油碳氫化合物污染的概況，因此往往也以總石油碳氫化合物(Total Petroleum Hydrocarbon，TPH)來作為法規中判斷污染狀況的基準。

苯(Benzene)、甲苯(Toluene)、乙苯(Ethylbenzene)、及二甲苯(Xylene)四者通常被合起來簡稱為 BTEX，這四種化學物質為常用的有機溶劑，大多油品中存在此四種化合物。BTEX 都具高揮發性、低沸點及不易溶於水之特性。這四種單環芳香族碳氫化合物對人類身體之影響可能因誤食、呼吸、接觸皮膚等造成慢性毒性、致突變性致畸胎性及對人體免疫系統干擾抑制，其中苯更證實有生物毒性、致癌性及突變性等(阮國棟、簡慧貞，1994；Kuiper-Goodman, T., 1995)，美國環保署已將 BTEX 列為 129 種優先列管污染物之一(阮國棟、簡慧貞，1994)。

甲基第三丁基醚(Methyl Tert-Butyl Ether，MTBE)是近年來被高度關切的有機污染物。在 1920 年代為了改善汽油的性能，因此添加四乙基鉛(Tetra -Ethyl Lead，TEL)到汽油中，藉以提高辛烷值及抗爆性。到了 1970 年代後期，因使用汽油而導致鉛排放造成嚴重的空氣污染，因此有替鉛劑的產生，比如乙醇、乙醚及 MTBE 等。這種替鉛劑的加入不但可提高辛烷值還可改善燃燒、減少震爆及改善空氣品質，MTBE 添加的體積百分比約為 7%。自 1979 年起

MTBE 開始被用作為氧化劑(Oxygenate)添加於汽油後，添加的體積百分比提高為 11 – 15%。這幾年 MTBE 較引人注目係因 MTBE 已被美國環保署認定為對動物具致癌性。美國飲用水諮詢委員會在 1997 年 12 月對 MTBE 建議在飲用水中的濃度範圍需小於 20-40 ppb，我國毒性化學物質管理法亦將 MTBE 列管為第四類毒性化學物質。

1.3 國內加油站與儲槽污染與整治概況

國內目前已公告儲槽污染控制場址中，土壤污染項目以總石油碳氫化合物(TPH)最普遍，地下水污染項目則以苯最常見。國內目前已公告之加油站污染場址，依污染類別分析，土壤污染項目以總石油碳氫化合物(TPH)最普遍，苯、甲苯、乙苯次之，地下水污染項目則以苯最常見。

目前國內公告之控制場址共 648 處，整治場址 49 處(環保署，2011)。控制場址中，加油站共 45 處，儲槽有 5 處；其中屬於油品儲槽的場址為：台灣中油股份有限公司油品行銷事業部東部營業處(北埔油庫)、高雄縣台灣中油股份有限公司石化事業部林園廠、國喬石化高雄廠(高雄縣大社鄉大社石油化學工業區興工路 4 號)儲油槽漏油污染地下水案等 3 個場址。整治場址中，加油站共 17 處，儲槽有 2 處；屬於油品儲槽的場址為：台灣中油股份有限公司煉製事業部高雄煉油廠 P-37 油槽區。解除控制場址中，加油站共 19 處，儲槽 1 處。已經解除列管的 2 處整治場址則皆為加油站。實際上是油品污染的場址中，台灣中油股份有限公司苓雅寮儲運所場址曾有大規模柴油滲漏，經將近二十年的整治，部分已列為解除控制場址，部分仍被列為控制場址和整治場址；台灣中油股份有限公司煉製事業部高雄煉油廠工廠區是目前南部現存油品污染最嚴重的區域，部分屬於控制場址，最嚴重的高雄煉油廠 P-37 油槽區屬於整治場址。

1.4 研究目的

本研究將利用 TMVOC 軟體模擬近年來油品污染整治場址常用之多相抽除法(Multi-phase Extraction, MPE)（包括 Bioslurping），因 TMVOC 中的 LNAPL 相可分別將油品中的各種成分包括 BTEX 與 MTBE 精確地模擬，故可藉以更深入瞭解在多相抽除過程中，除了浮油回收以外，BTEX 與 MTBE 從非飽和層與浮油中移除的狀況，以及在浮油回收過程中對 BTEX 與 MTBE 溶解至地下水抑制的效率與回收效率。透過不同回收井間距與負壓之配置，以及將地下水位同時洩降納入，藉 BTEX 回收與溶解至地下水中的總量找出提升 MPE 效能之方式。

由前述文獻回顧和國內外實際污染場址經驗可知，不論是單相或多相浮油回收（包括 MPE 在內），由於欠缺適當的模擬工具，因此都必須仰賴現場的先導試驗取得有限的資料決定設計參數。但這樣的方式卻無法更為全面性地評估在不同場址條件下的最佳操作條件。此外，往往現場的經驗多半是依照監測井中浮油的厚度來決定操作條件以及何時停止操作，並無法有效釐清浮油抽除量和 BTEX 控制效率之間的關係。因此，若只能用浮油回收量來看，在土壤顆粒較細的地層中往往認為 MPE 效率也不佳。但可能實際上，MPE 在 BTEX 氣相抽除上有頗大貢獻，且因同時抽除浮油所以比起放棄浮油抽取僅以 SVE 方式更有效率。

本研究將透過 TMVOC 模擬探討 MPE 在不同地層中在 LNAPL 抽除和 BTEX 氣相移除和土壤參數與系統操作參數的關係。

二、文獻回顧

2.1 油品污染概述

汽油（Gasoline）為原油蒸餾物之一部分，主要是 5 個碳至 10 個碳組成之碳氫化合物，沸點介於 15℃至 200℃之間。而碳氫化合物含有各種化學物質，對人體也都有一程度的危害，但是衡量這些物質對於人體與環境的危害輕重程度與行政管理上的務實，目前一般所公認石油碳氫化合物中的主要污染物有兩大類，一類為 BTEX，另一類為 MTBE（甲基第三丁

基醚)。苯（Benzene)、甲苯（Toluene)、乙苯（Ethylbezene)、二甲苯（Xylene）四者通常被合起來簡稱為 BTEX，這四種化學物質為常用的有機溶劑，大多油品中存在此四種化合物。這四種單環芳香族碳氫化合物對人類身體之影響可能因誤食、呼吸、接觸皮膚造成慢性毒性、致突變性、致畸胎性及對人體免疫系統干擾抑制，其中苯更證實有生物毒性、致癌性及突變性等，美國環保署已將 BTEX 列為 129 種優先列管污染物之一。BTEX 亦已被列為我國地下水污染管制標準中。(經濟部工業局, 2007）

大型地面儲槽洩、滲漏油量遠遠大於加油站的地下儲槽滲漏量，國內多起地面儲槽洩漏都屬於重大的土壤及地下水污染事件。除了石油公司的油庫與儲運所、港口與航站具有大型的地面儲槽之外，石化工業數量龐大的大型地面儲槽與管線都是潛在的污染源。依據環保署「地下水潛在污染源調查計畫」統計，全台容積 100 公秉以上的儲槽總計 3,351 座。由於油槽長期暴露在大氣中，受到日曬雨淋等環境力作用，可能造成底板外為基礎面因雨水或積水造成腐蝕或接頭焊接部位因不同材質間氧化還原引發腐蝕。地面儲槽最可能發生洩漏的方式為進出口管線洩漏、浮頂油槽之中心排水管斷裂、槽底洩漏、槽壁破裂或是操作不慎。(經濟部工業局, 2007）

2.2 LNAPL 於地表下之分布與移動

油品為輕質非水相溶液（Light Dense Non-Aqueous Phase Liquid, 以下簡稱 LNAPL）的一種，當油品出現在土壤中時，可以下面五相存在：汽相、溶解相、自由相、吸附相、殘餘相。以圖 2-1 為例子來說明，當地表發生洩漏時，油品受重力影響將會向下移動，移動過程中有些液體將會以殘留飽和度留在不飽和帶中而不向下移動，此即稱殘餘相。除了殘餘相，油品亦有機會在移動過程中揮發至不飽和帶或大氣中，形成汽相。當油品向下移動至毛細緣層（Capillary Fringe）時，將會在該處堆積形成浮油並隨水力梯度向下游移動，此即為自由相。若堆積造成的局部高壓足夠突破毛細緣層，則油品將有機會溶解至地下水體中，形成溶解相並隨地下水流動，溶解相亦有機會出現在油品掃過之不飽和帶中所含之孔隙水中。最後，當油品在與土壤顆粒接觸後，有機會被土壤顆粒中有機碳吸附在顆粒表面，形成吸附相。

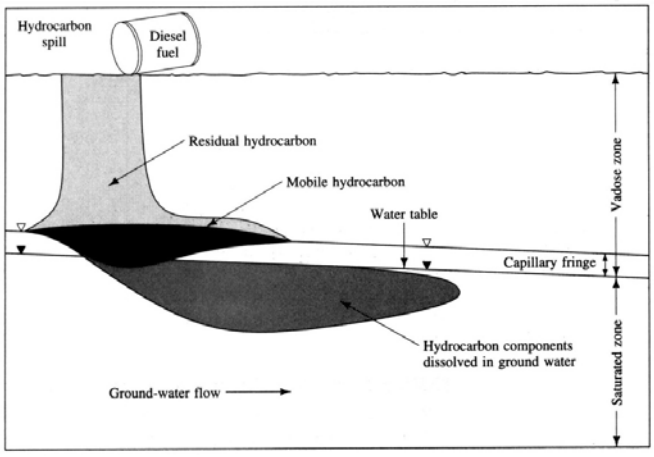

圖 2-1 LNAPL 於地表下的分布(Fetter, 2001)

探討不飽和帶傳輸時有兩個重要的曲線，其一為土壤水特徵曲線（Soil Water Characteristic Curve, 以下簡稱 SWCC)，其二為 K-S 曲線。SWCC 定義了土壤中含水量與孔隙張力的關係，圖 2-2 為典型粉土的 SWCC，當全飽和土體開始排水時，SWCC 將沿著 Desorption Curve 發展，當空氣突破 Air-entry Pressure 開始進入土體後，孔隙張力將明顯隨含水量下降而上升，當含水量降至某一程度後曲線斜率開始趨緩，最後將達到殘餘含水量，此時孔隙水不再排出。理論上殘餘含水量的定義為 Desorption Curve 斜率為 0 之處之含水量，但因孔隙張力隨含水量降低而持率上升的現象不易停止，斜率真實為 0 處不易尋找，實際使用上會設定一個張力停損點，van Genuchten（1980）建議使用凋萎點（15 m 水頭，約 147 kPa）

作為殘餘含水量張力停損點。從殘餘含水量為起點開始對土體進行濕潤動作時，SWCC 將會沿著 Adsorption Curve 發展，隨著含水量提高，土體的空氣含量也逐漸降低，當孔隙張力不再有明顯變化後含水量也將固定住，此時之含水量與初始全飽和土體含水量有差距，此差距即為殘餘空氣量（Residual Air Content），為無法再被壓力排出的空氣。所謂 K-S 曲線，是指土壤相對滲透係數（K）與飽和度（S）的關係曲線，當土壤飽和度降低時，相對滲透係數也跟著快速降低。。

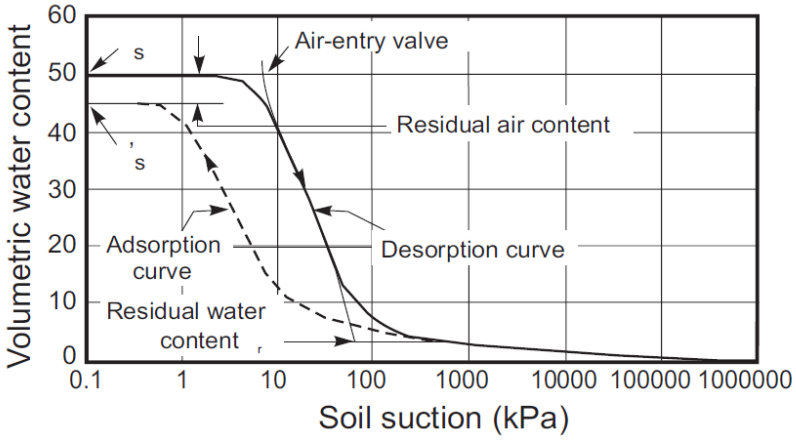

圖 2-2 典型坋土 SWCC （Fredlund and Xing, 1994）

2.3 油品污染場址之整治 – 浮油回收與多相抽除

由過去累積迄今的整治經驗顯示，很少有單一技術可以完全勝任整治工作，絕大多數的情況都將數種整治技術合併使用，以達最佳的效果。例如整治的初期可能需儘量回收洩漏的浮油，其次再利用土壤氣體抽除法或化學氧化法將殘留的油滴作進一步處理，再以地下水抽出處理的方法對高濃度區的地下水作初步的減量，以及在污染的下游區以抽水方式防止污染向下游擴散，接下來可考慮以現地地下水生物分解的方法，以及對未飽和層土壤施以生物通氣法，作長時間的整治，如果時間條件許可尚可考慮申請採用自然衰減等。

浮油回收一直是油品污染場址中移除污染源的主要方法，其現場的經驗非常多，但研究面的探討較少，直到近年來才逐漸有對其經濟與時間效益的探討(Campagnolo and Akgerman, 1995; Kirshner et al., 1996; Gerhard et al., 2001; Jennings and Patil, 2002; Mihopoulos et al., 2002)；且有部分研究是針對方法的研發與改良(Nadim et al., 2000; USEPA, 2001)。然而，對於浮油回收過程的模擬一向很少(Campagnolo and Akgerman, 1995; Mihopoulos et al., 2000, 2001, 2002; Jennings and Patil, 2002)。

初期以抽油來進行浮油回收可稱為「主要回收」(primary recovery)，僅能在 LNAPL 飽和度夠高時執行(Chevalier, 2003)且僅能以溝渠(Trench)或單相(One-phase)/多相(Multi-phase)抽除井達成。在抽除井以效率甚低無法抽除 LNAPL 時，因毛細力和浮力作用導致殘留在含水層中的 LNAPL 之回收稱為「二次」(Secondary)或「三次」(Tertiary)回收，使用的方法包括介面活性劑(Surfactant)降低毛細力(Chevalier, 2003)或超飽和水(Supersaturated water)放出高壓 CO2 (Nelson et al., 2009)。

早期傳統抽除浮油的方式是以浮油回收機（oil skimmer）進行，其目標是要在不回收地下水 (或非常少量)的條件下回收浮油。一般而言，這種方法涉及在開挖處、回收溝或回收井使用油水分離設備移除浮於地下水位上的浮油，通常用於臨時性或短期的處置。但僅靠重力自然的流動往往僅能回收開挖面周圍小範圍的區域，地質的孔隙愈小，浮油回收的效率愈差。所以下列浮油的抽除技術以效果比浮油回收機好很多的雙相抽除法（Dual Phase Extraction，DPE）為主要說明對象。

雙相抽除法亦稱為多相抽除法（Multi-phase Extraction）、真空抽除法（Vacuum-enhanced Extraction）以及生物漱洗法（Bioslurping）（中文另有譯為「生物啜吸法」）。主要於污染區土壤上方，挖設一個回收整治井，井中設置泵，由泵抽離、移除土壤及地下水中以不同型態

存在的污染物質，其中包括液態之地下水自由相（free product）、溶解相，以及不飽和土壤層中以氣相存在之揮發性有機物等物質，屬於油、水、氣可同時抽除處理之整治技術。抽除之各種型態之污染物，經處理之後排放或廢棄、回收。

在實際浮油回收方法中，雙相抽除法（Dual-phase(or two-phase) vacuum extraction (DPVE)）與 Bioslurping 相似，是一種高成本效益的技術(O'Melia and Parson, 1996)；過去對於這套方法的研究多半是探討其機制、執行方式與流程控制(Lamarre et al., 1997; Bailey and Schneider, 1998; Zahiraleslamzadeh et al., 1999; Roth et al., 1999; Vaughn and Turner, 2001)，例如 USEPA (1997)的手冊還提供了一份完整的系統特性、設計、效能、單價，甚至於是可提供服務的廠商名單。

雙相抽除法在不飽和土壤層中，由於土壤氣體遭不斷的抽除，造成不飽和層趨向真空的狀態，也因回收井附近之抽氣作用，使得污染區以外之遠方乾淨土壤氣體引入，造成通氣氣流之現象，持續補助整治區之土壤層供氣供氧，產生類似生物通氣法之作用，如此可以加強不飽和層土壤層之生物降解作用。雙相抽除法特別適用於油品類污染之場址，尤其是在自由相之浮油尚未移除之前，並不適合直接利用生物或化學方法進行整治的場址。因此，在污染場址採取多重處理方法併用原則下，針對有浮油層的場址，雙相抽除法往往優先於其他整治程序，被選擇來處理地下環境中之污染物。在系統的設計上，大致可分為單泵與雙泵兩種，其示意圖分別如**圖 2-3** 所示。

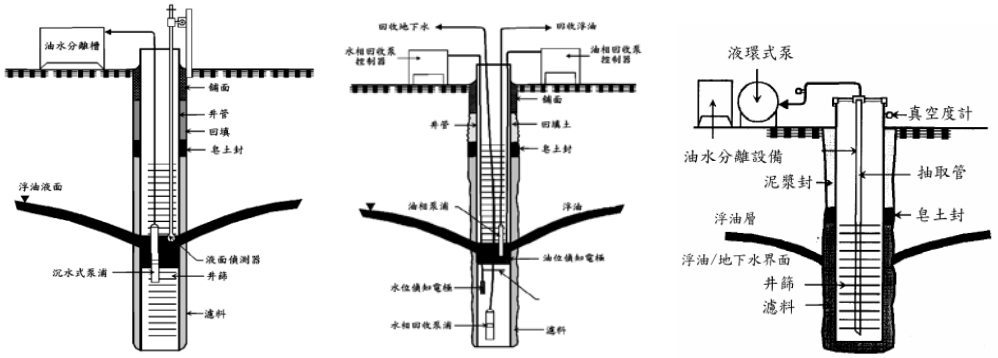

(a)單泵回收井　　(b)雙泵回收井　　(C) 單管雙相回收

圖 2-3 浮油回收井設備示意圖(API, 1996)

雙相抽除法在實際整治設計上已發展出多種形式，但主要有二種配置的概念，其差異僅在於抽取管在井中之垂直位置的不同。一般的真空/抽水系統如**圖 2-4** 所示，直接將抽出管出口置於地下水中，採用單一泵同時抽取水與浮油，由於回收井為氣密設計，所以回收井上部產生真空而有回收油氣之效果。另外一種系統則是設計同時用單一泵同時抽取浮油、空氣與水，所以將抽出管或抽氣管的出口置於空氣/浮油的界面（**圖 2-4**），這種設置即為一般所稱的生物漱洗(Bioslurping)。有時雙相回收系統可以藉由地下水抽取量與回收井的數量與位置的設計，達到利用水力控制來限制浮油團的擴散。

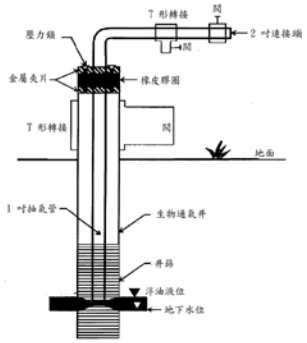

圖 2-4 生物漱洗井結構示意圖(API, 1996)

雙相回收抽除系統適用於土壤、地下水污染併同處理，甚至包括浮油之回收，具有氣、液、油共同處理之適用優勢。

雙相回收抽除系統的適用條件包括：

1. 低到中等的透水性地質 (水力傳導係數 $< 10^{-3}$ cm/s) 或較薄的浮油厚度(< 15 cm)。
2. 地下水位介於 1.5 到 6 m。
3. 傳統的抽出法或回收溝技術不適用。
4. 浮油位於鋪面或不透氣表面之下。

當雙相回收系統之浮油回收體積不夠多的時候，就該考慮停止操作，所以訂定停止運作之標準也是系統建置時必須審慎考慮的條件。停止運作的標準可能包括總浮油回收率 (例如：每個月少於 2 加侖或者浮油回收體積對地下水抽出速率的比例小於 0.1%) 與回收/監測井中浮油厚度 (例如：小於 3 cm)。浮油厚度應按季或按月進行監測，以確保回收/監測井中的浮油厚度在規定時間內 (如 2 年) 沒有超過閥值 (如 3 cm)，此閥值也可同時作為重新啟動回收設備的參考。

2.4 浮油回收與 LNAPL 抽除之數值模擬

Charbeneau 早期曾替 U.S. EPA 開發了相當原始的浮油污染模擬模組 HSSM，油品滲漏後在非飽和層的下滲行為可用 KOPT 程式計算、至形成浮流體可用 OILENSE 程式計算，溶解態的傳輸可用 TSGPLUME 程式計算。然而，這一套程式組無法計算地下水中(非溶解相)的油粒的傳輸。而且 U.S. EPA 並未提供蒸汽相(Vapor Phase)的油氣傳輸與分佈模式，因此無法計算油氣在非飽和土層中的濃度分佈(Weaver et al., 1994)。HSSM 是一初步篩選模式；它對包括許多化學和水文現象僅採取即為簡單的假設和排除某些現象，例如假設地表下為均質。在這模式中，許多潛在的重要過程是近似或完全被忽略，這模式的只是用來做同數量級的估計。HSSM 是根據一簡化之 LNAPL 釋放概念，「油品污染物動態傳輸」(Kinematic Oily Pollutant Transport (KOPT))和 OILENS 模組被整合到單一個電腦程式，HSSM-KO，可提供地下水含水層模式一個隨時間改變的污染源狀況。KOPT 和 OILENS 計算一同時溶解於 LNAPL 和水相的化學成分的蹤跡。一旦這個化學成分到達地下水位，它會經由和補注水接觸以及從 LNAPL 鏡體釋出污染地下水含水層。如此，這模式這第三部份模擬的是 LNAPL 的化學成分穿越地下水含水層的傳輸。由於從 OILENS 釋放的質量通量隨時間改變，因此地下水含水層模式必定得能夠模擬隨時間改變的污染源狀況。為了和使用於 KOPT 和 OILENS 的近似假設保持一致，一適當選擇是採用移流-分散等式解析解的瞬時態污染源高斯污染團模式 (Transient Source Gaussian Plume (TSGPLUME))。

另一方面，Parker et al. (1994)開發了 ARMOS 數值模式，模擬非拘限含水層中浮油移動和回收，可模擬 LNAPL 在自然梯度或浮動泵(Skimmer pump)抽取下（僅抽 LNAPL 未抽水）之流動。Waddill and Parker (1997a) 對數值模式加以修正，以考慮土壤水保持中遲滯現象對 LNAPL 困在土壤中的效應，並用在以抽水製造地下水位洩降加速 LNAPL 回收之狀況分析。之後 Waddill and Parker (1997b)在 ARMOS 中納入隨機統計分析(Stochastic analysis)評估含水層異質性對 LNAPL 回收之影響。其結果顯示含水層異質性對浮油回收與油品困在土壤中的影響不顯著；利用土壤性質的幾何平均數作為模擬參數可有效評估浮油回收。Cooper, Jr. et al, (1995)以二維有限元素模式 ARMOS 模擬浮油回收，利用間歇性啟動與可變化抽取速率的方式回收，間歇性啟動的目的在於侷限浮油往外擴散以提高抽取效率。研究結果顯示相較於一般「定速率」抽取浮油，其建議方案可提高浮油回收體積 11%，減少困在土壤中的 LNAPL 15%。Charbeneau and Chiang (1995)基於 Lenhard and Parker (1990)與 Farr et al. (1990)的成果開發出垂直向平衡數學模型，描述 LNAPL 滲漏後在地層中的分布；之後更提出了浮油回收的模擬工具。

Charbeneau et al. (2000)提出兩個浮油回收模擬的簡單模型來模擬抽油井和負壓增強系統(Vacuum enhanced systems)。其模式與 ARMOS 相較更為簡單，且有利於用來作為回收系

統的初步設計之用。但此模式僅考慮垂直向的平衡，無法真正用來模擬三維的現場狀況和同時使用多井回收的狀況(Charbeneau et al., 1999, 2000)。該模式後來經過更進一步的改良，並且將控制方程式以試算表方式處理(Charbeneau, 2003) 並整合為一套評估浮油回收用的專用軟體(Charbeneau, 2007; Charbeneau and Beckett, 2007)，這套軟體的開發是美國石油學會(American Petroleum Institute, API)支持的，可由該學會的網站上下載。

API/Charbeneau 模式因其已納入許多不同類型的場址參數，如非飽和流特性、水文地質參數、水-空氣-LNAPL 三相的性質(Huntley and Beckett, 2002; Adamski et al., 2005; US EPA, 2005)且易於使用，且可模擬單層(Charbeneau and Chiang, 1995; Charbeneau et al., 1999, 2000)、雙層(Charbeneau, 2003)、甚至於三層(Charbeneau, 2007; Charbeneau and Beckett, 2007)不同的含水層材料，故廣為工程界與學術界接受和使用。部分研究使用該模式模擬結果與現場浮油回收數據比較，誤差範圍約為 6%和 14% (US EPA, 2005; Adamski et al., 2005)。Adamski et al. (2005)利用 API/Charbeneau 模式模擬細顆粒土層中浮油回收。該場址監測井中浮油厚度最高達 4.6 m。模擬結果在 LNAPL 分布、飽和度、回收都與實際狀況頗為吻合。模擬結果預測 LNAPL 飽和度小於 3%，實際上為 2%。模擬預測可回收浮油 2009 L，實際上 1.5 年以高負壓抽除系統抽油後回收約 568 L。且該案例證明較小尺度的異質性當網格尺度較大(2 m)時可忽略。

但對於較細顆粒土壤中的 LNAPL 抽除，因 LNAPL 液相層厚度較小，所以似乎以負壓為主（如 MPE, Bioslurping）的整治方式較符合成本效益。但該研究結論為甚少 MPE 可以達成在短期內將 LNAPL 厚度降低到零的目標；即使在短期內可以達到目標的狀況，在 12 個月之後 LNAPL 的「回彈」(Rebound)導致 LNAPL 又出現在地下水位面上。因而，在較細顆粒土壤中 LNAPL 移除的較佳方式應為以長時間的蒸汽抽除（蒸汽相的質量轉移）為主。但研究中的模擬也顯示 MPE 在極細顆粒土壤中的功能不彰。因為 LNAPL 的滲透性對細顆粒土壤中含水比的變化極為敏感，因此若 MPE 可以進行數週，應可有效將 LNAPL 飽和度降低至不再進入含水層。

但在此方法的模擬方面之研究極少(Li et al., 2003a; Yen et al., 2003; Yen and Chang, 2003)。Li et al. (2003a)提出有限元素多相流程式模擬雙相負壓抽除整治；模式本身模擬效率高，因僅考慮在垂直方向將水、LNAPL、氣的流動之控制方程式整合。Yen et al. (2003)則提出 Bioslurping 的有限元素程式評估在異質性、異向性非拘限含水層中 LNAPL 的回收效率；該模式可模擬水、油、氣三向在地下水中的流動和非飽和層中的氣相流動，同時模擬用抽氣（負壓）回收 LNAPL 和多種溶質溶解至地下水中，且以南台灣的某案例實際應用。但上述的解析模型或模擬程式都是以解析解或二維數值模型，無法處理真三維問題；且模式選擇受現場的複雜程度影響極大，實際的三維流場（例如有儲槽或其他物體存在）或高度異質性含水層，上述的程式恐都無法提供較適當的模擬(Charbeneau et al., 2000)。

至今為止 VER 模擬甚少，多相之間的組合率關係為納入考量或考量時不夠嚴 (Blake and Gates, 1986; API, 1989; Baker and Bierschenk, 1995, 1996)。例如 Charbeneau et al. (1989)開發的兩層模型來模擬浮油回收。相對地，在過去主要研究多相流的學者在浮油回收、負壓加速抽除相關的模擬以三維三相流程式模擬似反而較為完整。

Beckett and Huntley (1998)使用 MAGNAS3 模擬 LNAPL 回收。MAGNAS3 (MAGNAS3. HydroGeoLogic, Inc., 1992; Panday et al., 1994; Huyakorn et al., 1994)為三維有限元素三相流模擬模式，該模式不考慮土壤水遲滯現象；該研究亦並未將蒸汽相 LNAPL 回收納入模擬。影響研究結果的重要現象為 LNAPL 在土層中的貯留和移動受土壤毛細作用特徵、滲透性、液體性質之控制；就監測井中浮油厚度一樣的情況下，細顆粒土層中 LNAPL 的飽和度通常較粗顆粒土壤者低。

考量以抽除井為中心的軸對稱狀況，Beckett and Huntley (1998)模擬區域為一扇形柱體，總地層厚度 15 m，半徑 57.5 m，地下水厚度 10 m（圖 2-5）。模擬周圍變界上，地下水定水頭邊界，LNAPL 為無滲流邊界（亦即 LNAPL 總體積不變）。LNAPL 回收之模擬係在井中

設定地下水位、浮油面、氣體勢能的洩降。

模擬 LNAPL 抽除的結果顯示（圖 2-6），因 LNAPL 移動性隨其在土壤中飽和度降低而變小，且細顆粒土壤滲透性(Intrinsic permeability)較粗顆粒土壤小，因此在細顆粒土壤層中進行浮油抽除不易成功，可抽除量極小；只有在抽除井周圍 3 – 5 m 範圍內 LNAPL 飽和度有顯著降低。在粗顆粒土壤中，LNAPL 回收較易，液相抽除就可回收達 95%。研究結果發現，在抽除井附近 LNAPL 滲透性因 LNAP 移除而降低的效應隨距離減緩，亦即在抽除井周圍的低 LNAPL 滲透性區域導致回收要擴大範圍受到阻礙。因此，以負壓輔助浮油回收應該可以提升水力回收率。因為垂直向勢能平衡必須滿足，因此若監測井中若有浮油存在時，其浮油厚度較地層中有液相油品的厚度小，且地層中的浮油厚度尚不包括在其上下土壤孔隙中殘留（因污染過程或地下水位變動導致）而不易移動的 LNAPL。但即使是所謂的「浮油」，其所存在的土壤孔隙中也還是有水和空氣的存在。

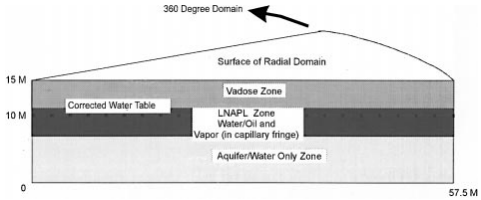

圖 2-5 模擬區域示意圖(Beckett and Huntley, 1998)

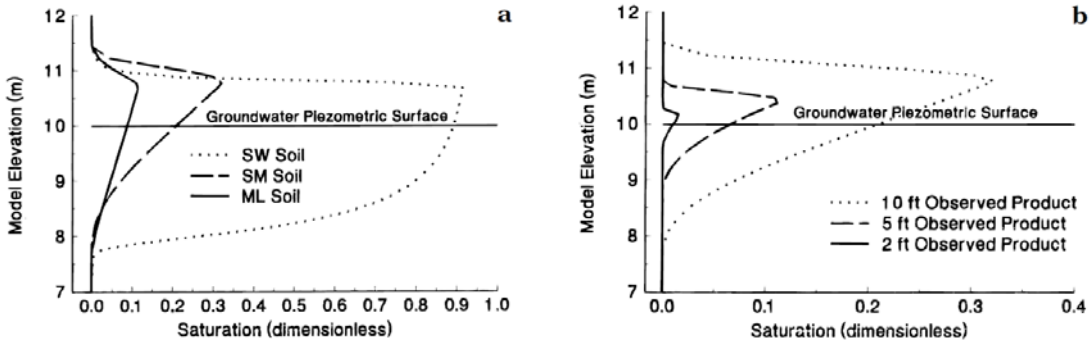

圖 2-6 (a) 初始浮油厚度 10 ft 模擬結果之 LNAPL 初始飽和度、(b)不同初始浮油厚度模擬結果之 LNAPL 初始飽和度(Beckett and Huntley, 1998)

對浮油回收效能來說，影響最大的是土壤種類；影響層面包括地下水位洩降、負壓輔助效能。在有 10 ft 初始浮油時，良好級配(SW)砂中，初始平衡飽和度最大值可達 90%；但在沈泥質砂(SM)中，最大飽和度只有 30%；沈泥(ML)中則僅 11%。飽和度之大小影響 LNAPL 相對滲透性，因而在原本滲透性(Intrinsic permeability)就已經比較低的細顆粒土壤中 LNAPL 移動性受飽和度影響而更小。

以抽取地下水製造洩降輔助抽油的雙相抽除，在粗顆粒土壤中有效（例如該研究中的良好級配砂），總抽除量 96%；井周圍(5 m 以內)抽除量更高達 98%，LNAPL 飽和度由 90%降低至 20%。浮動泵 LNAPL 抽除率由開始的 10 gal/min 以上在 3 年後降低至 1 gal/min。SM 土壤在井周圍 1 m 內的飽和度則在 3.2 年的浮油回收後由 30%降低至 10%，模擬範圍內的總抽除率只有 5%；LNAPL 抽除率由 0.045 gal/min 在 3.2 年後降低至 0.015 gal/min（**圖 2-7**）。模擬的 3.2 年中，ML 土壤的總清除率則亦僅 7%。

模擬加入負壓輔助之浮油回收（Vacuum-Enhanced Fluid Recovery, VEFR），以負壓提高流入回收井的有效勢能梯度，並同時以液相和蒸汽形式回收在地下水位面以上土壤孔隙中的 LNAPL。加入 VEFR 後，浮油回收效率顯著提升；在粗顆粒土壤中效益較細顆粒土壤顯著，在井附近的回收率幾乎倍增（**圖 2-8**）。

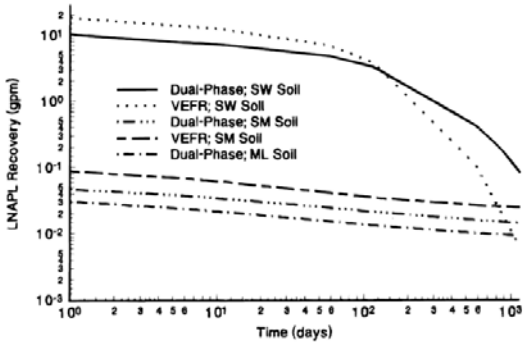

圖 2-7 不同種類土壤中 LNAPL 抽除率與時間之關係(Beckett and Huntley, 1998)

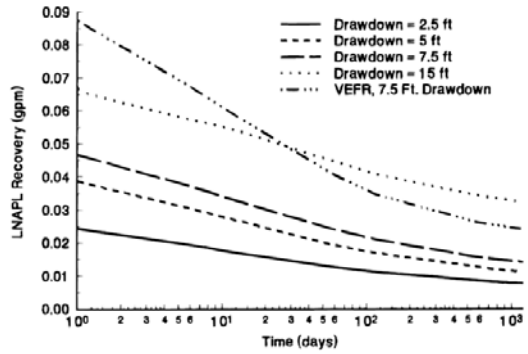

圖 2-8 SM 土壤中 VEFR 輔助之浮油回收率與時間之關係(Beckett and Huntley, 1998)

Peargin et al. (1999)利用 MAGNAS3 (Huyakorn et al. 1994; Panday et al., 1994)模擬浮油回收。以 MAGNAS3 模擬 MPE，包括均質狀況、砂與沈泥質黏土互層（厚度 0.25 m）、沈泥質砂與沈泥質黏土互層。模擬之 LNAPL 為汽油，在地下水位面上厚度 1 m；假設厚度均勻，體積固定。地下水水位在邊界上為定水頭。模型為軸對稱。下邊界為無滲流邊界(No flow)。抽取井位於圓柱形邊界中央，負壓 15 in.Hg，抽水、油、氣。井以洩降 2.25 m（低於靜止地下水位面）模擬，蒸汽流動範圍可容許高於靜止地下水位面 3 m。該研究顯示，短期 MPE 整治潛能以：(1) LNAPL 飽和度隨距離與時間之變化最大化；(2) 在回收井 10 m 範圍內任一時間的 LNAPL 體積變化；(3) 在土壤中的污染區中 LNAPL 蒸汽的流動。

該研究證實，在沈泥質黏土或沈泥質砂與黏土互層等 LNAPL 飽和度和體積小的狀況下，無論時間多長，MPE 幾乎沒有液相回收。有效的捕捉半徑隨時間較長、導水度較高、毛細上升較小而增大。對沈泥質砂和其他細顆粒土壤而言，8 小時之間，在井的 1 m 範圍以外，LNAPL 飽和度降低不到 0.1%。但若時間拉長至 30 天，MPE 井 10 m 以內 LNAPL 飽和度可降低 5%。對於透水係數低於 0.05 darcy (4.0×10^{-10} cm^2)的細顆粒土壤來說，除非浮油很厚且飽和度高於 35%（幾乎不可能），否則無法有效抽除。因為，一旦飽和度降低，LNAPL 相對導水度降低、流動速度減緩，MPE 效率也就愈來愈低。

無論是在較粗顆粒或較細顆粒土壤中，短期 MPE 對於抽除 LNAPL 蒸汽的效能不足（**表 2-1**）。在抽氣時負壓導致毛細水上升，以致於在抽除井周圍孔隙中含水量大幅提高，導致土壤氣體通路受阻，因此在通氣層中的污染區土壤氣體流通能力降低，嚴重影響 MPE 之土壤蒸汽移除效能。

表 2-1 模擬結果顯示不同土壤中之浮油回收效率(10 m 半徑內)(Peargin et al., 1999)

Simulation	Initial Volume (m^3)	8-hr Recovery (m^3)	30-day Recovery (m^3)
Sand (2 Darcy)	73.5	3.5 (4.8%)	21.4 (29.1%)
Silty Sand (0.4 Darcy)	34.6	1.0 (2.9%)	4.2 (12.1%)
Silt/Clay (0.01 Darcy)	2.8	0.0 (0%)	0.0 (0%)
Interbedded Silty Sand & Silt/Clay	14.5	0.2 (1.4%)	0.3 (2.1%)
Interbedded Sand & Silt/Clay	37.0	1.7 (4.6%)	8.5 (23%)

Chen et al. (2005)對 LNAPL 之負壓加速回收(Vacuum-enhanced recovery, VER)進行數值模擬，開發了一個三相流 LNAPL、空氣、水模擬程式。考量垂直向水頭平衡，將 3D 問題以 2D 處理；且可納入含水層之異質性。並以加拿大西部某場址為對象模擬。但該研究的 LNAPL 僅考慮 BTEX，並未考慮 LNAPL 的主成分烷類，也沒有考慮遲滯現象。

Rasmusson and Rasmusson (2009)以 **TMVOC** 模擬實際 LNAPL 污染場址的浮油回收，探討是否可以 LNAPL 之滲漏歷程和整治以及所需的時間。其場址模型為軸對稱之 3-D 圓柱形區域。其模擬之滲漏時間為 30 年，柴油滲漏總體積約 700 m^3。因模擬未考慮季節性地下水位變動與土壤之異質性，因此模擬結果高估了各監測井中柴油厚度和回收量。該研究另一重要結果為 LNAPL 的移動性(Mobility)隨時間快速降低，導致浮油回收時間緩慢。LNAPL 到回收井的滲流率(Flow Rate)在幾年之間減半。大量的 LNAPL 會以接近殘餘飽和度的狀態存在於回收井相反側（外圍）的土壤孔隙中。該論文作者建議日後應將材料的異質性，例如導水度、NAPL 殘餘飽和度等，在場址模型設定時納入考量。

2.5 污染物傳輸物理模型

孔隙介質中的污染物傳輸遵守質量守恆，其基礎概念為：空間裡某一區域中，其質量的增加速率會等於流進該區域之質量的淨通量加上生物反應以及非生物反應在該區域引致的質量增減。以上概念可用以下數學式子表示：

$$\frac{d}{dt}\iiint_{cv} m dV = -\iint_{cs} \vec{J}\cdot\hat{n} dA + \iiint_{cv} S dV \tag{2.1}$$

其中 *CV* 指空間中一任意控制體積，*CS* 為包圍該體積的封閉曲面，*m* 為污染物在控制體積中的質量分布，$\vec{J}$ 為污染物質量之流速，$\hat{n}$ 為封閉曲面上的法向量，S 為生物反應以及非生物反應造成的 sink／source。公式中質量流速可用散度定理做以下改寫

$$\iint_{cs} \vec{J}\cdot\hat{n} dA = \iiint_{cv} div(\vec{J}) dV \tag{2.2}$$

綜合上述二式可得

$$\iiint_{cv} \{\frac{\partial}{\partial t} m + div(\vec{J}) - S\} dV = 0 \tag{2.3}$$

或

$$\frac{\partial}{\partial t} m + div(\vec{J}) = S \tag{2.4}$$

此即為孔隙介質中污染物傳輸的連續方程式。就應用觀點而言，連續方程式的應用在於將將問題予以簡化，簡化的過程是透過一些假設將各種程序加以模式化。（顏伯穎, 2002）

質量分布 *m* 會以濃度的形式來表示其在控制體積的分布量多寡。控制體積中的空間分別被孔隙與土壤顆粒占據，而孔隙又分別被不同流體占據，一般來說流體可分為三相：水、空氣、油，質量 *m* 將分布在此四者之間。在應用上，會以單一相的濃度為基礎，透過函數關係來表示其他三相中的濃度，此稱為溶質分配（Solute Partitioning）。以水相濃度為基礎，並假設線性關係來進行溶質分配為常見的做法。土壤吸附屬溶質分配的範疇。

污染物流速 $\vec{J}$ 可以三種方式出現：平流傳輸（Advection Transport）、擴散（Diffusion）、機械延散（Mechanical Dispersion）。溶質隨著孔隙流體的運動而被帶走的現象稱為平流傳輸。平流傳輸是最顯著的質量移動方式，動力來源為流體的勢能梯度。擴散是指質量透過隨機分子運動傳輸的過程，擴散會將質量自高濃度區帶往低濃度區。在探討低傳導系數土壤中的傳輸、揮發性化學物質在汽相中的傳輸、殘留相 NAPL 的衰減等三種傳輸情境下，擴散為重要的機制，但一般來說擴散傳輸影響尺度較孔隙流體傳輸小得多。另外，擴散亦可對污染物被化學吸附的比率產生限制作用。平流傳輸為孔隙流體傳輸上的平均概念，機械延散則用來形容此平均值的偏差程度（Deviation），偏差值具有方向性，並隨模型尺度不同而改變。

實務上，時常將機械延散與擴散的影響合併，以水動力延散（Hydrodynamic Dispersion）來表示。（Randall, 2000）

2.6 TMVOC 及其物理模型

TMVOC 為美國勞倫斯柏克萊國家實驗室（Lawrence Berkeley National Laboratory）所開發，以 TOUGH2 為藍本改寫的三維積分式有限差分三相流模擬程式，它被設計來處理碳氫化合物與有機溶質在飽和及不飽和帶中的傳輸，並可模擬人工整治。Thunderhead Engineering 為其開發了使用者介面 PetraSim。已有許多研究使用 TMVOC 進行模擬（Battistelli, 2008, 陳等, 2009, Rasmusson and Rasmusson,2009, Erning, et al, 2009, Kererat and Soralump, 2010, et al.）。

TMVOC 使用積分式有限差分（Integral Finite Difference）處理空間域，在時間域上則使用一階有限差分，通量與 sink／source 使用 fully implicit 處理。控制體積中外延性質使用平均值取代，控制面積上內延性質通量的表面積分（Surface Integral）以離散空間下各連接面淨通量平均值的總和取代。對於空間中某個控制體積 V_n 以及其鄰接空間 V_m，若探討 V_n 中某 K 物質質量守恆行為，則有

$$\int_{V_n} M dV = V_n M_n^k \tag{2.5}$$

M 為 V_n 中的密度分布，M_n^k 為 M 在 V_n 中的平均值。而在離散空間下，控制面積上的淨通量可表示為

$$\int_{\Gamma_n} \vec{F}^k \cdot \hat{n} d\Gamma = \sum_m A_{nm} F_{nm} \tag{2.6}$$

Γ_n 為控制面積，$\hat{n}$ 為控制面積上法相量，$\vec{F}^k$ 為 K 的流速，A_{nm} 為 V_n 和 V_m 的交界，F_{nm} 為 $\vec{F}^k$ 在 A_{nm} 上的垂直分量平均值。圖 2-9 展示了 TMVOC 離散模型示意圖。

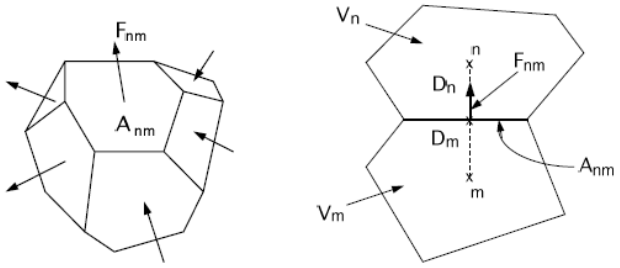

圖 2-9 TMVOC 離散模型 (Pruess et al., 2002)

而 K 可由不同相流體攜帶，故有

$$F_{nm} = \sum_\beta x_\beta^K F_{\beta,nm} \tag{2.7}$$

x_β^K 為 K 在 β 相流體的濃度，$F_{\beta,nm}$ 為 β 之流速在 A_{nm} 上的垂直分量平均值。而 $F_{\beta,nm}$ 遵循廣義達西速度

$$F_{\beta,nm} = -k_{nm}\left[\frac{k_{r,\beta}\rho_\beta}{\mu_\beta}\right]_{nm}\left[\frac{P_{\beta,n}-P_{\beta,m}}{D_{nm}} - \rho_{\beta,nm} g_{nm}\right] \tag{2.8}$$

K_{nm} 為 V_n 的本質滲透係數（intrinsic permeability），$K_{r,\beta}$ 為 β 的相對滲透係數，ρ_β 為密度，μ_β 為黏滯力，$P_{\beta,n}$ 與 $P_{\beta,m}$ 分別代表 β 在 V_n 及 V_m 的壓力，D_{nm} 為 V_n 及 V_m 的節點距離，g_{nm} 為重力加速度在節點 n、m 連線上的分量。

綜合以上公式可得到

$$\frac{dM_n^k}{dt} = \frac{1}{V_n}\sum_m A_{nm}F_{nm} + q_n^k \qquad (2.9)$$

其中 q 為 sink／source 在 V_n 中的平均值，此即為 TMVOC 的控制方程式。

TMVOC 假設在任意時間點上，整個模型皆達到化學平衡與熱平衡，即化學、熱平衡為瞬發反應。化學反應只發生在以下幾種情形：交界面上的質量交換、固體相的吸附以及 VOC 之生物降解。在 TMVOC 控制方程式中未考慮機械延散（Fickian Model for Hydrodynamic Dispersion），須額外配合其他套件來模擬機械延散對傳輸的影響。(Pruess et al., 2002)

三、研究方法

3.1 模擬場址與土壤與油品參數

本研究使用 TMVOC 軟體模擬煉油廠或儲運站等大型儲槽之洩漏與整治，並比較不同整治方案效率差異。本模擬所用數值模型的示意圖繪製於圖 **3-1**，圖中模型最上方區域為大氣連通邊界，而最底部為無通量邊界，此邊界用來模擬不透水層。最左下與最右下網格為固定端，用來給予流場一個穩定的左右端水頭差，而最左上與最右上網格亦為固定端，用來提供模擬大氣邊界所需的固定壓力。緊鄰大氣邊界的下方即為土層，在土層中引入一個洩漏源 S 來模擬油品洩漏，在 S 水平距離 L 外之處引入整治井 W，W 將開篩在地下水位面附近。而在本研究中透過改變 L 來比較不同佈井位置整治效益的差別，並改變土層孔隙率來探討孔隙率對整治效益的影響，最後改變 W 的負壓大小，探討負壓對整治效益的影響。

使用數值模型模擬污染場址之整治可分為三個階段，第一階段為建立未污染地下水流場，第二階段為模擬油品洩漏，第三階段為引進整治井並模擬抽油整治。以下分別就此三階段分別說明建模過程。本場址設定為煉油廠、儲運站、火力發電廠、機場、大型化工廠等具有大型儲槽之設施油品滲漏與整治。

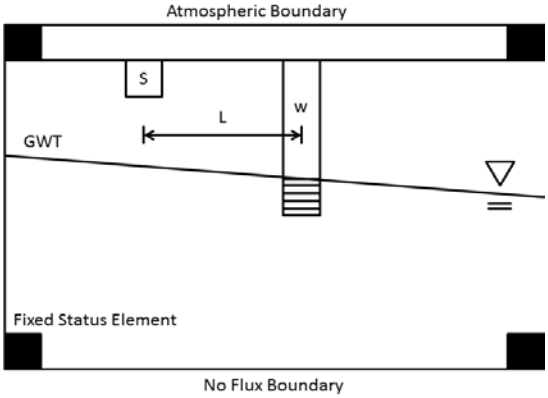

圖 3-1 模型示意圖

LNAPL 污染整治之模擬分為兩個階段：

1. 污染階段 – 油品由儲槽滲漏：探討問題 – 定滲漏率下不同土壤類型中 LNAPL 分布（厚度、範圍）。本階段建立之污染範圍與分布，將作為第二階段的初始條件。第一階段之輸出檔為第二階段之輸入檔。

2. 整治階段 – 浮油回收（滲漏已停止）：探討問題 – 浮油回收速率、負壓大小等整治系統控制因子對回收效率之影響。以第一階段之污染場址停止 LNAPL 滲漏，並在 TMVOC 模型中以適當之 Sink 假設，模擬 MPE 之負壓與浮油回收。

3.2.1 未污染場址之建立

本研究選定一長 400 公尺（X 方向）、寬 200 公尺（Y 方向）、深 16 公尺（Z 方向）之模型作為研究對象。模型土層使用單一砂層，絕對滲透係數在水平向（X&Y）為 1.0×10^{-11} m^2，

垂直向（Z）為 1.0×10^{-12} m^2，孔隙率為 0.3。SWCC 使用 Paker 3-phase 的理論，相關參數為：S_m=0、n=1.84、α_{gn}=100、α_{nw}=110；相對滲透係數使用 Stone's 3-phase 的理論，相關參數為：S_{wr}=0.1、S_{nr}=0.05、S_{gr}=0.05、n=3。模型所使用的土壤參數整理於**表 3-1**。

表 3-1 土壤參數

SAND			
Horizontal Intrinsic Permeability	Vertical Intrinsic Permeability		Porosity
1.0×10-11	1.0×10-12		0.3
Stone's Model Parameter			
n	Swr	Snr	Sgr
3	0.1	0.05	0.05
Paker 3-phase Model Parameter			
Sm	αgn	αgw	n
0	100	110	1.84

模型中深度-0 m 至-1 m 為大氣邊界，-1 m 開始為土層。土層分布在-1 m 至-16 m 間，厚度共 15 m。整個模型在 Z 方向分為 12 個網格，由-0 m 至-11 m 為加密網格，-11 m 至-16 m 為粗網格。X 方向分為 20 個網格，Y 方向分為 12 個網格，在此兩方向上於洩漏點預定位置做有網格加密的動作。網格示意圖繪製於**圖 3-2**。

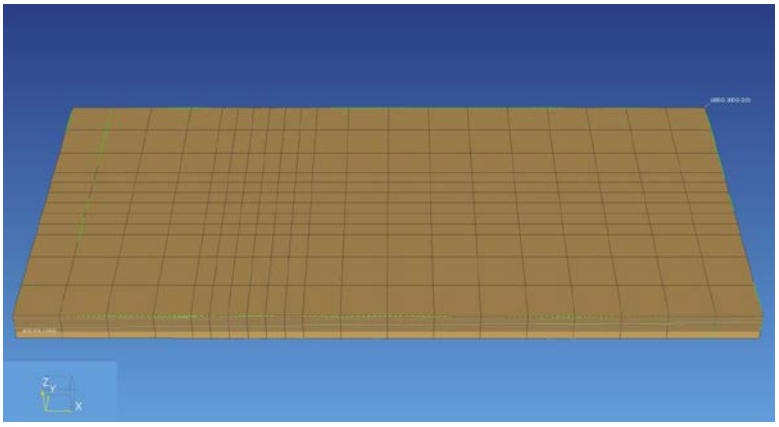

圖 3-2 網格示意圖

本研究中將地下水水位於左端設置於-6 m 而於右端設置於-7 m，從而使整個模型產生 0.0025 之水力坡降。地表降雨入滲在本研究中未予以考慮。因 TMVOC 無法求解穩態解，本研究中必須以長時間的暫態模擬來得到穩態解。在模擬長時間的地下水流後，可得到一相對穩定的流場，如**圖 3-3** 所示，該流場水流方向皆為平行 X 方向，而此流場將用於後續模擬油品洩漏。

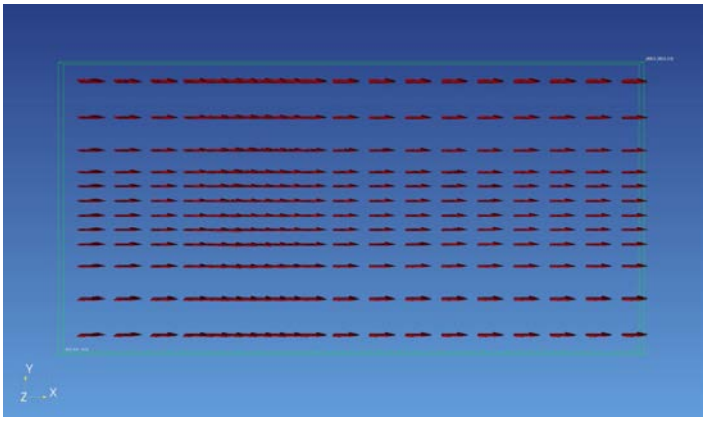

圖 3-3 穩定之地下水流場

3.2.2 洩漏階段之模擬

為了避免邊界效應，洩漏點位置將設在稍偏上游處，且為了模擬大型儲槽實際洩漏行為，洩漏點應設置於貼近地表之網格，最終本研究將洩漏點中心座標設為 X=110，Y=105，Z= -1.5，洩漏點在模型中的相對位置可參考**圖 3-4**。

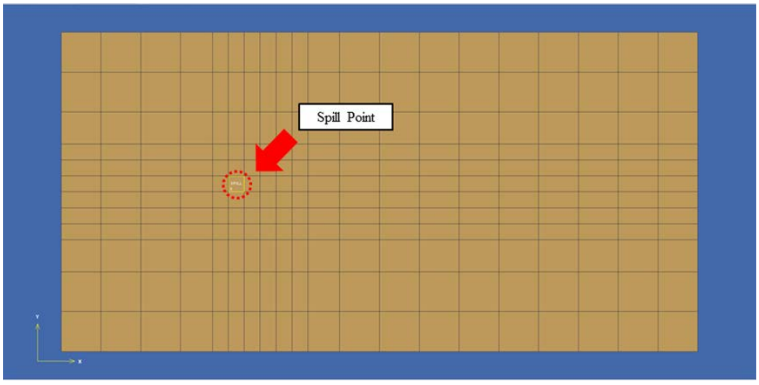

圖 3-4 洩漏點位置

本由究所使用之油品為汽油，而為了真實模擬油品於土壤中之遷移行為，本研究不將油品以單一物質替代，而將是將其中每個成分獨立設立一個 Source。本研究將汽油簡化為五成分，分別為苯、甲苯、乙苯、二甲苯、正辛烷，其各自的重量百分比如下：苯 3.5%、甲苯 7.0%、乙苯 5.5%、二甲苯 1.5%、正辛烷 82.5%。模擬洩漏速率設定為每天 0.5 m^3，即每天 1826.25 kg，據此計算各個污染物的洩漏速率如下：苯 1.58×10^{-4} kg/s、甲苯 3.15×10^{-4} kg/s、二甲苯 6.759×10^{-5} kg/s、乙苯 2.48×10^{-4} kg/s、正辛烷 3.72×10^{-3} kg/s。滲漏時間訂為 10 年，故可預估 10 年後總滲漏量可達到 1,142,802.8 kg。滲漏速率彙整於表 3-2。在 TMVOC 中所使用的化學參數請見附錄。而在研究過程中尋找油品化學性質時，時常只找到某一特定溫度下的數值，抑或是無法找到 TMVOC 內建公式所使用之參數。為了順利完成模擬，本研究將模型維持在恆溫 25℃，讓化學參數不會因溫度變化而產生改變。

為了研究孔隙率對整治效率的影響，本研究將對兩個不同孔隙率之場址以相同洩漏速率進行油品散佈。模擬結果，在孔隙率 0.3 之場址 10 年後留於場址中的總油品共有 1,422,851 kg，而在孔隙率 0.4 之場址共有 1,422,901 kg，與估計值 1,142,802.8 kg 相比僅有十萬分之三與十萬分之七的誤差。

表 3-2 洩漏量設定

	Benzene	Toluene	Ethylbenzene	Xylene	Octane
Weight Percent (%)	3.5	7.0	5.5	1.5	82.5
Leakage Rate (kg/s)	1.580×10^{-4}	3.150×10^{-4}	2.480×10^{-4}	6.759×10^{-5}	3.720×10^{-3}
Total VOC Mass after 10 Years (kg)	49,861.0	99,406.4	78,262.8	21,329.8	1,173,942.7

3.2.3 整治階段之模擬

本階段將前述洩漏場址作為模型的初始條件（Initial Condition），並在模型中引入 Sink 來模擬整治井。為了貼近現實狀況，Sink 形式採用 Deliverability Model，而非使用 Mass Out。Sink 之水平位置設置在一條通過洩漏點而平行於 X 軸之直線上，如**圖 3-5** 俯瞰圖所繪，整治井 W 將不會設在洩漏點 S 的 Y 方向上。而如**圖 3-5** 側視圖所繪，Sink 深度將設在地下水位所在的 Z＝-6~-7 m 網格。本研究中使用之 Sink 參數列於**表 3-3** 中。

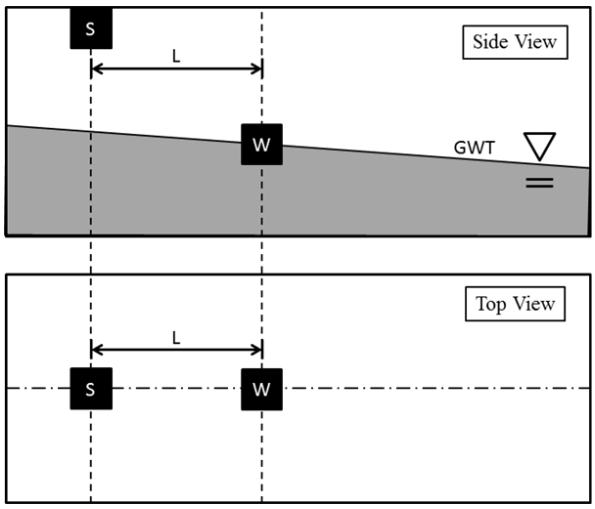

圖 3-5　Sink 位置示意圖

表 3-3 Sink 參數

Production Well Radius (m)	0.1016
Skin Factor	0
Productivity Index (m^3)	1.78×10^{-11}
Bottomhole Pressure (Pa)	90,000

3.3 汽油成分設定

油相是由不同 NAPL 所組成之一個流體相，油相之黏滯力、密度、莫爾體積等性質將由油品內各 NAPL 所佔百分比的不同而產生變化，而各 NAPL 在油相中所佔本分比將由各自的飽和蒸汽壓、溶解度、化學活性等互相制衡。油品成分簡化需保持三個原則，原則一，BTEX 四項為主要研究對象，應將其視為獨立的 NAPL，故新成分汽油中勢必要保留 BTEX，並保持此四物質的物理化學性質不變；原則二，新油品之流動性必須和原始油品相似，而在多相傳輸中流體通量大小與黏滯力和密度的比例有關，故在新成分汽油中，其黏滯力和密度的比例必須維持不變；原則三，TMVOC 在化學平衡過程中時常用到莫爾濃度此一物理量，故對於主要研究對象的 BTEX 四項，其在油品中之莫爾濃度應當維持不變。

本研究最終決定使用所謂「4+1」的五成分汽油來進行模擬，即保留 BTEX 並另外加上一個足以代表餘下成分的背景 NAPL 來組成汽油。陳培旼等（2010）所使用之簡化汽油，其成分可細分成三大類：芳香族、脂肪族、醚類。芳香族包含了苯、甲苯、乙苯、二甲苯，脂肪族飽含了環戊烷、庚烷、異辛烷，而甲基第三丁基醚被獨立歸到醚類中。芳香族四成分為欲保留的 BTEX 四項，不予以變動，故油品簡化重點在於將其他物質以單一物質取代。但受限於甲基第三丁基醚參數未收集完整，並且考量其只占有汽油 18.0%之下，此成分將被屏除於新汽油成分外，本研究只對脂肪族三物質作簡化的動作。

本研究參考 Gustafson et al. (1997)將汽油以等碳數（Equivalent Carbon Number）做分類的研究，以及 Rasmusson & Rasmusson (2009)以等碳數對柴油成分作簡化的研究，在此以等碳數概念將脂肪族簡化成單個物質。等碳數是將碳氫化合物之沸點對正烷類之沸點做正規化的概念，一般來說碳氫化合物之飽和蒸汽壓、溶解度、密度等化學性質與沸點具有正相關，一個等碳數 5 的碳氫化合物將可預期和碳數 5 之正烷類—即正戊烷具有相似的物化性質。

在確定新汽油成分後，須再調整正辛烷性質以便符合莫爾濃度以及流動性的要求。**表 3-4** 為原始 8 成分汽油的性質，整體油品代表性密度使用重量百分比來加權平均，整體油品代表性粘滯力則用 TMVOC 內定的公式計算

$$\mu_n = \prod_k \mu_k^{X_n^k} \tag{3.3}$$

式中 μ_n 為整體油相之黏滯力，μ_k 為油相中成分 k 之黏滯力，X_n^k 為成分 k 在油相中之莫爾濃度。

因黏滯力隨各成分莫爾濃度改變，故須先調整新汽油各成分莫爾濃度以符合要求。由於新成分中正辛烷取代了脂肪族與醚類，正辛烷重量百分比應當設定為此兩分類的加總—82.5%。據此計算出符合莫爾濃度要求的莫爾質量，正辛烷將從 114.231 g 修改為 86.580 g。莫爾濃度固定後，由黏滯力公式便可推出所需黏滯力，正辛烷黏滯力將從 0.533 cP 修改為 0.447 cP。最後須讓新汽油密度與原始汽油相近，正辛烷密度從 698.5 kg/ m^3 修改為 759.2 kg/ m^3。新汽油成分列於**表 3-5**，可發現在莫爾濃度、密度、黏滯力上與原始汽油相去不遠。

表 3-4 原始汽油成分

	Weight Percent (%)	Viscosity (cP)	Density (kg/ m^3)	Molar Mass (g)	Mole Fraction
Benzene	3.5	0.652	885.0	78.114	0.0393
Toluene	7.0	0.590	867.0	92.141	0.0667
Ethylbezene	5.5	0.669	867.0	106.168	0.0455
Xylene	1.5	0.620	864.0	106.168	0.0124
Cyclopentane	24.5	0.430	896.0	65.515	0.3282
Heptane	20.0	0.410	679.5	100.200	0.1752
Isooctane	20.0	0.510	688.0	114.231	0.1536
MTBE	18.0	0.470	740.6	88.150	0.1792
Density＝778.6 kg/ m^3　Total Moles＝1139.6 mole　Viscosity＝0.4733 cP					

表 3-5 簡化汽油成分

	Weight Percent (%)	Viscosity (cP)	Density (kg/ m^3)	Molar Mass (g)	Mole Fraction
Benzene	3.5	0.652	885.0	78.114	0.0393
Toluene	7.0	0.590	867.0	92.141	0.0667
Ethylbezene	5.5	0.669	867.0	106.168	0.0455
Xylene	1.5	0.620	864.0	106.168	0.0124
Octane (Edited)	82.5	0.447	759.2	86.580	0.8362
Density＝778.7 kg/ m^3　Total Moles＝1139.6 mole　Viscosity＝0.4726 cP					

3.4 指標參數與控制變因

3.4.1 指標參數

為了比較不同案例之間整治結果孰優孰劣，本研究選定兩個指標作為判別基準，其一為整治效率（Efficiency），其二為整治速率（Rate）。效率係指整治行動結束後，成功從場址中抽出的油品數量多寡，是一個時間上的積分結果。效率較好或效率較高的案例即為整治結束時油品抽出總量較多之案例。速率係指在某一時間區間內油品抽出量的多寡，可視為效率在某一時間區間中的平均值。

3.4.2 模型控制變因

<u>佈井位置</u>

不同佈井位置會改變整治井影響半徑內的初始條件，而且佈井位置不同對流場勢能變化亦有不同影響。本研究中以 Sink 對洩漏點的水平距離為變化基準，在不同佈井位置以相同的 Sink 設定進行整治，並進行比較。

<u>孔隙率</u>

在相同流體通量下，孔隙率不同影響了孔隙介質飽和度的發展。大孔隙率者飽和度變化將趨緩，從而讓 SWCC 與相對滲透係數的發展有所改變。本研究分別模擬孔隙率 0.3 以及 0.4 的場址，並分析不同孔隙率下整治效率的差別。

<u>井內負壓（水力梯度）</u>

油品往整治井方向移動之能量來源，來自整治井周邊的壓力梯度，當在場址中引入一負壓後（係指小於大氣壓力 101,325 Pa 之壓力源），由於跟大氣壓力之間的落差，負壓將在周邊

區域造成壓力梯度。與大氣的壓差越大，壓力梯度越陡峭，流體通量也越大。在本研究中，除了最初的井底壓力 90,000 Pa，另外將引入 44,246 Pa 的井底壓力進行整治模擬。此兩者與大氣之間的壓差約相差 5 倍，而此兩不同壓力場址間整治效率的比較將用於分析大壓力梯度帶來的效益。

四、結果與討論

4.1 整治井對油品分布之影響分析

圖 4-1 為在不同情況下，NAPL 飽和度於 Z=-7m 之分布。在洩漏剛停止時，洩漏點附近仍留有較高的 NAPL 飽和度。如**圖 4-1(A)**所示，洩漏點（X=110m，Y=105m）附近的飽和度達到 0.26 以上，明顯高於其他區域。但在停止洩漏並讓其自由流動一年後，就如前述的原因，原始的高飽和度區（飽和度 0.26 以上）範圍大大地縮小，由**圖 4-1(B)**可觀察到飽和度 0.31 以上區域消失，而飽和度 0.26 以上區域只殘留一小塊。另外，由於所擷取的圖片僅為某一深度之平面圖，會有誤導 NAPL 只在該深度向外擴散的可能，但事實上此為三維行為，該區域減少的 NAPL 將向四面八方散布到鄰近空間中。

若於洩漏停止後引進整治井，並進行為期一年之整治，則可預期擷取區附近 NAPL 飽和度將有所降低。在此以案例 8 的佈井位置（X=120m，Y=105m）為範例，來比較進行整治後 NAPL 飽和度的改變。由圖 C 可觀察到，整治 1 年後不僅飽和度 0.21 以上區域消失，鄰近整治井的區域其飽和度甚至降到比外圍區域還低。但遠離擷取區的 0.01、0.06、0.11 等高線，以及 0.16 等高線較下游區塊，在整治 1 年後其分布範圍與自由流動相較之下，並無明顯變化。

溶解相油品除了出現在地下水體以外，在油品重力滲流過程中所掃過的不飽和帶中的孔隙水，也有機會出現溶解相油品。**圖 4-2(A)**為滲漏剛停止時，在 Y=105m 剖面的溶解相油品莫耳濃度分布圖。可以發現主要污染區可分為兩部分，其一為為洩漏點下方油品滲流經過之不飽和帶，其二為地下水位上方推積的油品隨流場掃過的區域。在停止洩漏並讓油品自由流動一年後，濃度分布幾乎無變化，**圖 4-2(B)**可看出原本的高濃度區仍侷限在同樣範圍裡，並無特別擴大或縮小。

為了說明引進整治井對溶解相油品的影響，在此同樣以案例 8 的佈井位置（X=120m，Y=105m）為範例來進行為期 1 年之整治，並比較、說明結果。**圖 4-2(C)**為整治 1 年後之濃度分布，在不飽和帶中濃度有明顯降低，但地下水位附近的區塊其濃度則無太大變化，此乃因為該區域孔隙中仍殘留有一定量的自由相油品，造成油品持續溶解到水中。要讓濃度有效降低，前提便是將孔隙中的油品飽和度降至一定水平以下，而地下水位附近之自由相油品即為本研究所稱之浮油，故若是想要有效控制油品溶解相濃度，便需先將足夠量的浮油給清理掉。

在本研究的模擬中，汽相油品包含了苯、甲苯……等多種不同的蒸氣在內，為了方便解說，在此僅以苯蒸氣來說明整治井對汽相油品的影響。同樣先觀察剛洩漏完與洩漏完後自由流動 1 年之場址，方便與整治後場址做比較。**圖 4-3(A)**為滲漏剛停止時，在 Y=105m 剖面的汽相苯莫耳濃度分布圖，與溶解相油品同樣地可分為不飽和帶以及地下水位附近兩區塊。在洩漏停止後讓其自由流動 1 年，濃度分布亦沒有什麼變化，由**圖 4-3(B)**可觀察到高濃度區範圍近乎不變。

在洩漏停止後引進案例 8 整治井進行為期 1 年的整治，整治後汽相苯濃度剖面繪製圖 4-3(C)，可以觀察到和溶解相油品相似的狀況，不飽和帶濃度有效地降低，地下水位附近濃度仍近乎維持不變，原因如下：在數值模擬中，汽相與溶解相的分佈行為皆使用溶質分配（Solute Partitioning）來形容，此即為兩相行為相近的原因。在自由相油品未降至一定量以下時，NAPL 將持續被平衡至溶解相與汽相中。

TMVOC 無法計算浮油厚度，但自由相油品飽和度 SO 一定程度上可反應浮油厚度多寡。**圖 4-4** 為 SO 於 Y=105 m，Z= -7m 直線上的分布，在案例 8 整治過後整治井周圍 SO 明顯降低，但下游 250 m 過後便無影響。整治井周邊約 20 m 範圍內 SO 降低程度最明顯。

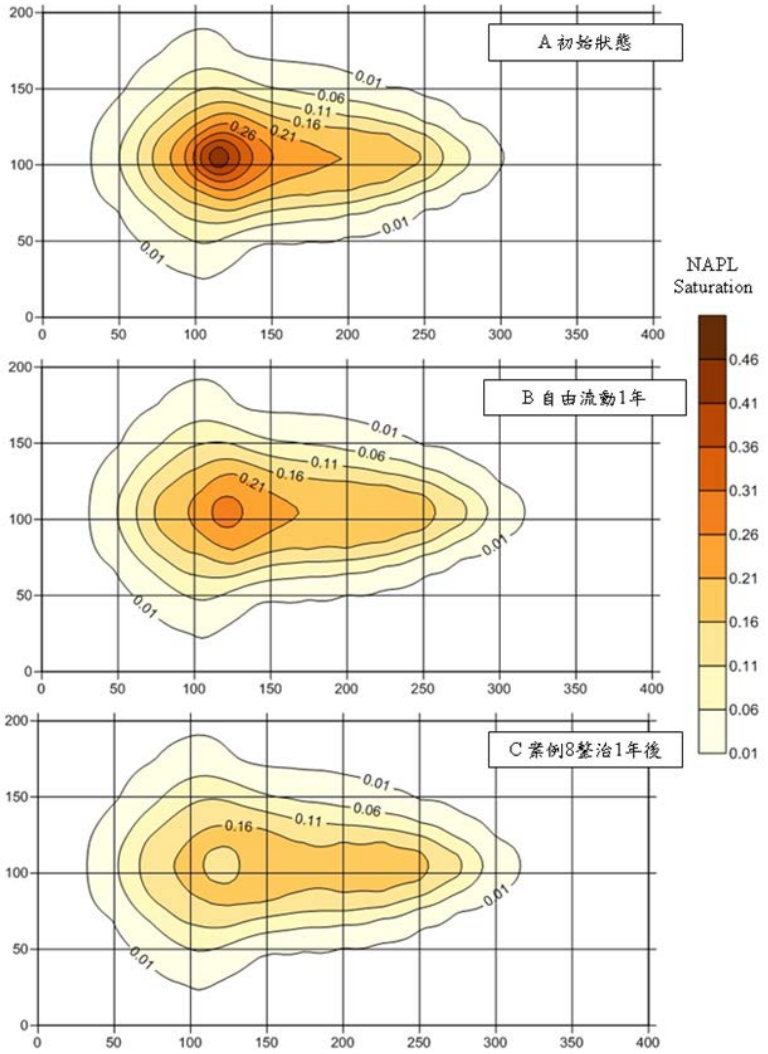

圖 4-1　Z=-7m 之 NAPL 飽和度分布圖

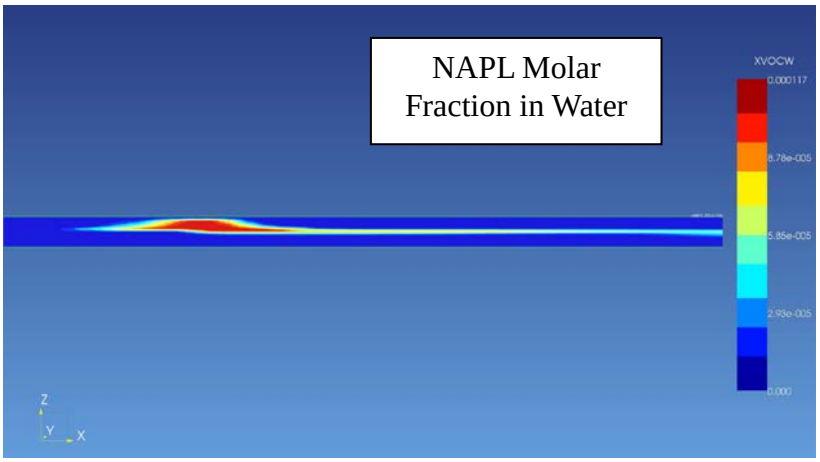

圖 4-2(A) Y=105m 剖面之溶解相油品莫耳濃度，初始狀態

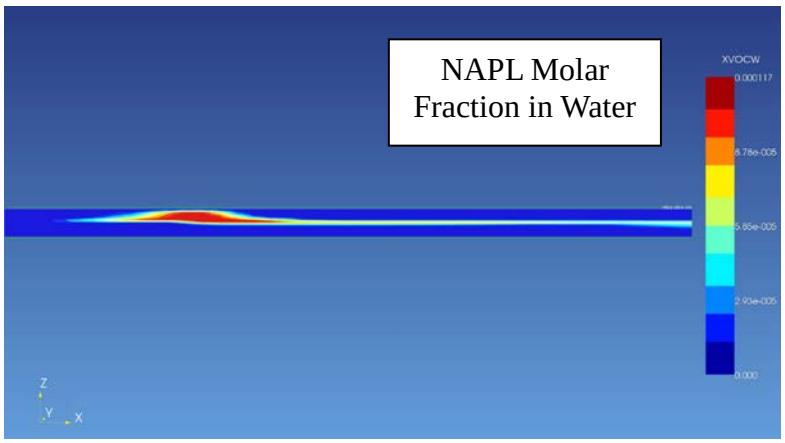

圖 4-2(B) Y=105m 剖面之溶解相油品莫耳濃度，自由流動

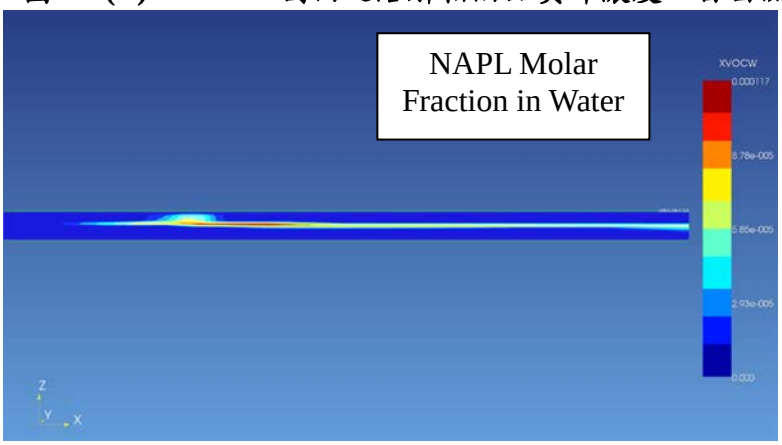

圖 4-2(C) Y=105m 剖面之溶解相油品莫耳濃度，案例 8 整治 1 年後

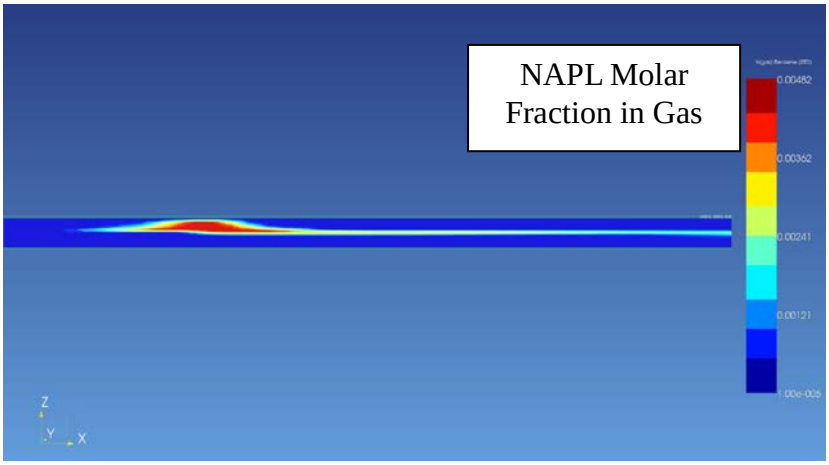

圖 4-3(A) Y=105m 剖面之汽相苯莫耳濃度，初始狀態

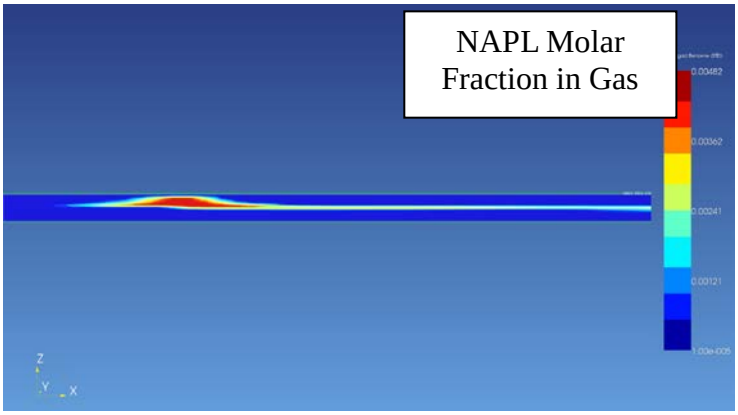

圖 4-3(B) Y=105m 剖面之汽相苯莫耳濃度，自由流動 1 年後

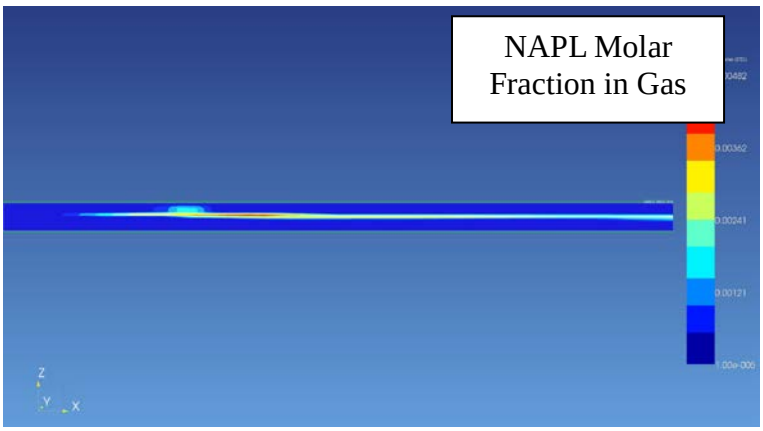

圖 4-3(C) Y=105m 剖面之汽相苯莫耳濃度，案例 8 整治 1 年後

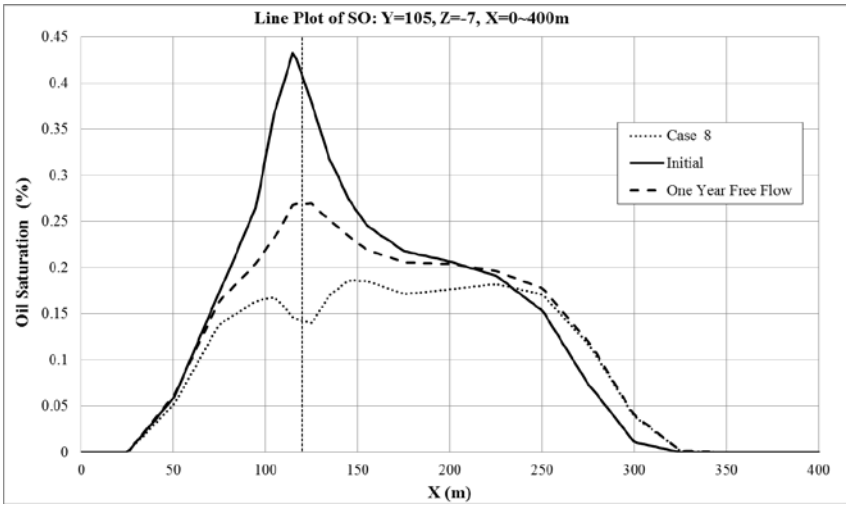

圖 4-4　Y=105 m, Z=-7 m 之油品長軸方向飽和度分布

4.2 佈井位置影響分析

本節中將整治井與油品洩漏點之 X 方向水平距離作為變數，在相同的污染場址及整治井抽取能力下，探討不同佈井位置的整治效率。如**圖 4-5(A)**所示，在經過一年整治後，整治井使整個場址內的油品減少了 1,049 至 203,949 kg 不等。最大減少量發生在佈井於洩漏點下游 10 m 之案例 8，油品減少了 20,3949 kg，以此為中心向上游與下游佈井則整治效率開始下降；在下游 77.5 公尺之後變化程度趨緩，最終於 152.5 m 處降至 1,049 kg，只為最高效率案例的千分之五。整治一年後留於場址中的油品總質量隨佈井距離之變化繪製於**圖 4-5(B)**，發展趨勢與**圖 4-5(A)**相反，從下游 10 m 向開始向兩側增加，同樣在下游 77.5 m 之後變化程度趨緩，最終於 152.5 m 處幾乎回收不了任何油品。

若以整治一年後留於現地之油品總量為基準來計算油品的整治百分比，則整治井成功地抽出了 0.07~14.33%不等的油品。由**圖 4-5(C)**可觀察到，同樣地在下游 77.5 m 之後變化程度趨緩，效率驟降至 2.46%；最終於 152.5 m 處降至 0.07%。

整治井的整治速率發展可分為兩個不同特性之群組，分別為：群組 A（案例 6、7、8、9、15）以及群組 B（案例 11、12、13、14），各案例與佈井位置的對照表列於**表 4-1**。群組 A 佈井位置距離洩漏點較近，其整治速率變化大致有一定規律，並有著相對於群組 B 較高的整治速率；群組 B 佈井位置距離洩漏點較遠，整治速率發展較無規律，且有著相對於群組 A 較低的整治速率。

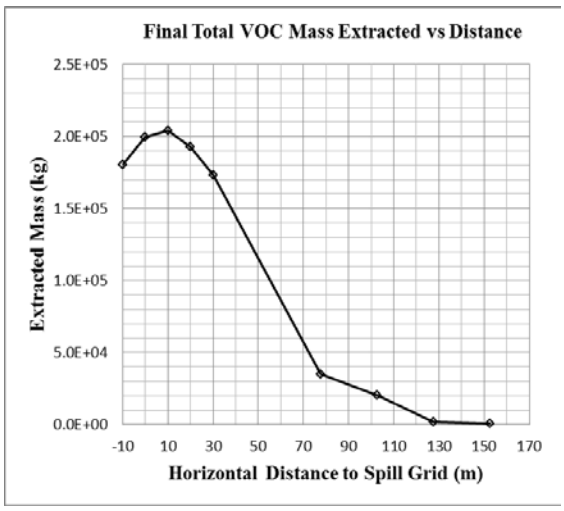

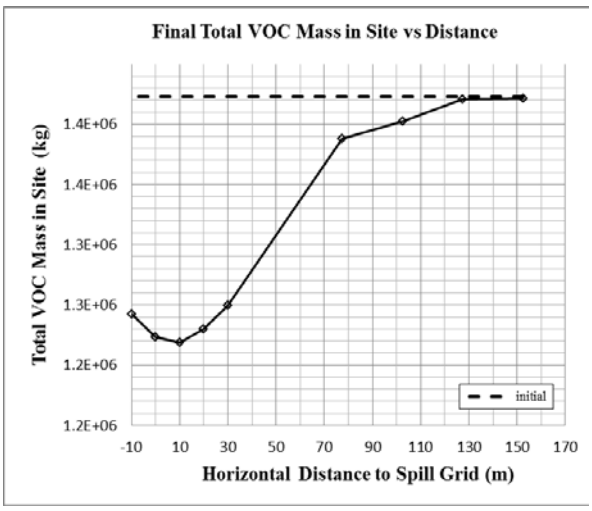

(A)油品整治量與整治井距離之關係　(B)整治一年後場址之油品總量與整治井距離之關係

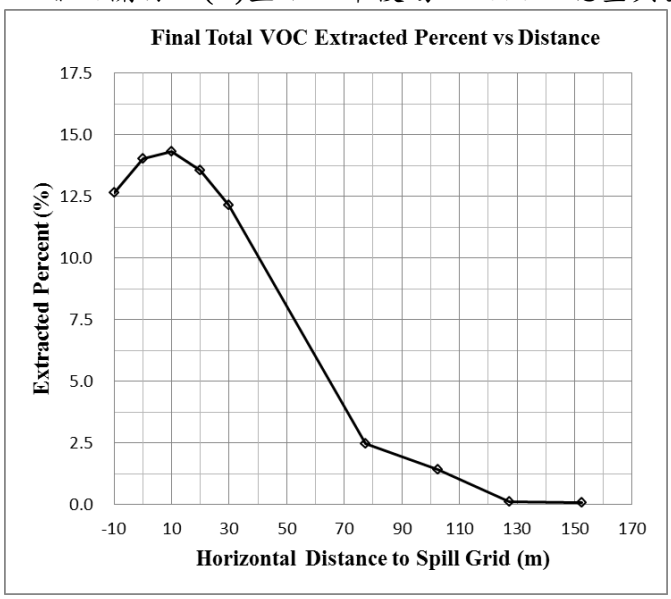

(C)油品整治百分比對整治井距離之關係

圖 4-5　整治井位置對整治效果影響

在群組 A 的部分，整治速率在第一個月達最高峰，但隨整治持續進行有逐漸減小的趨勢；由**圖 4-6(A)**可看出，離洩漏點越遠者其初始速率越小。案例 6 雖然在第二個月速率有所提升，但之後仍然持續下降；其速率提升是因整治井周邊油品隨壓力梯度遷移，造成整治井附近油品飽和度在整治初期有所增加，且案例 6 抽取量相對較低，一來一往使得整治速率在第二個月小幅提升。後續月份因油品相對滲透係數降低，補注量不再足以填平整治井的抽取量。群組 A 所有案例在六個月後整治速率都降至最高峰的 50%左右，特別是高整治效率的案例 8、案例 9、案例 15，早在第二個月便降至 50%左右。而群組 A 案例在一年整治後速率分別降至 10%~30%不等。由**圖 4-6(A)**另可觀察到群組 A 整治速率隨整治進行皆趨近同個數值，平均約落在每個月 7,069 kg。此數值可視為系統達穩定下之穩定整治速率。由模擬結果可知，佈井於洩漏點上游 10 m 至下游 30 m 內，系統達穩定後之整治速率皆約略落在同一範圍。

群組 B 整治速率對時間的變化呈現於**圖 4-6(B)**，可觀察到群組 B 整治速率變化複雜。案例 11 前三個月速率提升，並在第三個月達到最高峰每個月 3,635 kg，第四個月開始速率持續降低，在一年後整治速率降至最高峰的 65%，但仍高於第一個月的整治速率（每個月 2,317 kg）。案例 12 整治速率維持在每個月 1,700 kg 上下，並無明顯起伏。案例 13 以及案例 14 整治速率隨時間前進持續上升。群組 B 整治速率減少之趨勢較群組 A 緩和，在案例 13 與 14 甚至逆勢成長，但群組 B 整治速率比群組 A 小了 1 至 3 個數量級，以整治效益來看並不建議佈

井於此。兩群組數量級之比較呈現於**圖 4-7**。

綜合以上所述，佈井於洩漏點稍偏下游處可以取得最大的整治效率，在本研究中共回收了 14.33%的油品，在此點之上游或是下游佈井整治效率將下降，效率下降程度在佈井距離 77.5 m 後開始趨緩，但此時整治效率已大幅降低。佈井接近洩漏點的案例其速率變有一定規律，一年後整治速率都將收斂至同樣範圍；佈井較遠離洩漏點者整治速率變化複雜。

表 4-1 案例與佈井位置對照表

Case	Case 15	Case 9	Case 8	Case 7	Case 6	Case 11	Case 12	Case 13	Case 14
Horizontal Distance to Spill Grid (m)	-10.0	0.0	10.0	20.0	30.0	77.5	102.5	127.5	152.5

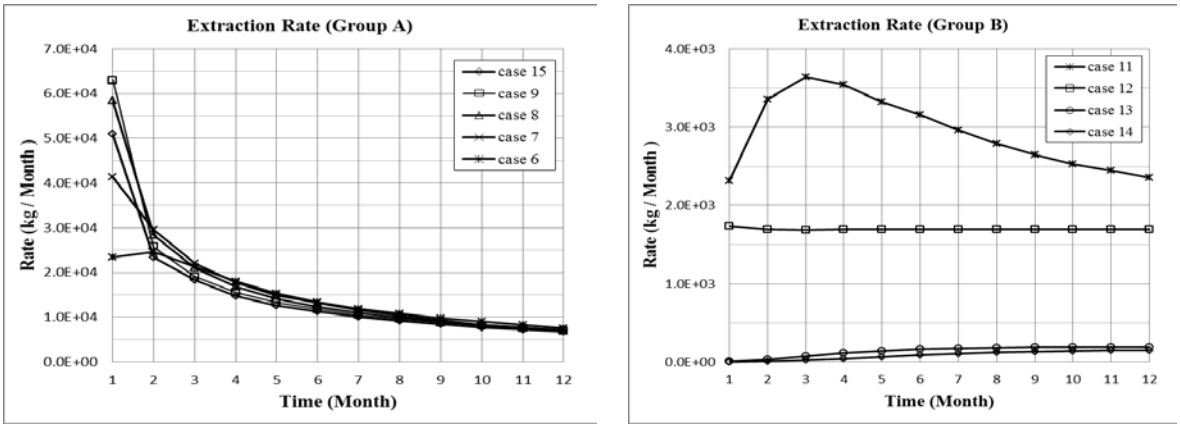

(A)群組 A 整治速率對時間之變化　　(B) 群組 B 整治速率對時間之變化

圖 4-6　油品回收速率與時間之關係

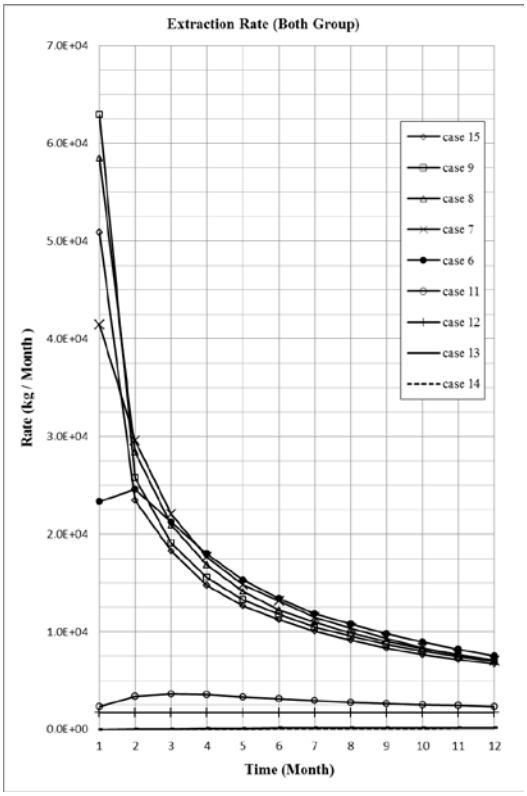

圖 4-7 群組 A 與群組 B 之整治速率比較

本研究透過設定的監測井（點）位置的水溶液相與蒸汽相苯濃度數據加以彙整，正如同在實體整治中利用監測井來進行觀測，以瞭解 TMVOC 模擬整治時對於水溶液相和蒸汽相中

有機污染物濃度降低的效果。四個監測點的位置如**圖 4-8** 所示，監測井與洩漏點之距離如**表 4-2** 所示。

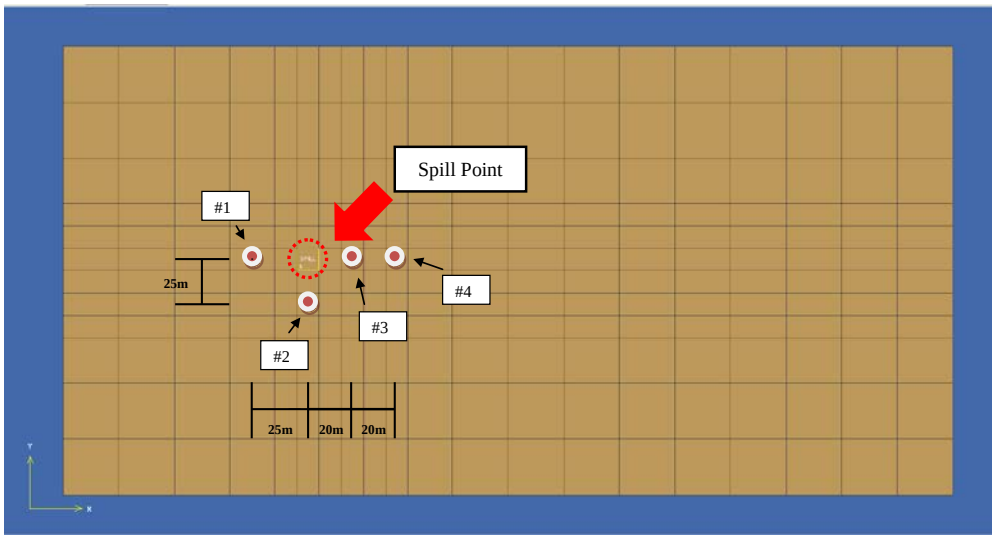

圖 4-8　假設之地下水監測井和土壤氣體監測點位置圖

表 4-2　監測點與洩漏點之距離

井編號	#1	#2	#3	#4
離洩漏點距離	25m	25m	20m	40m

整治效率較高的 A 組整治井在整治期間在水中的苯濃度和土壤氣體中的苯濃度如**圖 4-9** 所示。由於油品污染團本身的縮小，所以非飽和層土壤中苯蒸汽的濃度降低頗為快速。但是因為整個油品污染團在單一一口整治井的抽取下，在一年的整治期間後其所佔面積仍頗大，所以污染團上非飽和層的土壤仍有相當濃度的土壤氣體存在。這也和一般的油品污染場址實際的狀況相吻合。

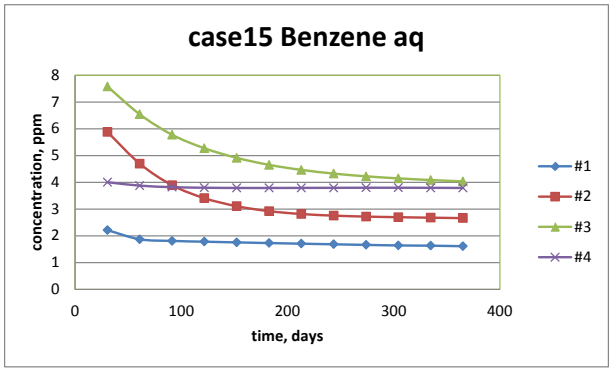

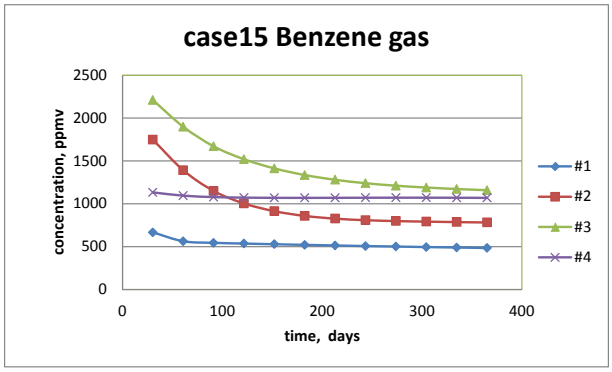

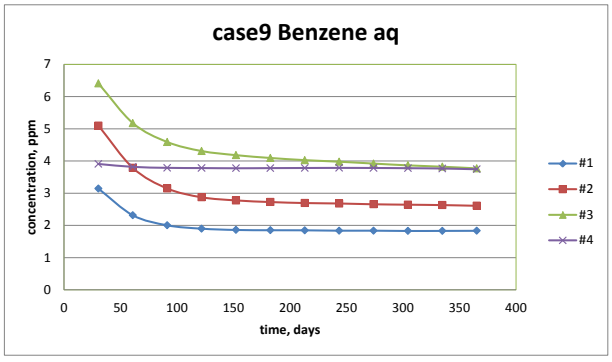

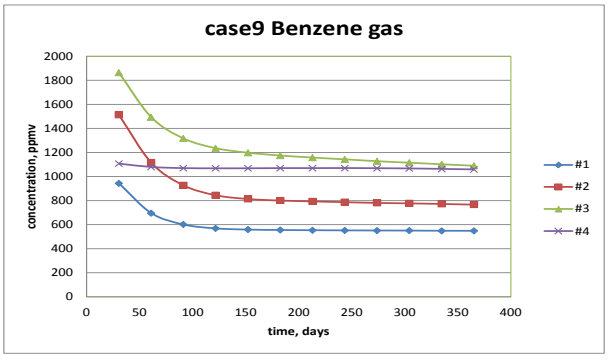

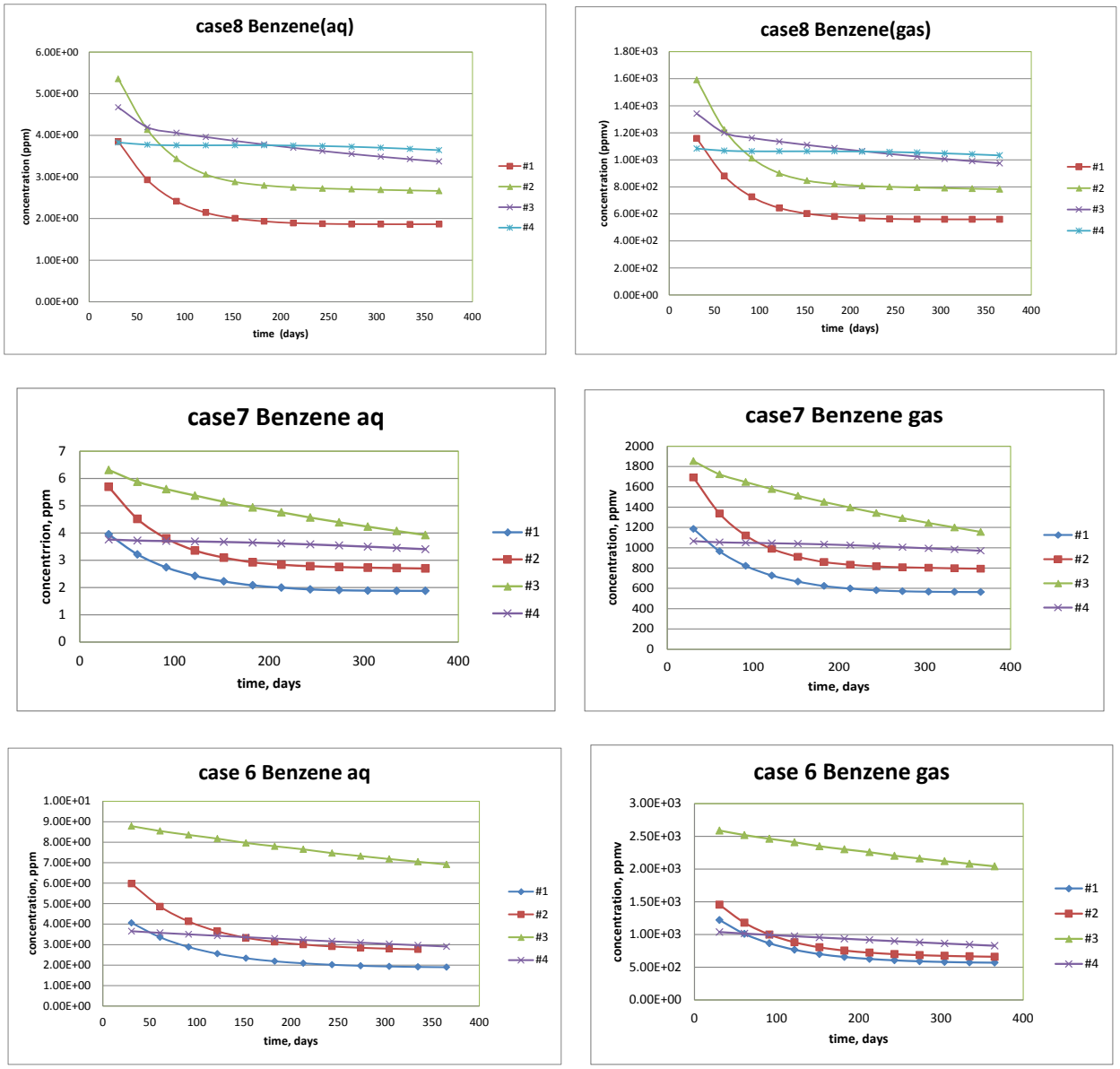

圖 4-9　各監測點位置地下水和土壤氣體中苯濃度隨時間的變化

4.3 孔隙率影響分析

若基本案例的孔隙率從 0.3 提高至 0.4，以相同洩漏速率模擬十年的場址洩漏，洩漏停止後以相同整治井設定進行同樣為期一年的整治，並將整治結果與孔隙率 0.3 者做比較。模擬結果顯示，較高孔隙率之場址在各個佈井距離的整治效率都比較低孔隙率者來得好。高孔隙率場址無論在效率、速率上皆表現較佳原因有二：①高孔隙率場址油品分佈集中。②高孔隙率場址相對滲透係數下降速度緩和。以下分別說明之。

較高孔隙率之場址（以下簡稱 BNN）在洩漏十年後場址內油品質量達到 1,422,901 kg，而較低孔隙率之場址(以下簡稱 LN) 總質量為 1,422,852 kg，兩者僅存在約萬分之四的誤差，可視為相等。但模擬結果顯示，BNN 油品分佈範圍較小。**圖 4-10** 為 BNN 與 LN 洩漏十年後，在高程-7 m（即地下 6 m）油品飽和度的分佈圖，而**圖 4-11** 為高程-7 m 之油品飽和度在 Y=105 m 之水平線的分佈。由此兩張圖可觀察到 BNN 之飽和度 0.01 範圍較 LN 小。

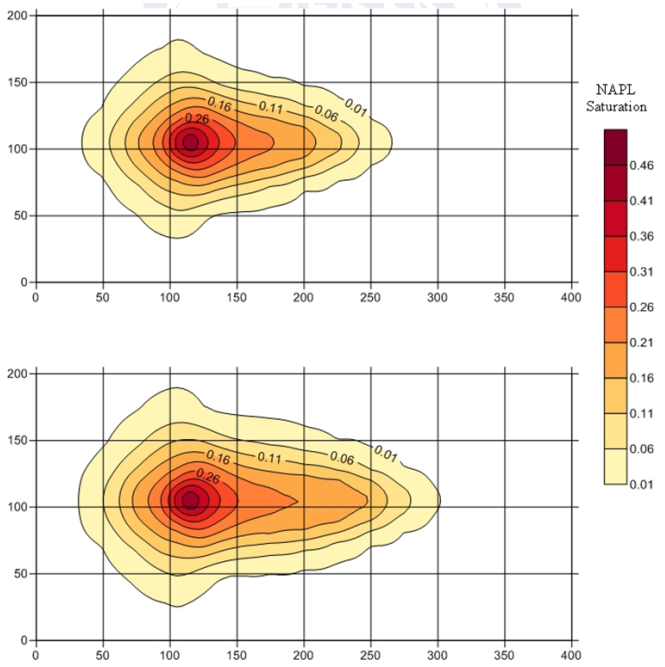

圖 4-10　Z=-7m 之油品飽和度分佈圖，上方為 BNN 場址，下方為 LN 場址

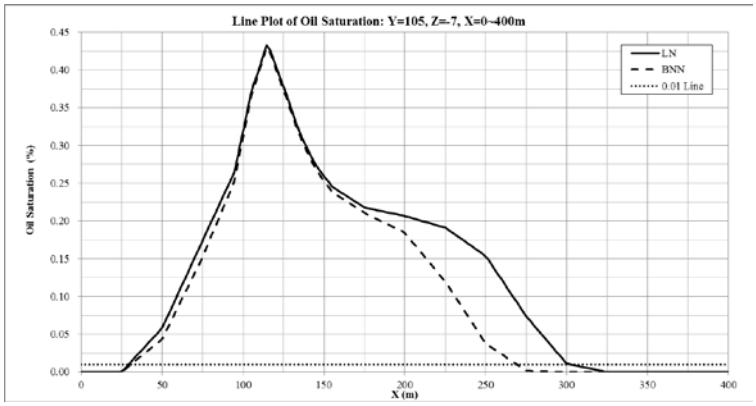

圖 4-11　Z=-7m 之油品飽和度 X 方向分佈圖

高孔隙率者在相同質量淨通量下，其飽和度降低的速度較低孔隙率者緩和。而較緩和的飽和度降低速度可讓流體之相對滲透係數得以在較長的時間區間內維持高數值。而高相對滲透係數對於井的抽取能力有正面幫助。綜合以上兩點可知，BNN 除了整治井抽取能力能可在較長時間區間中維持較高數值之外，在擷取區內亦分佈著較大量的油品。此即為 BNN 效率、速率較佳的原因。

BNN 整治量、整治百分比、一年後留於場址污之染物總量，三者隨佈井距離的變化趨勢和 LN 相同，如**圖 4-12(A)**、**圖 4-12(B)**、**圖 4-12(C)**所示。最高效率同樣發生在洩漏點下游 10 m，由此向兩側效率開始下降，且同樣在下游 77.5 m 之後變化程度趨緩。由圖上也可觀察到 BNN 無論在哪個距離佈井，其效率始終較 LN 好。

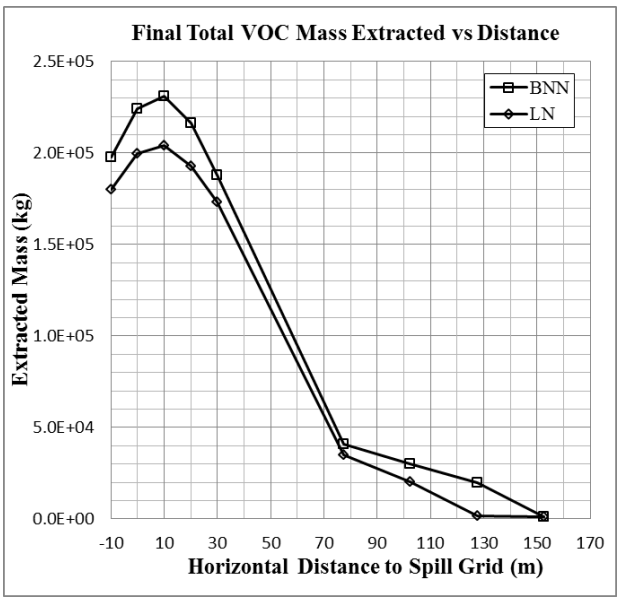

圖 4-12(A) n=0.3 與 0.4 油品整治量對佈井距離之變化

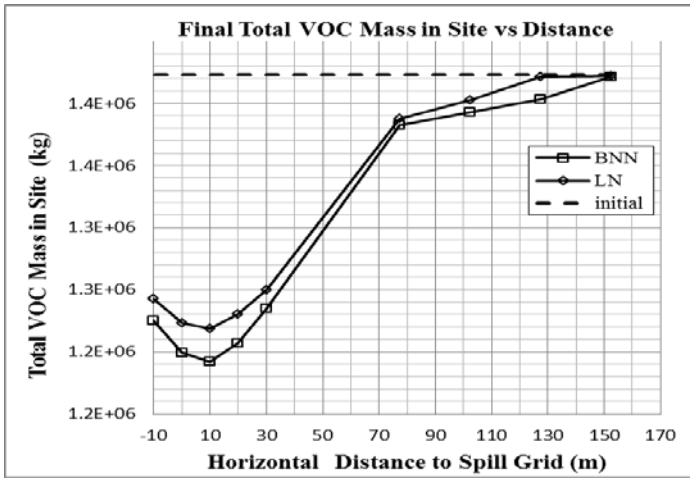

圖 4-12(B) n=0.3 與 0.4 整治一年後留在場址之油品總量對佈井距離之變化

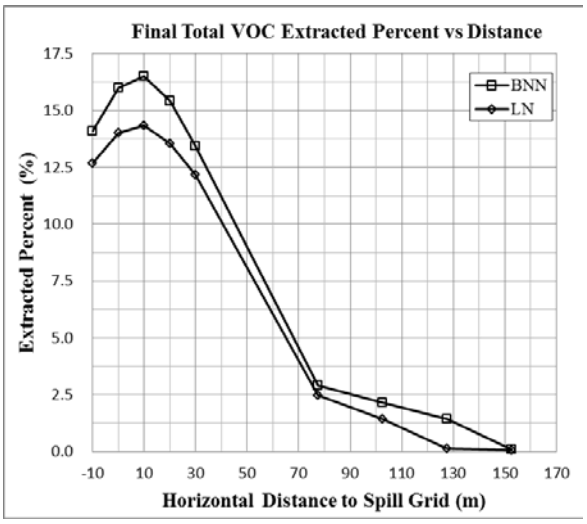

圖 4-12(C) n=0.3 與 n=0.4 油品整治百分比對佈井距離之變化

BNN 的群組 A（案例 15、9、8、7、6）中除了案例 6 以外，其餘案例在任意時間點整治速率皆較 LN 高，此可由**圖 4-13(A)**至 **4-13(E)**觀察到。由先前圖 4-8 可知，案例 6 佈井位置（X=140m）所在網格油品項飽和度，無論在 BNN 或是 LN 中皆無太大差別；即 BNN 或 LN

在案列 6 中整治井周遭的初始相對滲透係數並無太大差別，連帶使得井的出水能力相去不遠。但 BNN 由於孔隙率較大，整治井周邊油品飽和度上升得較 LN 慢，即相對滲透係數上升較慢，致使整治初期 LN 速率會比 BNN 來得高。

相對滲透係數在周邊環境制衡下，會有發展上限存在，當相對滲透係數發展至上限並且當油品質量通量無法再補足整治井抽除量後，整治井所在網格油品飽和度開始下降，伴隨飽和度下降的便是相對滲透係數下降，以及整治井抽取能力下降。由**圖 4-14** 可觀察到，LN 在一個月後以及 BNN 在兩個月後，整治井所在網格的相對滲透係數開始降低。而 BNN 因飽和度降低速度較緩和，在第二個月後油品相對滲透係數始終維持比 LN 高，因而讓 BNN 較 LN 有較佳的整治速率。

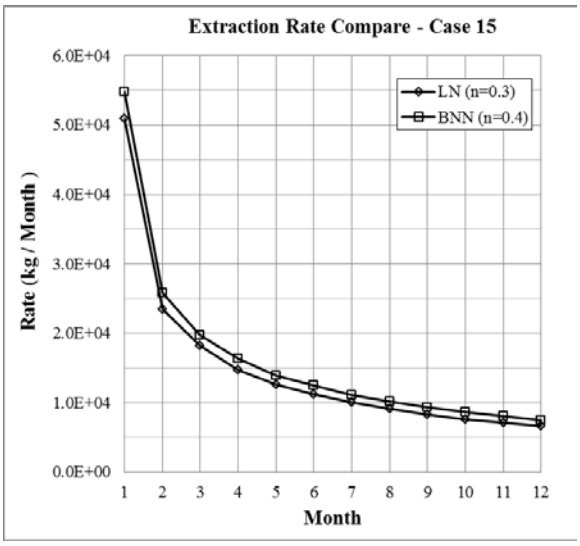

(A) 案例 15 整治速率比較

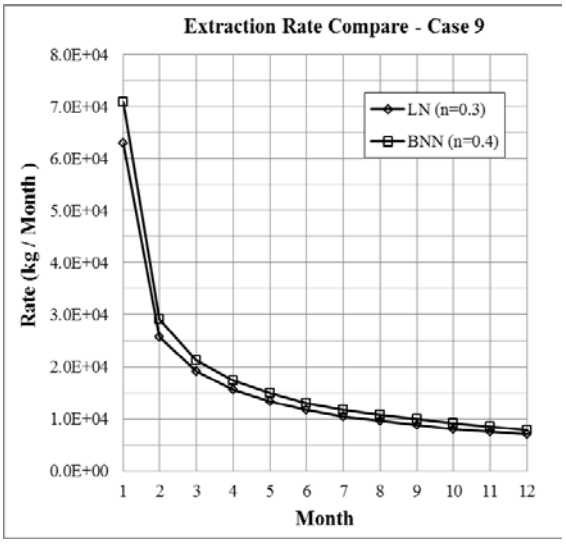

(B) 案例 9 整治速率比較

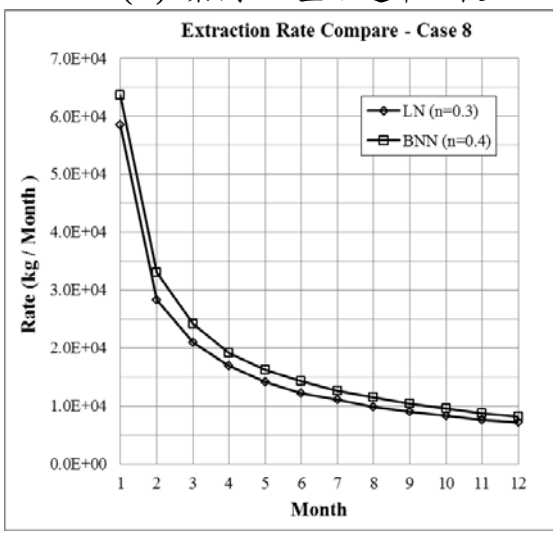

(C) 案例 8 整治速率比較

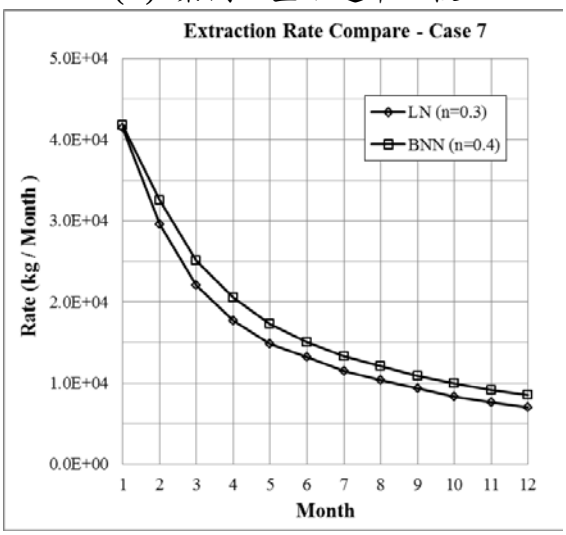

(D) 案例 7 整治速率比較

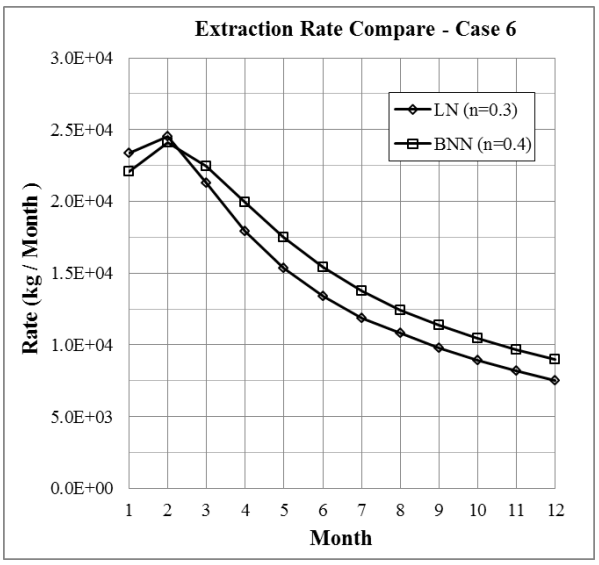

(E) 案例 6 整治速率比較

圖 4-13　n=0.3 與 n=0.4 整治速率比較

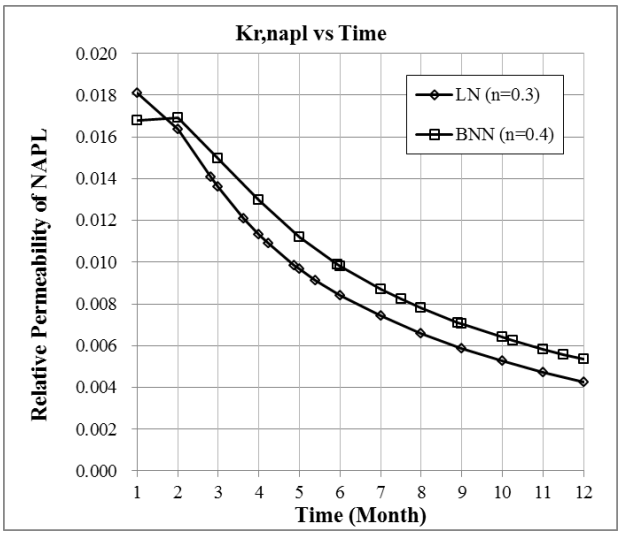

圖 4-14 n=0.3 與 n=0.4 案例 6 整治井所在網格油品相對滲透係數隨時間之變化

BNN 的群組 B（案例 11、12、13、14）整治速率與 LN 同樣複雜，且在某些案例中速率變化趨勢與原本的 LN 有所不同。BNN 案例 11 同樣先上升後下降，但初期速率較 LN 高，如圖 **4-15(A)**所示，整治速率最高達到每個月 6,243 kg。BNN 案例 12 整治速率未像 LN 案例 12 一樣持平，趨勢反而比較趨近案例 11 的先上升後下降，由**圖 4-15(B)**可觀察到 BNN 與 LN 在案例 12 整治速率上的明顯不同。由**圖 4-15(C)**可觀察到，BNN 案例 13 開始出現持平段，但在最末一個月速率忽然降低。水平段速率約維持在每個月 1,679 kg。此速率與 LN 案例 12 的持平速率相近（約每個月 1,700 kg），但中間的關聯性牽涉到兩整治井鄰近區域油品飽和度、相對滲透係數與壓力梯度的相互制衡，本研究中仍未找出確切原因。案例 14 則兩場址都有相同的趨勢（**圖 4-15(D)**），速率隨時間增大。

總體來看，高孔隙率之場址整治表現較好。群組 A 污染物整治量增加了 11%左右，群組 B 有著更大幅度的增加量。整治速率部分除了少數例子外，較高孔隙者在各個佈井距離與各個時間點上都取得較高的整治速率；群組 A 之穩定整治速率平均落在每個月 8,184 kg，為較低孔隙率者（每個月 7,069 kg）的 1.15 倍。

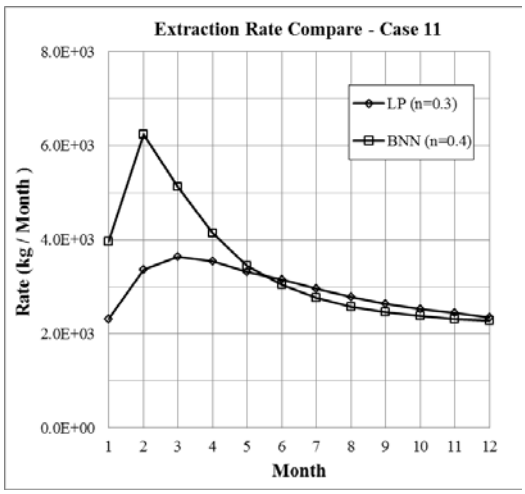

(A) 案例 11 整治速率比較

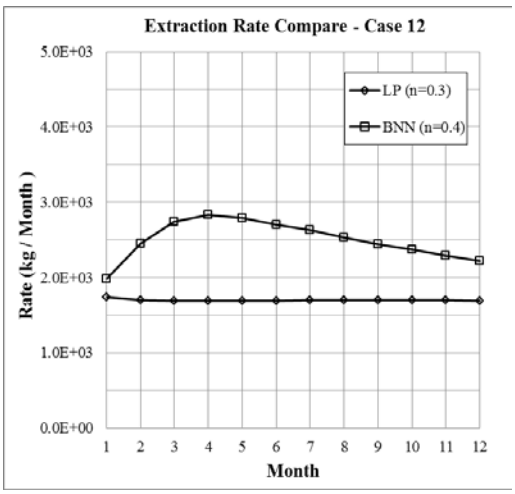

(B) 案例 12 整治速率比較

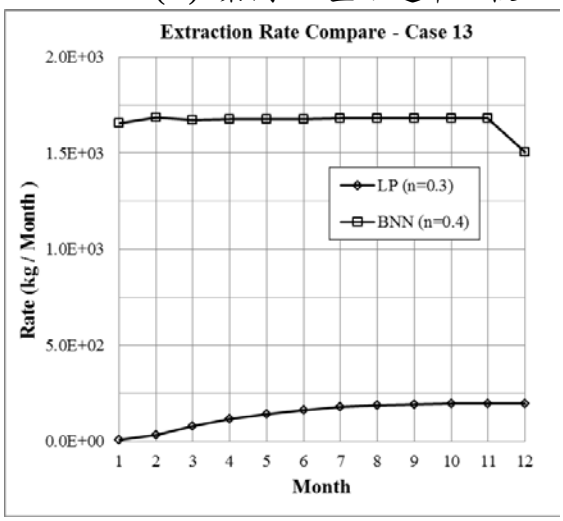

(C) 案例 13 整治速率比較

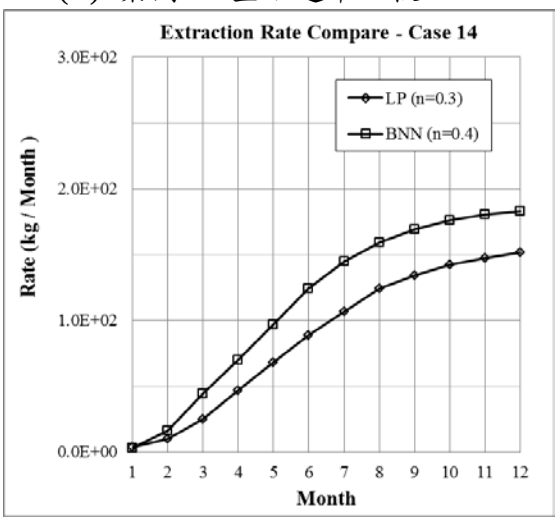

(D) 案例 14 整治速率比較

圖 4-15　n=0.3 與 n=0.4 整治速率比較

在 n=0.4 的條件下，監測點地下水中苯的濃度和土壤氣體中苯的濃度，與 n=0.3 的狀況自整治起始時就差異甚小。整治效率較高的 A 組整治井在整治期間在水中的苯濃度和土壤氣體中的苯濃度如**圖 4-6** 所示。只有 Case 6 與**圖 4-9** 中的 n=0.3 的狀況有稍微較明顯的差異。

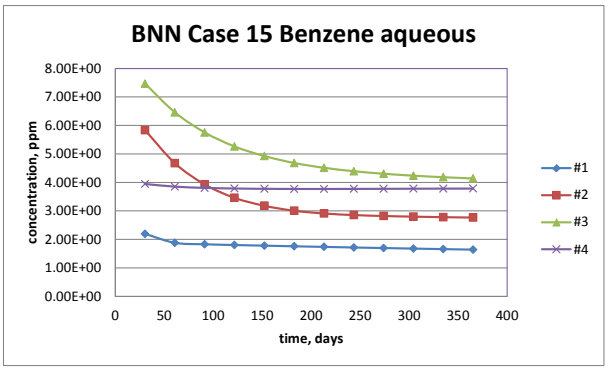

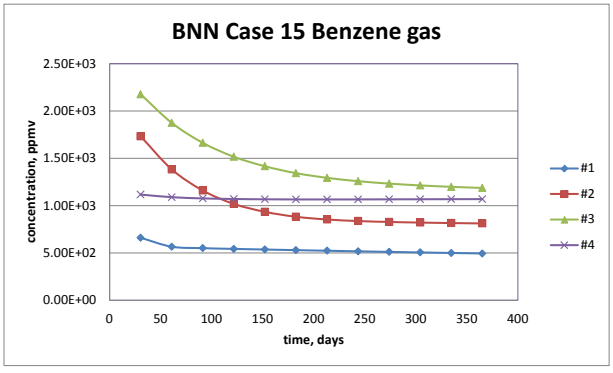

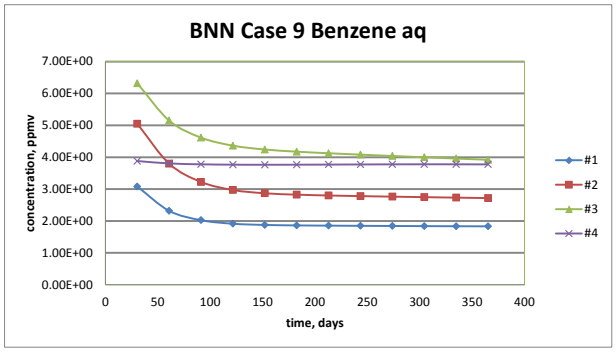

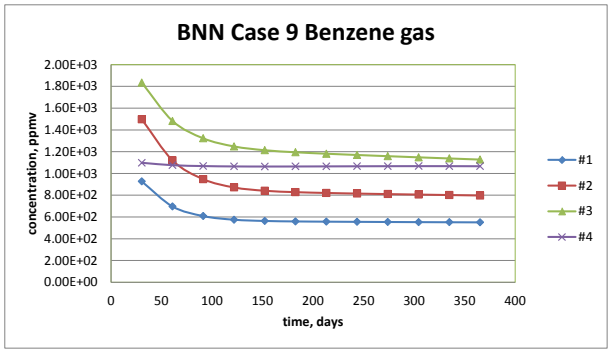

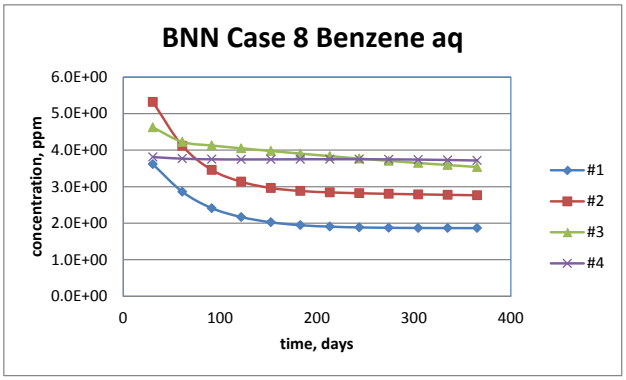

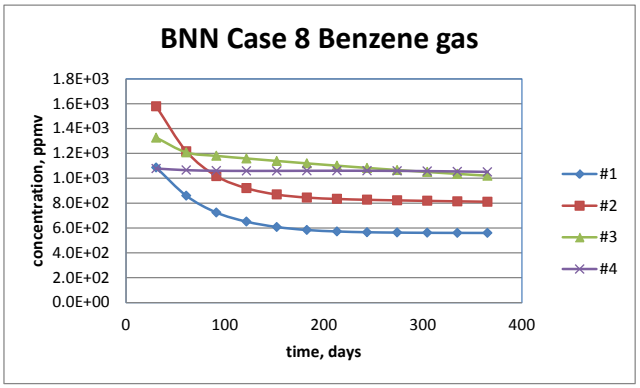

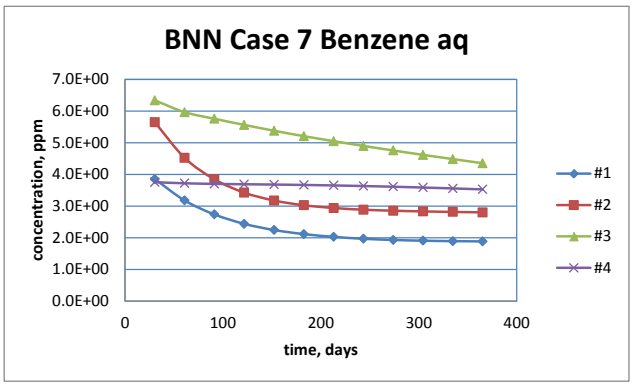

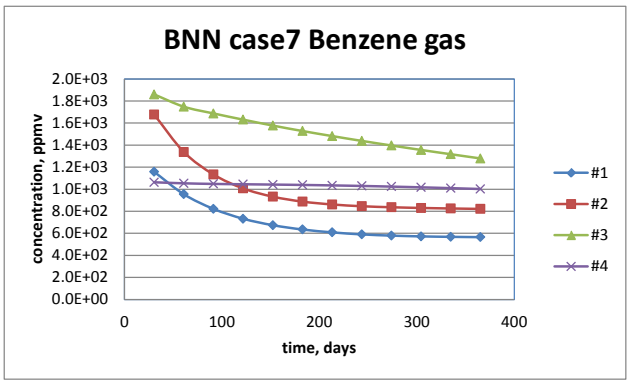

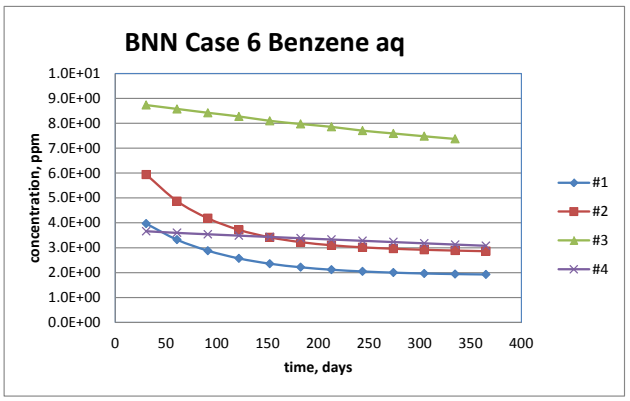

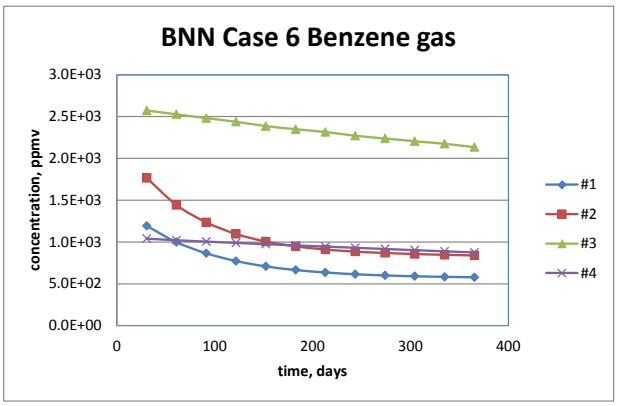

圖 4-16　n=0.4 各監測點位置地下水和土壤氣體中苯濃度隨時間的變化

4.4 壓力梯度影響分析

本研究中使用孔隙率 0.3 之洩漏場址，將整治井內的壓力調整為 44,246.2 Pa，使整治井與大氣（101,325 Pa）的壓差增大至 57,078.8 Pa，為 BNN 與 LN 的 5.04 倍，並以此壓力同樣進行為期一年的整治。在模擬過程中，受限於軟體所需模擬時間過長，有些案例甚至達到三個禮拜以上，本研究中唯一完成的只有案例 6 的比較。在案例 6 中，大壓差場址（以下簡稱為 HP）一年後的總整治量達到 25.3%，為 BNN 和 LN 的兩倍左右。**表 4-3** 為 HP 模擬結果與

LN 和 BNN 之比較。HP 在一年後，場址中殘留有 1,622,293 kg 的油品，較 BNN 和 LN 為低；油品整治量達到 360,559 kg，整治效率分別為 BNN 和 LN 的 1.92 倍以及 2.08 倍。

表 4-3　HP 模擬結果與比較

	LN	BNN	HP
Pressure in Well (Pa)	90,000.0	90,000.0	44,246.2
ΔP (to Atmosphere, Pa)	11,325.0	11,325.0	57,078.8
Porosity	0.3	0.4	0.3
Final total VOC Mass in Site after 1 Year (kg)	1,249,879	1,234,771	1,062,293
Mass of Total VOC Extracted (kg)	172,973	188,130	360,559
Percent of Total VOC Extracted (%)	12.16	13.22	25.34
Efficiency Ratio to LN	-	1.09	2.08
Efficiency Ratio to BNN	0.92	-	1.92
Efficiency Ratio to HP	0.48	0.52	-

本研究在 TMVOC 模擬過程中使用 Deliverability Model 來描述整治井的 sink 行為。此模式中使用一個生產力指標（Productivity Index, PI）以及井底壓力來形容 sink 的強度，PI 定義了孔隙介質在每單位壓差下每單位時間的出水量。對任意流體 β 有以下公式

$$S_\beta = \frac{k_{r,\beta}}{\mu_\beta}\rho_\beta \cdot PI \cdot \left(P_\beta - P_{wb}\right) \qquad (4.1)$$

式中 S_β 為 sink 強度、$K_{r,\beta}$ 為相對滲透係數、μ_β 為絕對粘滯力、ρ_β 為密度、PI 為生產力指標、P_β 為井周邊區域流體 β 的壓力、P_{wb} 為井底壓力。對於任意物質 K 其質量隨整治井抽出的速率，可用物質 K 在不同流體相中的濃度乘以該流體相之 sink 強度來加總，公式如下

$$S^K = \sum C_\beta^K \cdot S_\beta = \sum C_\beta^K \cdot \frac{k_{r,\beta}}{\mu_\beta}\rho_\beta \cdot PI \cdot \left(P_\beta - P_{wb}\right) \qquad (4.2)$$

式中 C 為物質 K 在流體 β 中的濃度。由公式可觀察到，若只對井底壓力做改變，則井底壓力與周邊網格的壓力差變化倍數，將恰為 sink 強度之變化倍數。在本研究中，壓差被加大到 5 倍，可預期 sink 強度將增為 5 倍，即整治量將為 5 倍。但模擬結果 HP 整治效率只分別為 BNN 的 1.92 倍與 LN 的 2.08 倍，sink 強度並未達到 5 倍。

整治速率可視為 sink 強度的平均值。由**圖 4-17** 可觀察到，HP 的整治速率

隨整治持續進行逐漸趨向 BNN 和 LN 的數值，從第一個月的每月 80,903 kg 經過五個月後降至每月 23,768 kg，最終降至每月 13,546 kg，此可說明 HP 的 sink 平均強度為一隨時間下降的函數。若將 HP 整治速率分別除 BNN 以及 LN 整治速率，來得到一倍率，則由**圖 4-18** 可觀察到 HP 的整治速率倍率有隨整治進行逐漸下降的趨勢；由最初的對 LN3.67 倍、對 BNN3.46 倍，經過七個月發展降為對 LN1.70 倍、對 BNN1.48 倍，自此維持在此一水平上。換句話說，HP 之 sink 強度平均值會向 BNN 以及 LN 的水平靠近，並在長時間發展後維持一穩定比例。

改變了井底壓力 P_{wb}，連帶得也改變了式中各項參數的發展。各參數的發展為一個互相牽制的複雜過程：改變井底壓力 P_{wb} 會使洩降錐改變並影響整治井周邊壓力 P_β 的發展，而 P_β 變化會使整治井周邊流體質量淨通量有所改變，從而讓相對滲透係數 $K_{r,\beta}$ 發展產生改變。$K_{r,\beta}$ 改變後又會反過來影響淨通量，連帶影響到 P_β 的發展。流體質量淨通量直接影響到物質濃度 C 變化速率，而濃度 C 直接影響了 sink 強度 S_β，另外濃度 C 又影響了流體 β 的密度與粘滯力。密度與粘滯力又會反過來影響淨通量及 sink 強度，又使濃度 C 變化速率改變。如以上所述，整治速率與整治效率的變化是一個綜合效應，非由單一參數的變化來決定。若探討 P_{wb} 對公式中各項參數的影響，再將參數變化與整治效率的變化綜合起來將過於複雜，本研究中只著墨於 P_{wb} 與整治效率的相關性。

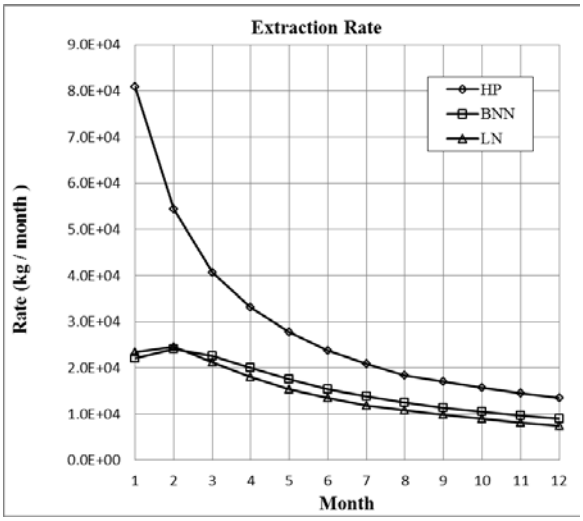

圖 4-17 整治速率隨時間變化之比較

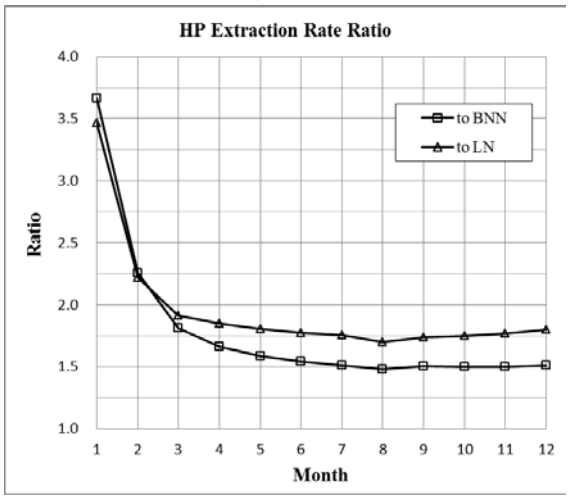

圖 4-18 速率倍率隨時間變化之比較

由**圖 4-19** 來看，以 Case 6 為例，提高整治井的壓力梯度後，監測點的地下水中苯濃度降低的幅度明顯提升，#1 與#3 都達到 2 ppm 以下、#3 也降低到 4 ppm 以下。在非飽和層的土壤中苯蒸汽濃度也較低，尤其是洩漏點下游的#3 差異較大。

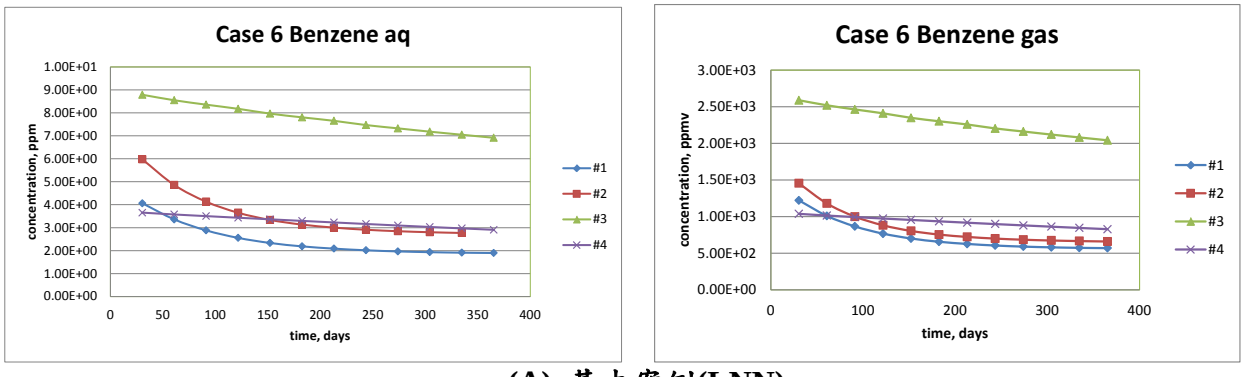

(A) 基本案例(LNN)

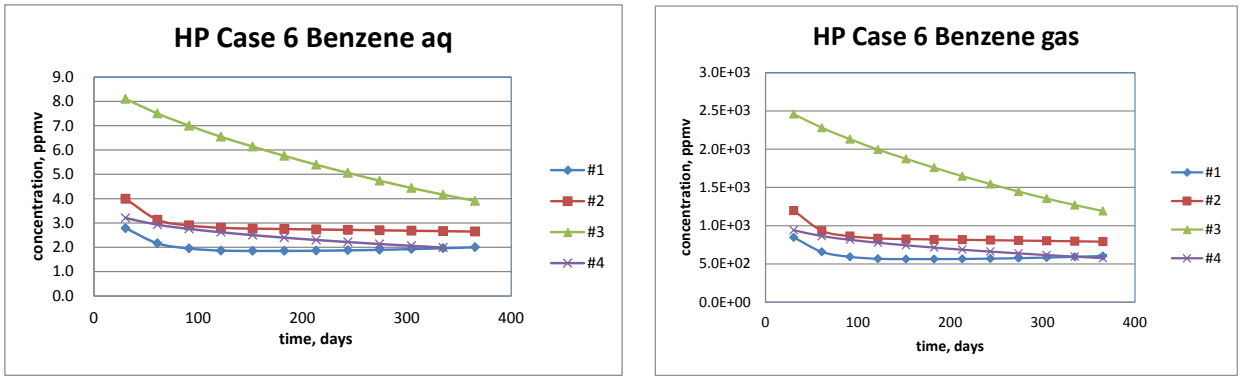

(B) 提高壓力梯度(HP)

圖 4-19　改變整治井壓力梯度監測點位置地下水和土壤氣體中苯濃度隨時間的變化

受限於本研究中只成功模擬出案例 6 在 5 倍壓力梯度下的整治模擬，沒有足夠數據將 P_{wb} 與整治效率做統計回歸，在此只對此成功案例做數值上的分析，分析結果如下：

I. 整治效率與 P_{wb} 引致之壓力梯度之間並非線性地成正比，但具有正相關性。5 倍壓力梯度下整治效率只上升為 2 倍左右。

II. P_{wb} 的下降在第一個月對整治速率會有最大的影響，第一個月過後整治速率的倍增率開始減少，並在約 6 個月後維持在一定水平。5 倍壓力梯度下可讓 6 個月後整治速率倍增率達到 1.5 倍（BNN）與 1.75 倍（LN）。

III. 同個佈井位置在加大井底壓力後，其整治速率隨時間變化的特性可能改變。在 **圖 4-17** 中，HP 之曲線速率持續降低，與 BNN 和 LN 的先上升後下降有所區別。

五、結論

本研究成功地以 TMVOC 模擬 MPE 整治。本研究針對 400 m×200 m×16 m，恆溫 25°C 砂質含水層模擬油品洩漏，洩漏品為汽油，洩漏量每日 0.5 m^3，洩漏時間 10 年。洩漏 10 年後以井底壓力 90,000 Pa（約 1.15 m 水頭差）之整治井進行整治模擬，模擬過程中允許油、水、汽等三相流體被抽出以便模擬多相抽除。根據佈井位置不同最高可回收 14.33%油品，而最高效率井在第 3 個月便達成 7.58%回收率，約為總回收量的一半。整治效率會隨時間降低，最高效率井在第 6 個月達成總回收量的 75%，三個月內抽出 3%油品；在第 9 個月達成總回收量的 90%，三個月內抽出 2.14%油品；而在最末 3 個月只抽出了 1.58%的油品。整治速率有隨時間下降之趨勢。

本研究中首先將佈井位置作為變數，在相同的污染場址及整治井抽取能力下，探討不同佈井位置的整治效率。模擬結果顯示，於洩漏點稍偏下游處佈井可以取得最大的整治效率，在此點之上游或是下游佈井整治效率將下降。整體來說，在洩漏點上游 10 m 至下游 30 m 範圍內佈井，整治效率都可達到 11%以上。整治速率部分，根據佈井距離不同可區分為 A、B 兩群組。佈井接近洩漏點的 A 群組其速率變化循一定規律，且一年後整治速率都將收斂至近似的數字；佈井較遠離洩漏點的 B 群組速率變化複雜，且速率比前者小了 1 至 3 個數量級。

後續本研究將基本案例的孔隙率從 0.3 上修至 0.4，以相同洩漏條件與整治條件進行模擬，並將整治結果與孔隙率 0.3 者做比較。模擬結果顯示，較高孔隙率之場址在各個佈井距離的整治效率都比較低孔隙率者來得好。群組 A 污染物整治量增加了 11%左右，而群組 B 有著更大幅度的增加量。整治速率部分除了少數例子外，較高孔隙者在各個佈井距離與各個時間點上都取得較高的整治速率；群組 A 之穩定整治速率平均落在每個月 8,184 kg，為較低孔隙率者（每個月 7,069 kg）的 1.15 倍。

最後，本研究改變整治井內的壓力，使其與大氣之間壓差增大至基本案例的 5.04 倍，並進行整治模擬。在唯一完成的案例 6 比較中，大壓差場址一年後總整治量達到 25.3%，約為

基本案例之兩倍。整治速率在第一個月達高峰，約為基本案例 3.5 倍，之後隨時間逐漸降低至 1.6 倍。

綜合以上所述，佈井於洩漏點稍偏下游處可取得最大整治效率，而大孔隙率場址又可取得較好的整治效率。遠離洩漏點（下游 77.5 公尺之後）的整治井整治效率不佳，只有高效率區的 0.5 至 0.1 倍，佈井位置若遠離洩漏點則 MPE 整治效率將大打折扣，此時可嘗試尋求其他整治方法。整治井壓力梯度變化與整治效率變化並非線性成正比，但具正相關性。加強井底負壓對各個時間階段的整治速率皆有正面幫助。但是加強負壓的助益僅在整治初期最明顯，其後隨整治持續進行助益逐漸減少。

參考文獻

行政院環保署，油品類儲槽系統土壤及地下水污染調查、驗證作業及整治工作等技術規範建置計畫期末報告，附冊七，油品類儲槽系統土壤及地下水污染整治技術選取、系統設計要點與注意事項參考手冊，2006。

陳文福，2005，台灣的地下水，遠足文化。

陳培旼，2010，加油站土壤氣體及地下水監測模擬，碩士論文，國立交通大學。

陳華清、李義連，2009，淺層地下水 PCE/TCE 污染原位曝汽修復模擬研究，理論學與技術，第 32 卷，第 11 期，第 53-57 頁。

陳維良，2007，定流量非水量液體於土壤中之滲流分析，碩士論文，國立交通大學。

單信瑜、陳培旼，2011，加油站儲槽與管線滲漏模擬，第十五屆土壤與地下水污染整治研討會，台北，2011年6月29日

單信瑜、陳培旼、楊凱仁，2011，加油站滲漏監測有效性評估，第 14 屆大地工程研討會，桃園，2011 年 8 月 25-26 日

楊凱仁，2012，水位波動對地下儲油槽洩漏之影響，碩士論文，國立交通大學。

經濟部工業局，2007，土壤及地下水污染預防手冊。

經濟部工業局，2009，石油碳氫化合物 土壤及地下水污染預防與整治技術手冊。

經濟部工業局，土壤及地下水污染整治技術手冊－評估調查及監測，2004。

經濟部水利署，2010，水利統計。

經濟部能源委員會，加油站漏油檢測作業程序參考手冊，2003。

龍元祥，2004，含非水量液體土壤之透水性，碩士論文，國立交通大學。

顏伯穎，2002，應用數值方法模擬地下水空氣注入法整治受非水相污染區域之研究，碩士論文，國立成功大學。

Adamski, M., Kremesec, V., Kolhatkar, R., Pearson, C., Rowan, B., 2005, “LNAPL in finegrained soils: conceptualization of saturation, distribution, recovery and their modeling,” *Ground Water Monitoring and Remediation*, Volume 25, No. 1, pp.100–112.

Air Force Center for Environmental Excellence, 1994, “Technology Profile: Vacuum-Mediated LNAPL Free Product Recovery/Bioremediation(Bioslurper),” Issue 1, March, 1994.

API (American Petroleum Institute). 1989. Guide to the Assessment and Remediation of Underground Petroleum Releases, 2nd ed. API Publication 1628, Washington, DC: API.

API, A Guide to the Assessment and Remediation of Underground Petroleum Releases, Third Edition, API Publication 1628, Washington, D.C.，1996.

Bailey, W.M., Schneider, A. (1998). Enhanced Fuel Oil Recovery Using Steam Injection and Dual Phase Vacuum Extraction at a Paper Recycling Facility in Dublin, Georgia. Proceedings of TAPPI Environmental Conference and Exhibit, Vancouver, Canada, April 5–8, 1998, pp. 745–746.

Baker, R. S. 1995. One-, two-, and three-phase flow during free product recovery. In: Applied Bioremediation of Hydrocarbons, Hinchee, R. E., J. A. Kittel, and H. J. Reisinger (eds.). Columbus, OH: Battelle Press, 349–359.

Baker, R. S., and J. Bierschenk. 1995. Vacuum-enhanced recovery of water and NAPL: Concept and field test. Journal of Soil Contamination 4(1):57–76.

Baker, R. S., and J. Bierschenk. 1996. Bioslurping LNAPL contamination. Pollution Engineering March:38–40.

Battistelli, A.,2008 , "Modeling Multiphase Organic Spills in Coastal Sites with TMVOC V.2.0," *Vadose Zone Journal*, Volume 7, pp.316-324.

Beckett, G.D., and Huntley, D., 1998, "Soil Properties and Design Factors Influencing Free-Phase Hydrocarbon Cleanup," *Environment Science and Technology*, Volume 32, pp. 287-293.

Blake, S. B., and M. M. Gates. 1986. Vacuum-enhanced hydrocarbon recovery: A case study. Proceedings: Petroleum Hydrocarbons and Organic Chemicals in Ground Water. Houston, TX, November 1986. NGWA/API, Dublin, OH, 709–721.

Campagnolo, J.F., Akgerman, A., 1995. Modeling of soil vapor extraction (SVE) systems – part II, biodegradation aspects of soil vapor extraction. Waste Management 15, 391–397.

Charbeneall, 2006, "Groundwater Hydraulics and Pollutant Transport," Waveland Press Inc., 4180 IL: Route 83, Suite 101, Long Grove, IL 60047-9580, USA.

Charbeneau, R. J., N. Wanakule, C. Y. Chiang, J. P. Nevin, and C. L. Klein. 1989. A two-layer model to simulate floating free product recovery: Formulation and applications. In: Proc. Conf. on Petroleum Hydrocarbons and Organic Chemicals in Ground Water: Prevention, Detection, and Restoration. Dublin, OH: Natl. Ground Water Assoc., 333–345.

Charbeneau, R.J., 2007, "LNAPL Distribution and Recovery Model," Distribution and Recovery of Petroleum Hydrocarbon Liquids in Porous Media, Volume 1, API Publication 4760. API Publications, Washington, DC.

Charbeneau, R.J., Beckett, G.D., 2007, "LNAPL Distribution and Recovery Model," User and Parameter Selection Guide, Volume 2. API Publication 4760. Publications, Washington, DC.

Charbeneau, R.J., Chiang, C.Y., 1995. Estimation of free hydrocarbon recovery from dual-pump systems. Ground Water 33 (4), 627–634.

Charbeneau, R.J., Johns, R.T., Lake, L.W., McAdams, M.J., 1999. Free-product Recovery of Petroleum Hydrocarbon Liquids. API Publication 4682. API Publications, Washington, DC.

Charbeneau, R.J., Johns, R.T., Lake, L.W., McAdams, M.J., 2000, "Free-product recovery of petroleum hydrocarbon liquids," *Ground Water Monitoring and Remediation*, Volume 20, pp.147-168.

Chevalier, L.R., 2003. Surfactant dissolution andmobilization of LNAPL contaminants in aquifers. Environmental Monitoring and Assessment 84, 19–33.

Erning, K., Schäfer, D., Dahmke, A., Luciano, A., Viotti, P. and Papini, M.P., 2009, "Simulation of DNAPL Infiltration into Groundwater with Differing Flow Velocities Using TMVOC Combined with Petrasim," *Proceedings of the TOUGH Symposium 2009*, Lawrence Berkeley National Laboratory, Berkeley, September 14-16, 2009

Farr, A.M., Houghtalen, R.J., McWhorter, D.B., 1990. Volume estimation of light nonaqueous phase liquids in porous media. Ground Water 28 (1), 48.

Fetter, C.W., 1999, "Contaminant Hydrogeology," 2nd Edition, Prentice-Hall Inc., Upper Saddle River, New Jersey 07458, USA.

Fetter, C.W., 2001, "Applied Hydrogeology," 4th Edition, Prentice-Hall Inc., Upper Saddle River, New Jersey 07458, USA.

Fredlund, D.G. and Xing, A., 1994, "Equations for the soil-water characteristic curve," *Canadian Geotechnical Journal*, Volume 31, No. 3, pp. 521-532.

Gerhard, J.I., Kueper, B.H., Hecox, G.R., Schwarz, E.J., 2001. Site-specific design for dual phase recovery and stabilization of pooled DNAPL. Ground Water Monitoringand Remediation 21, 71–88.

Grant S. Cooper, Jr.“, Richard C. Peralta, Jagath J. Kaluarachchi, 1995, “Stepwise pumping approach to improve free phase light hydrocarbon recovery from unconfined aquifers,” *Journal of Contaminant Hydrology*, Volume 18 (1995), pp. 141-159.

Gustafson, J.B., Tell, J.G. and Orem, D., 1997 , “Selection of Representative TPH Fraction Based on Fate and Transport Consideration,” Total Petroleum Hydrocarbon Criteria Working Group Series, Volume 3, Amherst Scientist Publisher, Massachusetts.

Hayes, D., E. C. Henry, and S. M. Testa. 1989. A practical approach to shallow hydrocarbon recovery. Ground Water Monitoring Review Winter:180–185.

Hoeppel, R., M.C. Place, C.T. Coonfare, S.H. Rosansky. 1998. Application Guide for Bioslurping, Vols. I and II. Tech. Memo. TM-2300-ENV and TM-2301-ENV. Naval Facilities Engineering Service Center, Port Hueneme, CA

Huyakorn, P. S.; Panday, S.; and Wu, Y. S. J. Contam. Hydrol. 1994, 16, 109-130.

Jennings, A.A., Patil, P., 2002. Feasibility modeling of passive soil vapor extraction. Journal of Environmental Engineering and Science 1, 157–172.

Kaluarachchi, J. K., and Elliott, R. T., 1995, Design Factors for Improving the Efficiency of Free-Product Recovery Systems in Unconfined Aquifers, Vol. 33, No. 6, Ground Water, November-December, 1995

Kererat, C. and Soralump, S., 2010, “Modeling of Organic Contaminant Migration through Soil Cement Barrier Using TMVOC,” *The 17th Southeast Asian Geotechnical Conference*, Taipei, Taiwan.

Kirshner, M., Pressly, N.C., Roth, R.J., 1996. In situ remediation of jet A in soil and groundwater by high vacuum dual phase extraction. Ground Water Monitoring and Remediation 16, 73–79.

Kittel, J.A., R.E. Hinchee, R. Hoeppel, and R. Miller. “ Bioslurping -vacuum enhanced free product recovery coupled with bioventing: A case study Petroleum Hydrocarbons and Organic Chemicals in Groundwater: Prevention, Detection, and Remediation, 1994 NGWA/API Conference Proceedings, Houston, TX, 1994.

Lamarre, M.A., Foster, T.D., Lucas, D.H., 1997. Dual phase (‘‘Hi-Vac’’) extraction: an effective remediation alternative for enigmatic geologic conditions (case studies). Contaminated Soils 2, 317–338.

Lenhard, R.J., Parker, J.C., 1990, “Estimation of free hydrocarbon volume from fluid levels in monitoring wells,” *Ground Water*, Volume 28, Issue 1, pp. 57–67.

Li, J.B., Huang, G.H., Chakma, A., Zeng, G.M., 2003a, “Numerical simulation of dual phase vacuum extraction to remove non-aqueous phase liquids in subsurface,” *Practice Periodical of Hazardous, Toxic, and Radioactive Waste Management (ASCE)*, Volume 7, pp. 106–113.

M. Th. Van Genuchten, 1980, ”A Closed-form Equation for Predicting the Hydraulic Conductivity of Unsaturated Soils,” *Soil Science Society of America Journal*, Volume 44, No.5 pp. 894-898.

MAGNAS3. HydroGeoLogic, Inc., Herndon, VA, 1992.

Mihopoulos, P.G., Suidan, M.T., Sayles, G.D., 2000. Vapor phase treatment of PCE by lab-scale anaerobic bioventing. Water Research 34, 3231–3237.

Mihopoulos, P.G., Suidan, M.T., Sayles, G.D., 2001. Complete remediation of PCE contaminated unsaturated soils by sequential anaerobic-aerobic bioventing.Water Science and Technology 43, 365–372.

Mihopoulos, P.G., Suidan, M.T., Sayles, G.D., Kaskassian, S., 2002. Numerical modeling of oxygen exclusion experiments of anaerobic bioventing. Journal of Contaminant Hydrology 58, 209–220.

Nadim, F., Hoag, G.E., Liu, S., Carley, R.J., Zack, P., 2000. Detection and remediation of soil and aquifer systems contaminated with petroleum products: an overview.Journal of Petroleum Science and

Engineering 26, 169–178.

Nelson, L., Barker, J., Li, T., Thomson, N., Ioannidis, M., Chatzis, J., 2009. A field trial to assess the performance of CO2-supersaturated water injection for residual volatile LNAPL recovery. Journal of Contaminant Hydrology 109, 82–90.

O'Melia, B.C., Parson, D.R., 1996. Dual-phase vacuum extraction technology for soil and ground-water remediation: a case study. In: Wang, W., Schnoor, J., Doi, J. (Eds.), Volatile Organic Compounds in the Environment (ASTM STP 1261). American Society for Testing and Materials, pp. 272–286.

Panday, S.; Wu, Y. S.; Huyakorn, P. S.; Springer, E. P. J. Contam. Hydrol. 1994, 16, 131-156.

Parker, J.C., Zhu, J.L., Johnson, T.G., Kremesec, V.J., Hockman, E.L., 1994, "Modeling free product migration and recovery at hydrocarbon spill sites," *Ground Water*, Volume 32, pp. 119–128.

Peargin, T.R., Wickland, D.C., Beckett, G.D., 1999, "Evaluation of Short Term Multi-phase Extraction Effectiveness for Removal of Non-Aqueous Phase Liquids from Groundwater Monitoring Wells," *Conference Proceedings of the 1999 Petroleum Hydrocarbons & Organic Chemicals in Ground Water*, Houston, Texas, sponsored by the National Ground Water Association & American Petroleum Institute.

PetraSim 5, 2008, "PetraSim User Manual," Thunderhead Engineering, Manhattan, USA.

Place, M., C.T. Coonfare, A.S.C. Chen, R.E. Hoeppel, S.H. Rosinsky. 2001. Principles and Practices of Bioslurping. Battelle Press, Columbus, OH.

PolinFg, B.E., Prausnitz, J.M. and O'Connell, J.P., 2001, "The properties of Gases and Liquids," 5th Edition, McGraw-Hill Companies, USA.

Pruess, K. and Battistelli, A., 2002, "TMVOC User's Guide," Lawrence Berkeley National Laboratory, Berkeley.

Pruess, K., Oldenbug, C. and Moridis, G., 1999, "TOUGH2 User's Guide Version 2.0," Earth Sciences Division, Lawrence Berkeley National Laboratory, Berkeley.

Rasmusson, K., and M. Rasmusson, 2009, NAPL spill modeling and simulation of pumping remediation, Master Thesis, Department of Earth Sciences, Air, Water and Landscape Science, Uppsala University, Villavägen 16, SE-752 36 Uppsala Sweden. ISSN 1401-5765

Roth, R.J., Kirshner, M., Chen, H.Y., Frumer, B., 1999. High vacuum dual phase extraction wells remediating jet-fuel contaminated soil and groundwater at JFK International Airport. Contaminated Soils 4, 59–66.

Shaw, D.G. and Maczynski, A., 2005, "IUPAC-NIST Solubility Data Series. 81. Hydrocarbons with Water and Seawater Revised and Updated. Part 7. C8H12–C8H18 Hydrocarbons," *Journal of Physical and Chemical Reference Data*, Volume 34, No. 4, pp. 2261-2298.

Suthersan, S.S. Remediation Engineering: Design Concepts. CRC Press, Inc., 1997

U.S. Army Corps of Engineers. Engineer Manual. Multi-Phase Extraction, Engineering and Design. EM 1110-1-4010. June 1999.

U.S. Environmental Protection Agency. Analysis of Selected Enhancements for Soil Vapor Extraction. EPA-542-R-97-007. September, 1997b.

U.S. Environmental Protection Agency. Cleaning Up the Nation's Waste Sites: Markets and Technology Trends; 1996 Edition. EPA 542-R-96-005. April, 1997a.

U.S. Environmental Protection Agency. EPA REACH IT database, 1998. URL <http://www.epareachit.org>

U.S. Environmental Protection Agency. Presumptive Remedy: Supplemental Bulletin Multiphase Extraction (MPE) Technology for VOCs in Soil and Groundwater. EPA 540-F-97-004. April, 1997c.

U.S. EPA, Record of Decision (Amended), Tinkham's Garage, NH. EPA/ROD/R01-89/046. March 10, 1989.

U.S. Geological Survey. “Ground-Water Contamination and Movement at the Defense General Supply Center”, Richmond, Virginia, U.S. Geological Survey, Water- Resources Investigations Report 90-4113, 1990.

US Army Corps of Engineers, 1999, “Engineering and Design Multi-Phase Extraction,” Washington, DC 20314-1000, USA.

US Environmental Protection Agency, 1996, “How to Effectively Recover Free Product at Leaking Underground Tank Sites,” OSWER National Risk Management Research Laboratory, ORD, USA.

US Environmental Protection Agency, 1998, “MTBE Fact Sheet #2: Remediation of MTBE Contaminated Soil and Groundwater”, Washington, D.C., USA.

US EPA, 2005, ”Cost and Performance Report for LNAPL Characterization and Remediation. Multi-phase Extraction and Dual-pump Recovery of LNAPL at the BP Former Amoco Refinery,” Sugar Creek, MO. Office of Solid Waste and Emergency Response, EPA 542-R-05-016, US EPA.

USEPA, “Field Applications of In Situ Remediation Technologies: Ground-Water Circulation Wells”, (EPA-542-R-98-009), October 1998.

USEPA, 1997. Guiding Principles for Monte Carlo analysis, Risk Assessment Forum, U.S. Environmental Protection Agency, Washington, DC, USA, pp. 35.

USEPA, 2001. Abstracts of Remediation Case Studies (Vol. 5), U.S.. Environmental Protection Agency, Washington, DC, USA.

USEPA, How to Evaluate Alternative Cleanup Technologies for Underground Storage Tank Sites-A Guide for Corrective Action Plan Reviewers (EPA 510-B-94-003)，2004.

Vaughn, S.C., Turner, J.C. (2001). Dual-phase Extraction in South Texas Using the RSI S.A.V.E. System. Proceedings of Petroleum Hydrocarbons and Organic Chemicals in Ground Water: Prevention, Assessment and Remediation Conference and Workshops, Houston, TX, USA, pp. 166–172.

Waddill, D.W. and Parker, J.C., 1997a., “A semianalytical model to predict recovery of light, nonaqueous phase liquids from unconfined aquifers. *Ground Water*, Volume 35, pp. 280–290.

Waddill, D.W., Parker, J.C., 1997b. Simulated recovery of light, nonaqueous phase liquid from unconfined heterogeneous aquifers. Ground Water 35, 938–947.

Weaver, J. W., Charbeneau, R. J, Tauxe, J. D., Lien, B. K., and J. B. Provost, 1994, The Hydrocarbon Spill Screening Model (HSSM) Volume 1: User's Guide, EPA/600/R-94/039a

Wickramanayake, G.B., J.A. Kittel, M.C. Place, R. Hoeppel, A. Walker, E. Drescher, J.T. Gibbs. 1996. Best Practices Manual for Bioslurping. Tech. Memo. TM-2191-ENV. Naval Facilities Engineering Service Center, Port Hueneme, CA.

Yen, H.K. and Chang, N.B., 2003, “ Bioslurping model for assessing light hydrocarbon recovery in contaminated unconfined aquifer. II: optimization analysis,” *Practice Periodical of Hazardous, Toxic, and radioactive Waste Management*, Volume 7, pp. 131–138.

Yen, H.K., Chang, N.B., Lin, T.F., 2003, “Bioslurping model for assessing light hydrocarbon recovery in contaminated unconfined aquifer. I: simulation analysis,” *Practice Periodical of Hazardous, Toxic, and radioactive Waste Management*, Volume 7, pp. 114–130.

Z. Chen, L. Liu, G. H. Huang, Y. F. Huang & I. Maqsood (2005): Modeling for the Separation of Light NonAqueous Phase Liquids from Contaminated Subsurface Through Vacuum-Enhanced Oil Recovery, Energy Sources, 27:1-2, 123-138

Zahiraleslamzadeh, Z.M., Bensch, J.C., Cutler, W.G., 1999. Enhanced soil vapor extraction for source area remediation using dual phase extraction with pneumatic fracturing. Contaminated Soils 4, 359–372.

附件

國科會補助專題研究計畫成果報告自評表

請就研究內容與原計畫相符程度、達成預期目標情況、研究成果之學術或應用價值（簡要敘述成果所代表之意義、價值、影響或進一步發展之可能性）、是否適合在學術期刊發表或申請專利、主要發現或其他有關價值等，作一綜合評估。

1. 請就研究內容與原計畫相符程度、達成預期目標情況作一綜合評估

■達成目標

□ 未達成目標（請說明，以 100 字為限）

□ 實驗失敗

□ 因故實驗中斷

□ 其他原因

說明：

2. 研究成果在學術期刊發表或申請專利等情形：

論文：□已發表 □未發表之文稿 ■撰寫中 □無

專利：□已獲得 □申請中 □無

技轉：□已技轉 □洽談中 □無

其他：（以 100 字為限）

撰寫中的中文期刊論文：汽油污染場址 MPE 整治下各相中污染物之變化評估

撰寫中的國內研討會論文：汽油污染場址多相整治效果評估之數值模擬

撰寫中的英文期刊論文：Assessment of effectiveness of MPE based on simulation of multi-species VOC

撰寫中的國際研討會論文：Simulation of free-product recovery at gasoline contamination site with TMVOC

3. 請依學術成就、技術創新、社會影響等方面，評估研究成果之學術或應用價值（簡要敘述成果所代表之意義、價值、影響或進一步發展之可能性）（以500 字為限）

本研究之成果已由主持人在國內相關的教育訓練，包括環保署環訓所辦理的加油站地下儲槽與管線監測訓練班、台中港加工出口區辦理的土壤與地下水污染講習會、南投縣政府的土壤與地下水監測計畫講習會等相關教育訓練中，向與會者進行報告。且在參與環保署土壤與地下水整治基金會、各縣市環保局的相關計畫審查會議中，提出與環保署官員和計畫執行單位討論。且在台灣中油、縣市政府的污染整治計畫案審查會議中，與相關單位進行討論。對於利用 MPE 的效果向各單位進行討論，許多場址已實際上用 MPE 進行抽油，但往往效果不佳，本計畫之成果，也可以說明為何其然。並說明未來各單位應否與如何利用數值模式先期模擬，可先期研判 MPE 之效果。

附

國科會補助專題研究計畫項下出席國際學術會議心得報告

日期：102 年 8 月 31 日

計畫編號	NSC 101-2221-E-009 -135 -		
計畫名稱	LNAPL 多相抽除法對 BTEX 移除效能提升之探討		
出國人員姓名	單信瑜	服務機構及職稱	國立交通大學土木工程系副教授
會議時間	101 年 12 月 13 日至 101 年 12 月 16 日	會議地點	泰國　曼谷 Bangkok, Thailand
會議名稱	(中文)　GEOSYNTHETICS ASIA 2012-第五屆亞洲地區地工合成材料研討會 (英文) GEOSYNTHETICS ASIA 2012 - 5th Asian Regional Conference on Geosynthetics		
發表論文題目	(中文)夯實黏土與地工皂土毯之透氣性 (英文) AIR PERMEABILITY OF COMPACTED CLAYS AND GEOSYTHETIC CLAY LINERS		

一、參加會議經過

本次研討會在泰國曼谷舉行，是每兩年一次，亞洲國家地工合成材料界定期的大型國際研討會。由本次研討會的狀況來看，亞洲地區在金融風暴與金融海嘯的影響後似乎並未完全恢復，且泰國本身歷經曼谷的水災也受創嚴重，所以研討會的時間曾經數度延期。因此，相較於過去的盛況，今年台灣與會者比往年少了許多。

本人於 2012.12.14 下午進行簡報發表論文，與各國的專家分享掩埋場覆蓋系統使用地工皂土毯或夯實黏土在透氣性上的表現。因為一般廢棄物掩埋場若掩埋生垃圾（台灣在推動垃圾焚化之前，以及目前東南亞國家大多數的狀況）會產生甲烷氣，不僅是溫室氣體，且若氣溫過高或有意外（保特瓶、廢玻璃等具凸透鏡效果的物品聚焦）易引發火災或爆炸。因此透氣性愈低愈好，且應配合排氣系統控制。因此，這一議題也在會議中和各國代表進行討論。

本次大會的專題演講如下：

Keynote speech

- Embankments of soft ground and ground improvement , J. Chu
- Geosynthetics for riverbank and coastal protection in Asia , C. Lawson
- Geosynthetics for environmental protection – compatibility and integrity, T. Katsumi
- Geosynthetics innovation for sustainable engineering, H. Y. Jeon

本次大會期間，國際地工合成材料學會的相關代表，歐美各國地工合成材料的產學界代表，也都紛紛與會。在國內代表部分，暨南大學的劉家男教授、台灣科技大學的楊國鑫教授、屏東科技大學的謝啟萬教授、海洋大學的林三賢教授也都參與，廠商部分包括盟鑫企業、惠光企業等廠商代表也都與會。此外，所有台灣代表也都與國際地工合成材料協會的理事長 Prof. Zongberg 進行午餐會談，商談有關台灣分會的強化方向。

大會會場

研討會會場外

與台灣參展廠商盟鑫公司工程師討論

研討會廠商展覽會場

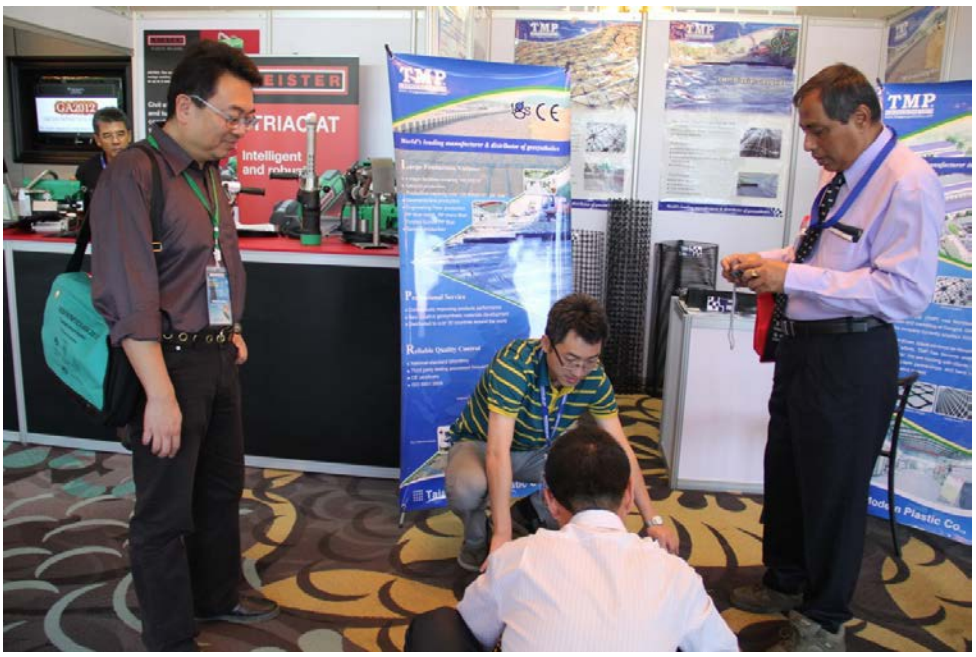

廠商展示該公司生產的 Geoweb


印度廠商介紹椰纖防沖蝕毯

二、與會心得

本次研討會各國人士的參與狀況仍然頗為踴躍。由研討會與展覽的參與者來看中國與韓國的與會者在今年與過去近幾年來一樣，仍是持續成長中。

在研討會的論文主題來看，在加勁相關議題部分，無論是加勁擋土牆、加勁邊坡、地盤改良、河海堤護岸、道路鋪面加勁等議題仍佔了主要的部分，有關地表加勁與防沖蝕的相關應用方面也維持一定的比例。但在和廢棄物處理或土壤地下水污染相關的部分，例如掩埋場的阻水材料、集排水材料，在污染場址圍堵用的垂直隔水牆或具電動勢能整治的材料的比例原本就較低，

今年看來較過去更少。

地工合成材料歷經了這些年的快速發展，最近幾年的較少有重大的突破或創新。因此在研討會中可看出在材料的應用方式與試驗上的創新頗為有限，但在數值模擬等相關研究上有較過去更多的成果。

另一方面，地工合成材料在「永續」面向上的優勢也較以往更受到重視，因此與使用地工合成材料可促進永續性與節能減碳的相關工程案例介紹的數量也較往年顯著增加。

三、考察參觀活動(無是項活動者略)

參觀活動需自費參加，未報名。

四、建議

我國的地工合成材料產業歷經二十餘年的發展，歷史雖然不長，但是其間的變化甚鉅。此外，我國的產官學界所組成的中華地工合成材料協會也從成立到持續的運作。

然而，因林肯大郡事件之後，山坡地住宅社區的開發數量驟降；且山坡地開發高爾夫球場、遊樂園區的案件也逐年減少。曾經因為這些工程而急速成長的地工加勁材料市場在國內顯得停滯多年，即使少部分的大型公共工程與道路災修工程近年來有部分使用加勁擋土牆或加勁邊坡，但數量遠不如過去多。且在因近幾年實際上的公共建設經費減少，且其中「生態工法」的應用上也遇到一些困境，也導致了國內地工合成材料的應用與研究受到直接的影響。

五、攜回資料名稱及內容

1. 研討會論文集（紙本與光碟）
2. 展示廠商之相關資料

六、其他

LOCAL ORGANIZING COMMITTEE

Prof. Dennes T. Bergado	Thailand
Dr. Sompote Youwai	Thailand
Mr. Nuttapong Kovittayanun	Thailand
Dr. Suttisak Soralump	Thailand
Dr. Montri Dechasakulsom	Thailand
Dr. Panich Voottipruex	Thailand
Dr. Yip Poon Lai	Malaysia
Dr. Pham Van Long	Vietnam

INTERNATIONAL ADVISORY COMMITTEE

Prof. Guangxin Li	China
Prof. Rajagopal	India
Mr. Gouw Tjie Liong	Indonesia
Dr. Hiroshi Miki	Japan
Prof. Han Yong Jeon	Korea
Mr. Thomas Wintermar	Philippines
Dr. Dave Chang	West Pacific Region

TECHNICAL COMMITTEE

Prof. Dennes T. Bergado	Thailand/Chairman
Prof. Chungsik Yoo	Korea
Prof. Han Yong Jeon	Korea
Mr. John Cowland	Hong Kong
Prof. Jun Otani	Japan
Prof. Jiro Kuwano	Japan
Prof. Shui Long Shen	China
Prof. Xiao Wu Tang	China
Prof. San Shyan Lin	Taiwan
Dr. Ennio Palmeira	Brazil
Dr. Abdelmalek Bouazza	Australia
Mr. Mike Sadlier	Australia
Mr. Sam Allen	U.S.A.

VENUE

GA2012 will be held at Centara Grand at Central Plaza Ladprao Bangkok (CGLB), a newly renovated 5-star hotel superbly located near the elevated highway system, the underground Mass Rapid Transit and the BTS Skytrain. CGLB provides an easy access to Suvarnabhumi International Airport which takes just over 30 minutes. It also has a direct link to the Central Plaza shopping complex through a covered walkway.

REGISTRATION

The Registration Fees which covers the Conference Proceedings, Lunch and Coffee Breaks are as follows:

Participants	US$ 500
IGS Member	US$ 450
IGS Corporate Member (up to 5 each members)	US$ 450
Student Participants	US$ 250

IMPORTANT DATES

For Technical Papers:

Deadline for Abstract Submission	29 February 2012
Notification of Abstract Acceptance	30 April 2012
Deadline for Paper Submission	15 July 2012
Notification of Paper Acceptance	15 August 2012
Final Paper Submission	01 October 2012
Deadline for Author Registration	01 October 2012

For Student Papers:

Deadline for Abstract Submission	15 July 2012
Deadline for Paper Submission	31 July 2012
Notification of Paper Acceptance	15 September 2012
Final Paper Submission	01 October 2012
Deadline for Author Registration	01 October 2012

For Case Histories, Country Reports, Keynote and Theme Lectures:

Deadline for Paper Submission	31 August 2012
Final Paper Submission	01 October 2012
Deadline for Author Registration	01 October 2012

According to the International Geosynthetics Society regulations, participants may have only one paper as first authors (no limit for co-authoring papers). Chapters of IGS may submit up to 3 "Case Histories of Geosynthetics Engineering Practice" in addition to individual submission.

Contact Information:

GA2012 Secretariat
c/o Asian Center for Soil Improvement and Geosynthetics
Asian Institute of Technology, Bangkok, Thailand
E-mail: geosyntheticsasia2012@gmail.com

Conference Chairman: Prof. Dennes T Bergado
E-mail: bergado@ait.ac.th

website: http://geosynthetics-asia2012.com/

GA2012

GEOSYNTHETICS ASIA 2012

5th Asian Regional Conference on Geosynthetics
13 to 16 December 2012
Bangkok, Thailand

BULLETIN NO. 7

" Geosynthetics for Sustainable Adaptation to Climate Change"

Organized by:

International Geosynthetics Society—Thailand Chapter

Asian Center for Soil Improvement and Geosynthetics

Suranaree University of Technology

Under the auspices of:

International Geosynthetics Society

GA2012

5th Asian Regional Conference on Geosynthetics

- Geosynthetics for Sustainable Adaptation to Climate Change -

Conference Program
13-16 December 2012, Bangkok, Thailand

IGS THAILAND
International Geosynthetics Society Thailand Chapter

Asian Center for Soil Improvement and Geosynthetics

Suranaree University of Technology

Under the auspices of:

IGS
International Geosynthetics Society

口頭發表場次表

Friday, 14th December 2012

08:30 – 09:15	Geosynthetics for environmental protection – compatibility and integrity – ***Keynote Lecture 3 - T. Katsumi*** ***Chair- P. H. Giao*** ***Co-Chair- W. Kongkitkul***
09:15 – 09:45	Award Ceremony
09:45 – 10:15	Coffee Break and Trade Expo
10:15 – 11:00	Geosynthetics innovation for sustainable engineering ***Keynote Lecture 4 - H. Y. Jeon*** ***Chair- S. Chandra*** ***Co- Chair- S. Youwai***
	Technical Committee on Barriers Session ***Chair- K. P. Von Maubeuge*** ***Co-Chair- N. Touze-Foltz***
11:00 – 11:10	GCLS to mitigate natural contamination from excavated rocks ***T. Katsumi***
11:10 – 11:20	A literature review on lifetime prediction of this HDPE geomembranes in the exposed environment ***R. Denis***
11:20 – 11:30	Hydraulic performance of geosynthetic clay liners (GCLS) compared with compacted clay liners (CCLS) in landfill lining systems ***K. P. von Maubeuge***
11:30 – 11:40	Peel and shear test comparison and geosynthetic clay liner shear strength correlation ***K. P. von Maubeuge***
11:40 – 11:50	Flow rate in composite liners including GCLS and bituminous geomembranes ***H. Bannour***
11:50 – 12:00	Geotextile barriers in the tailing dump inwash technology in permafrost region ***A. B. Lolaev***
12:00 – 13:00	Lunch at Rooms: Lardprao Suite and Krungthep 2
	Technical Committee on Reinforcement Session ***Chair- Y. Miyata*** ***Co-Chair- G. Brau***
13:00 – 13:10	Behavior of geosynthetics reinforced walls in back-to-back configuration ***C. S. Yoo***
13:10 – 13:20	EBGEO2010 – experience with German design procedures for geosynthetics reinforced structures ***G. Bräu***
13:20 – 13:30	Real-time monitoring for geosynthetics reinforced systems ***T. Abdoun***
13:30 – 13:40	A new type reinforced soil structure with inserting pile foundation ***T. Hara***
13:40 – 13:50	Load transfer mechanism of geocells ***A. Emersleben***
13:50 – 14:00	Effect of geogrid type on performance of reinforced dense-graded aggregate base ***R. Ghabchi***
14:00 – 14:30	Coffee Break and Trade Expo

11

	Ballroom B	Ballroom C
	Theme Session 3-Barrier/ Environmental *Chair- S. Soralump* *Co-Chair- A. Ritirong*	*Theme Session 4-Natural Fibers/Innovations* *Chair- P. Voottipruex* *Co-Chair- P. Jamsawang*
14:30 – 15:00	Geomembranes in mining works ***Theme Lecture 3 – A. Bouazza***	Sustainable infrastructure development including limited life geosynthetics ***Theme Lecture 4 - K. Rajagopal***
15:00 – 15:10	Air permeability of compacted clays and geosynthetic clay liners ***H. Y. Shan***	Experimental study on natural bamboo geogrid encased stone column ***J.N. Mandal***
15:10 – 15:20	The influence of bag's shape and internal friction angle of sand on ultimate capacity of sand-bag by using analytical and numerical analysis ***A. Haddad***	Application of fibers from Sabai grass in construction of subbase of roads in conjunction with sands ***J. Maity***
15:20 – 15:30	Ground improvement with geotextile reinforcement: case studies – embankment over soft clay in Australia and sludge pond capping in China ***W.C. Loh***	Preponderance of jute as geotextiles ***T. Sanyal***
15:30 – 15:40	Centrifuge model tests on the connecting form between cut off wall and composite geomembrane of cofferdam ***B. Li***	Study on impact absorbency of soil mixed with crushed EPS waste – relation to the deformation characteristics of soil – ***T. Kimata***
15:40 – 15:50	A feasibility study for the drainage and protection of GMC (Geo Multicell Composite) as a leachate collection system in landfill ***J. H. Kim***	Deformation and strength characteristics of lightweight geomaterial mixed with EPS beads for subgrade ***K. Yamanaka***
15:50 – 16:00	Hanging bag test of sludge filter through geotextiles ***Y. C. Wu***	Experimental study on one-dimension compression and creep characteristics of EPS in the application for stabilizing slope of expansion soil canal ***W. Zou***
16:00 – 16:10	A study on using waterproof asphalt to make frost heave-resistant drainage ditches ***T. Adachi***	Experimental study on the thermal conductivity of light soil mixed with EPS particles ***G. Liu***
16:10 – 16:20	The study on swelling index of sodium bentonite under different conditions ***P. Wu***	Eco-friendly engineering performance evaluation of PLA geosynthetics ***H. Y. Jeon***

12

AIR PERMEABILITY OF COMPACTED CLAYS AND GEOSYTHETIC CLAY LINERS

Hsin-Yu Shan [1], Jenn-Tien Yao [2]
[1] Department of Civil Engineering, National Chiao Tung University, Taiwan; Tel: +886-35131562; Fax: +886-35716257; Email: hyshan@mail.nctu.edu.tw,
[2] Fareastern General Construction, Inc., Taiwan; Tel: +886936292783; Email: ponyao@mail.fegc.com.tw

ABSTRACT

Two of most important functions of a landfill cover are to minimize the infiltration of water and to control the emission of landfill gas. Compacted clay liner (CCL), geosynthetic clay liner (GCL), and geomembrane (GM) are the three major types of hydraulic barrier materials used in the bottom lining systems as well as cover systems of landfills. However, it is well recognized that clay liners crack upon desiccation. The cracked liner may enhance the capacity to conduct fluid, which not only increase the infiltration of the downward moving water but also the emission of upward moving gas. Laboratory air permeability tests were conducted to quantify the rate of air passing through desiccated clay liner specimens. In addition, the equilibrium water content of clay liners in the field condition is also studied. The results show that desiccated clay liners may allow considerable amount of landfill gas to pass through. In addition, the air permeability of desiccated GCLs are much higher than that of desiccated CCLs. Accordingly, it is suggested that geomembranes should be used to contain landfill gas for landfills located in areas where landfill gas emission are to be controlled effectively.

Keywords: landfill, clay liner, air permeability, landfill gas emission

INTRODUCTION

In recent years, landfill gas emission has raised considerable concerns since methane is a major greenhouse gas. As a result, for closed landfills, the effectiveness of the cover system to control the emission rate of methane and non-methane organic compounds (NMOCs) needs to be assured. Gas passes through the landfill cover system by means of advection and molecular diffusion. In MSW landfills where large amount of gas is produced, the internal pressure is usually greater than atmospheric pressure such that landfill gas will be released not only by diffusion but also by pressure-driven advection. In the meantime, the natural fluctuation of atmospheric pressure can also cause gas to flow into or out of the landfill. Furthermore, a change in leachate/water table or difference of temperature across the cover system may also lead to gas migration. In many cases, the temperature within the landfill reaches higher than 40°C due to the heat generated by the anaerobic degradation process (Tchobanoglous et al. 1993).

Gas movement by diffusion is driven by gradient of concentration. When a gas is more concentrated in one region of a mixture more than another, it will diffuse into the less concentrated region. Thus the molecules move in response to a partial pressure gradient or concentration gradient of the gas. The present paper will focus only on advective transport.

Figueroa and Stegmann (1991) performed several field tests on a 0.6 m-thick soil cover (SC-SM) at a German landfill. They found that the landfill gas flow rates ranged from 5.2×10^{-6} to 9.6×10^{-5} $m^3/m^2/s$. They suggested that the dominant gas transport mechanism was

advection.

In most of the modern landfills, compacted clay liner (CCL), geosynthetic clay liner (GCL), and geomembrane (GM) are the three major types of hydraulic barrier materials used in the bottom lining systems and cover systems.

Many landfills have used compacted clays as hydraulic barrier in the cover system since the hydraulic conductivity of well-constructed CCL can be as low as 1 x 10^{-10} m/s and can meet the regulatory requirements. However, the major disadvantage of compacted clay liner is that they will crack as a result of desiccation, freeze-thaw cycles, and differential settlement (Koerner and Daniel 1992, Daniel and Koerner 1993). For clay minerals with high swelling potential, the cracks may heal upon rehydration. Kraus et al. (1997), McBrayer et al. (1997), and Day (1998) have looked into the phenomenon of crack-healing of compacted clay. Furthermore, Day (1998) suggested that an important factor in the healing of cracks upon wetting is the type of clay mineral. He stated that for montmorillonite the desiccation cracks are completely healed upon wetting. The hydraulic conductivity of cracked Otay Mesa natural clay specimen decreased from 7 x 10^{-7} m/s to 3 x 10^{-10} m/s as a result of healing of cracks.

Geosynthetic clay liners have not only been used in bottom liners for landfills and surface impoundments (Schubert 1987; Daniel and Koerner 1991; Trauger 1991, 1992; Clem 1992), but also in final covers for landfills and remediation projects as well (Koerner and Daniel 1992, Daniel and Richardson 1995; Woodward and Well 1995). The main advantages and disadvantages of GCLs have been discussed by Boardman (1993) and Manassero et al. (2000) amongst many others.

Although GCLs are usually installed to limit advection of liquids (e.g., water through a cover system) they may also serve an important role in covers as a gas barrier. Theoretically, hydrated GCLs as well as wet compacted soils should hardly allow any gas to pass through (Daniel, 1991). Nevertheless, Trauger and Lucas (1995) did measure the rate of methane gas migrating through GCLs via diffusion. Their results show that the rate of gas transport through GCL was very low as long as its water content was greater than 90%. The permeance is about 2 x 10^{-6} m/s for GCL sample with a water content of around 50% and drops below 1 x 10^{-9} m/s when water content reached above 90%. This suggests that the gas permeability of GCLs is dependent on the water content.

GCLs are known to have a phenomenal ability to retain moisture such that they might have the potential to be effective barrier to gas migration. Research on GCLs buried in sands showed that they were able to absorb water from the environment very quickly why buried dry or hardly lose any water when buried saturated (Geoservice, 1989; Daniel et al., 1993).

With GCLs being increasingly used as part of the capping, their gas performance has come under a growing scrutiny. Recent work has shown that the gas permeability of GCLs is affected by the manufacturing process and the form of bentonite (Didier et al., 2000; Bouazza and Vangpaisal, 2000; Shan and Yao, 2000; Aubertin et al. 2000; Vangpaisal and Bouazza, 2001, 2003).

This paper presents a test method developed speci.cally to assess the gas permeability of GCLs. It is based on the method developed by Matyas (1967) for the measurement of air permeability in soils. The testing apparatus has been designed to accommodate the GCL sample and gas. Flowmeters are used to monitor gas outflow from the device. The test method offers the possibility of carrying out gas permeability tests at different pressure gradients and confining stresses.

EXPERIMENTAL PROGRAM

The air permeability of soil depends on factors such as the size and number of cracks, the air porosity (n_a), and the degree of saturation. Many of these factors are dependent on each other or on some other factors. For example, the degree of saturation depends on both the water content and the void ratio. Among these factors, the air permeability of soils is most sensitive to the variation of degree of saturation. On the other hand, the void ratio of a clay liner in the cover system will be almost constant, since effective stress is kept unchanged throughout the service period. Therefore, the degree of saturation solely depends on water content. Furthermore, the cracking of clay liners is also closely related to the water content. Therefore, in a cover system, the water content is the single most important factor that affects its air permeability of a clay liner. As a result, this research focused on determining the effect of water contents on the air permeability of the clay liners.

Materials

The three clays selected to represent the compacted liners were kaolinite, Hsin-chu clay, and Chung-li clay. The properties of the clays are listed in Table 1.

Table 1 Properties of soils samples.

Soil	Finer than #200 sieve (%)	LL*	PL*	PI*	G_s	USCS
Hsin-chu clay	48.88	25.4	21.1	4.3	2.58	SM-SC
Chung-li clay	92.51	58.5	22	36.5	2.65	CH
Kaolinite	100	56.5	41.1	15.4	2.71	MH

Note:*Portion Finer than #40 Sieve s

The CCL samples were compacted with 48% of the energy produced by standard Proctor compaction test. The results of the compaction tests are listed in Table 2 and the compaction curves are shown in Fig. 1. The shrinkage limits of the bentonite in the clays were determined according to standard test method ASTM D427-92 and are listed in Table 3. The results of hydraulic conductivity of the CCL specimens are listed in Table 4.

Table 2 Results of compaction tests.

Soil	$\gamma_{d,\,max}$ (g/cm^3)	Optimum water content (%)
Hsin-chu clay	1.72	18
Chung-li clay	1.48	27
Kaolinite	1.27	36

Note: Specimens were compacted with 48% of Standard Proctor compaction energy.

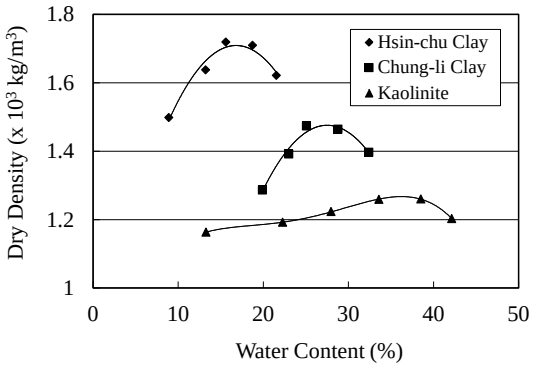

Fig. 1 Compaction curves of clays tested.

Table 3 Shrinkage Limit of Soils.

Soil	Shrinkage limit (%)	Volume change (%)
Hsin-chu Clay	16.7	15.61
Chung-li Clay	19.6	39.88
Kaolinite	40.5	30.64

Table 4 Results of fixed-wall hydraulic conductivity tests.

Soil	k (m/s)
Hsin-chu Clay	4.6×10^{-9}
Chung-li Clay	1.2×10^{-9}
Kaolinite	2.8×10^{-9}

Note: Hydraulic gradient = 100.

The two GCLs tested in this study were a needle-punched GCL and a stitch-bond GCL, which will be designated as GCL-A and GCL-B, respectively. GCL-A is comprised of a nonwoven needlepunched geotextile that is needle punched again through a layer of bentonite into a woven slit-film geotextile. The bentonite content is 3.6 kg/m^2. The water content of the bentonite in dry GCL-A is about 10 - 12%. In GCL-B, 3.6 kg/m^2 of bentonite is sandwiched between woven geotextile on the top and open weave geotextile at the bottom.

The shrinkage limits of the bentonite in the GCLs are listed in Table 5. It is interesting to note

that the shrinkage limits of the bentonite are very low comparing to the high water content of saturated bentonite.

Table 5 Results of shrinkage limit tests on bentonite in the GCLs.

GCL	Shrinkage limit (%)	Volume change (%)
GCL-A	35.2	87.86
GCL-B	29.9	88.15

Water Retention Test

Clay liner specimens were placed under 0.5 m of moist sand and loosely compacted moist clay in two 86-liter plastic buckets separately. The specimens had been allowed to absorb water under dead weights that imposed a vertical stress that is equivalent to 0.5 m of soil before they were put in the buckets. The test was performed over a 90-day period spanning from March to May. The monthly average temperatures were 17.2°C, 21.1°C, and 24.6°C, respectively. The average humidity during the test period was about 85%. The suction in the cover soils was monitored with tensiometers.

The soil water characteristics of the clay liner samples were determined with a 15-bar pressure cell. The main drainage curves (MDC) of the compacted clay specimens are shown in Fig. 2. The specimens were soaked to enhance saturation before the test. On the other hand, the specimens of water retention tests were placed in the surrounding soils immediately after they had been cut from the compacted samples. As a result, the water contents of the retention test specimens were a little less than those indicated by the MDC.

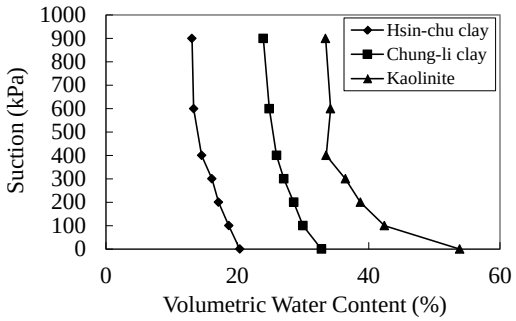

Fig. 2 Soil water characteristic curves of compacted clay samples.

Air Permeability Test

The diameter and the height of the CCL specimens were 101.6 mm and 19.5 mm, respectively. The clays were compacted at a water content 2% wet of optimum with 48% of standard Proctor compaction energy. In order for the cracks to develop more easily, it was decided to use shorter CCL specimens. Therefore, the specimens were compacted in a compaction mold of reduced size. The compacted samples were trimmed and then retrieved from the compaction mold.

The GCL specimens were cut from the rolls supplied by the manufacturer to a diameter of 114.5 mm. The specimen was placed in an acrylic mold with an inner diameter of 114.5 mm. The specimen was then hydrated with tap water for 1 day.

Both CCL and GCL specimens were placed inside an oven and heated under a temperature of around 35°C for a given period of time. During the desiccation period, a dead load weighing 4 kg was put on top of each specimen to provide a normal stress equivalent to that created by 300 mm of topsoil. In addition, the CCL specimens were put on top of a sheet of sand paper to prevent them from shrinking as a whole so that cracks could develop. This process was repeated for different drying times to obtain specimens with various water contents.

The air permeability tests of CCL specimens were performed with flexible-wall permeameters (Fig. 3). During the tests, a low cell pressure of 3.5 kPa (0.5 psi) was applied to ensure good contact between the membrane and the specimen.

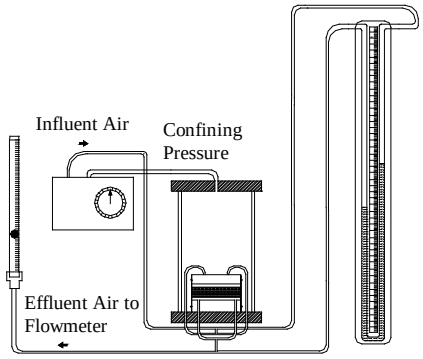

Fig. 3 Schematic diagram of the compacted clay air permeability testing system.

Fig. 4 shows the schematic diagram air permeameter for testing the GCL specimens. GCL specimens were clamped between two ring-shape holders. Bentonite paste was placed along the edges of the specimens to prevent air leakage.

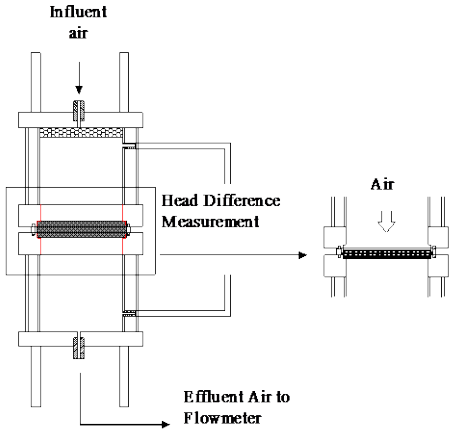

Fig. 4 Schematic diagram of the permeameter for measuring air permeability of GCL (Shan and Yao 2000).

For testing of both types of materials, the flow rate of air was adjusted by regulating influent air pressure with the pressure control panel (Fig. 5). Very low influent air pressure was used for the tests (less than 2 kPa). The range of flow rate was as high as 27 l/min for the more permeable specimens under larger gradients and as low as 0.5 l/min for less permeable specimens under smaller gradients. The head loss across the specimen was measured by U-tube manometer. For each specimen, head differences corresponding to 5 different flow rates were measured. The linear relationship between flow rate and gradient justified that the gas flow was in the laminar range. The test results of one of the compacted Chung-li clay specimen are shown in Fig. 6 as an example. After each test, the water content and the dimensions of specimen were measured.

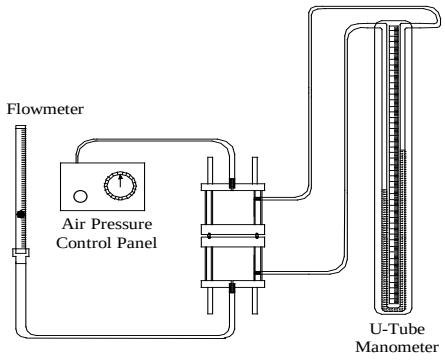

Fig. 5 Schematic diagram of the gcl air permeability testing system (Shan and Yao 2000).

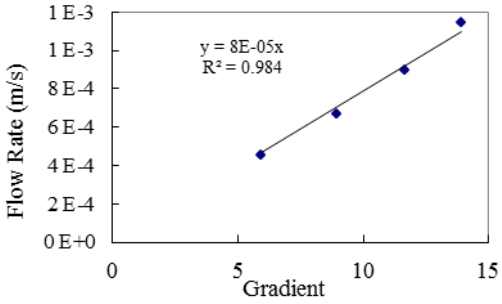

Fig. 6 Relationship between flow rate and gradient of air permeability tests.

The air permeability of the specimens was computed with the following equation:

$$k = \frac{q / A}{\left(\frac{\Delta h_{total} - \Delta h_{equipment}}{t} \right)} \quad (1)$$

where Δh_{total} is the total head loss measured (mm); $\Delta h_{equipment}$ is the head loss of system without specimen in it (mm); k is the air permeability (mm/s). The compressibility of air has been taken into account when computing the flow rates that passed through the specimens from the values measured with the flowmeter.

RESULTS AND DISCUSSION

Water Retention Tests

Results of the water retention tests show that the hydrated GCLs did not have a strong ability to retain water. The variations of the water content of GCL specimens with time are shown in Fig. 7. The final water content of GCL-A and GCL-B buried in sand are 48% and 53%, respectively. The final water content of GCL-A and GCL-B buried in clay are 27% and 28% which are lower than the shrinkage limit of bentonite. The water contents of the specimens at the end of the tests were much lower than those reported by Geoservice (1989). On the other hand, the final water contents of the specimens are comparable to the results of absorption tests performed by Daniel et al. (1993).

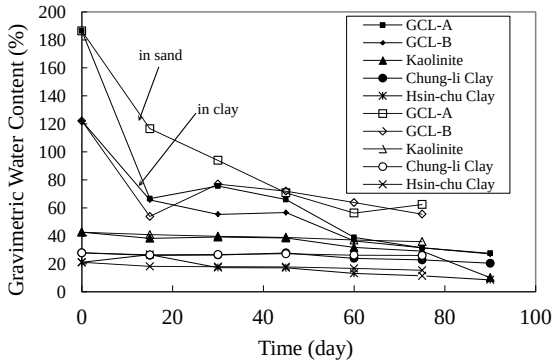

Fig. 7 Variation of water content of CCL and GCL specimens with time.

The CCL specimens also lost considerable amount of water during the test period. The difference between final water contents of specimens buried in sand and clay is most significant for kaolinite. On the other hand, only a small difference in water content was measured for Chung-li clay. In addition, the final water contents of kaolinite and Hsin-chu clay were all lower than their shrinkage limits. By comparing the results with the index properties, it can be concluded that clays with higher plastic limit are capable of retaining more water.

Air Permeability Tests on CCLs

The relationship between air permeability and water content of CCLs are depicted in Fig. 8(a), Fig. 9 (a), and Fig. 10 (a). The air permeability of the compacted clay specimens shows a slight increase as the water content decreases. The trend is most obvious for kaolinite.

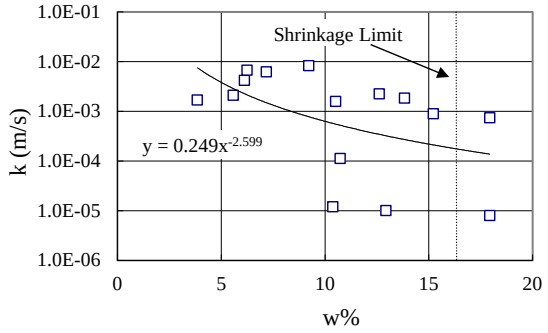

(a) Relationship between air permeability and water content

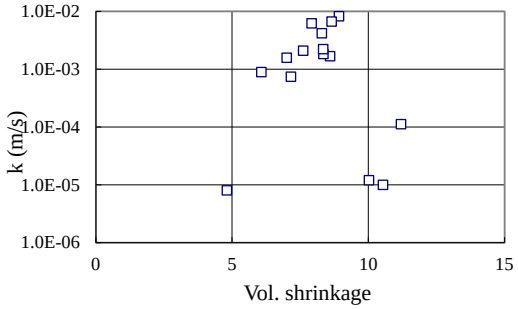

(b) Relationship between air permeability and volume change

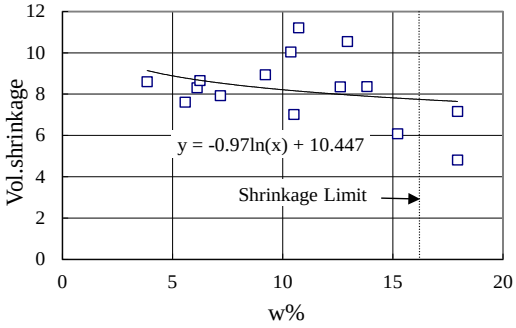

(c) Relationship between volume change and water content

Fig. 8 Relationship between air permeability, water content, and shrinkage of compacted hsin-chu clay.

Among three CCLs, kaolinite has the lowest air permeability while Hsin-chu clay has the highest. It is interesting to note that the hydraulic conductivity of Hsin-chu clay is also the highest among the three clays (Table 4).

The increase of air permeability with decreasing water content did not seem to be solely related with the increased number of cracks. The cracks developed before the water content of the specimens fell below the shrinkage limit. The loss of water of clay particles along the cracks might actually widen the pathway for air.

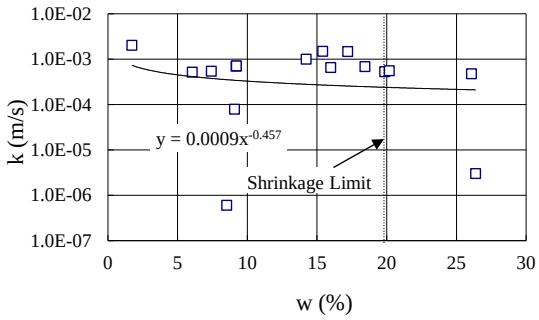

(a) Relationship between air permeability and water content

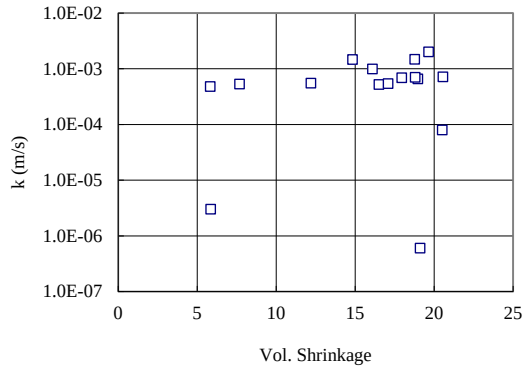

(b) Relationship between air permeability and volume change

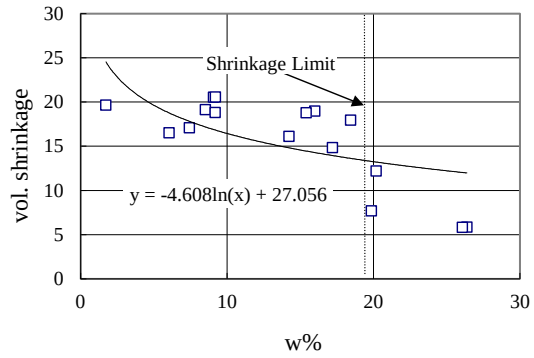

(c) Relationship between volume change and water content

Fig. 9 Relationship between air permeability, water content, and shrinkage of compacted chung-li clay.

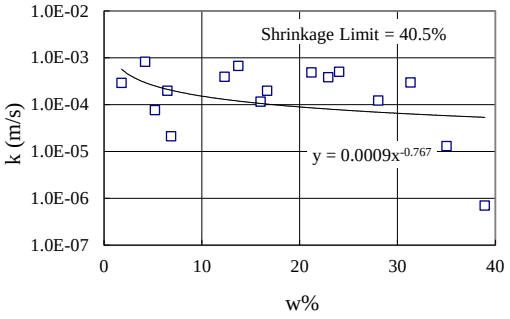

(a) Relationship between air permeability and water content

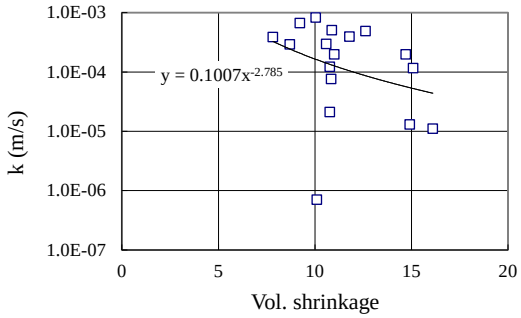

(b) Relationship between air permeability and volume change

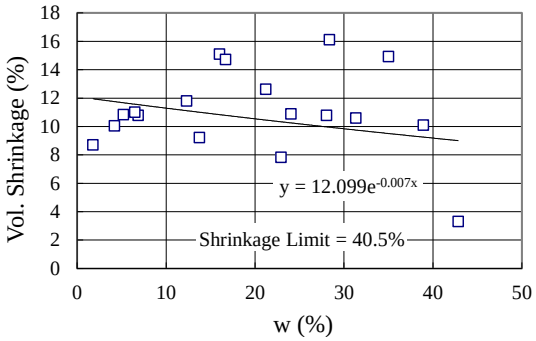

(c) Relationship between volume change and water content

Fig. 10 relationship between air permeability, water content, and shrinkage of compacted kaolinite.

The relationship between the air permeability and shrinkage of the clay specimens are shown in Figs. 8 (b), Fig. 9 (b), and Fig. 10 (b). Only the air permeability of compacted kaolinite decreased at the same time when it shrank (Fig. 10(b)). For Hsin-chu clay and Chung-li clay, there did not seem to be any relationship between air permeability and shrinkage (Figs. 8 (b) and 9 (b)). Again, the reason is that the air permeability of the CCLs is related to the widening of the cracks rather than the reduction of the total volume.

It is interesting to note that the optimum water content of Hsin-chu clay and Chung-li clay are higher than the shrinkage limits whereas the optimum water content of kaolinite is lower than the shrinkage limit. As a result, the volume change of kaolinite specimens was only about 1/3 of the volume change determined from shrinkage limit test, while this ratio was about 1/2 for the other two clays. In addition, kaolinite has more fine particles and lowest plastic index value. These factors may contribute to the low air permeability of desiccated kaolinite.

On the other hand, the content of fines of Hsin-chu clay is slightly below 50% such that the sand particles may be in contact with each other.

Therefore, as the water content decreases, the clay in between the sand particles shrank and pathways of air formed. As a result, Hsin-chu clay had higher air permeability than the other two types of CCLs.

Theoretically, the volume of the clays does not change after the water content dropped below the shrinkage limit. However, as shown in Figs. 8 (c) and 9 (c), for Hsin-chu clay and Chung-li clay, the specimens still experienced noticeable volume change when dried to a water content below the shrinkage limit. In addition, visual observation showed that as the water content decreased, the number of cracks remained approximately the same. The water left in the desiccated specimens either occupied the smallest pores or adhered to the surface of the clay particles. Further decrease of water content made the pathways become wider and allowed faster flow of air. As a result, the air permeability of Hsin-chu clay and kaolinite increased slightly as the water content decreased below the shrinkage limit (Figs. 8 (a) and 10 (a)).

On the contrary, for Chung-li clay, which has more than 90% of clay-size particles and the highest plastic index value, the air permeability remained almost unchanged when dried beyond the shrinkage limit (Fig. 9 (a)). It is noted that the desiccated Chung-li clay specimens shrank considerably with decreasing water content although the water content is lower than the shrinkage limit (Fig. 9 (c)). However, it is possible that compacted Chung-li clay liner may have much larger cracks than the other two clays in the field such that air will flow through it more easily.

The air permeability of the CCL specimens with water content drier than their shrinkage limits are listed in Table 6. Desiccated Kaolinite has the lowest air permeability, followed by Chung-li clay and then Hsin-chu clay. Daniel and Benson (1990) have concluded that compacted sandy clay (SC) is best suitable for hydraulic barrier because it has low permeability, high shear strength, and low shrinkage potential. However, the Hsin-chu clay (SM-SC), which consists of about 50% of sand has the highest air permeability. The most possible reason is that air not only passed through the cracks but also through the primary pores more easily than the other two clays. Although the structure formed by sand particles in contact with each other made the soil have low shrinkage potential, it also had larger pathways for air to go through when the clay shrank. The pathways were developed as the clay particles between the sand particles shrank such that additional pore space became available for transmitting air. Shrinkage of this scale is difficult to be measured or even be observed by visual inspection.

Table 6 Average air permeability of compacted soils drier than shrinkage limit.

Soil	k_a (m/s)
Hsin-chu Clay	2.8×10^{-3}
Chung-li Clay	8.2×10^{-4}
Kaolinite	2.7×10^{-4}

The ability of CCLs to transmit air can also be expressed as the permittivity to air in order to allow for comparison between barrier materials with different thickness. The permittivity is computed with the following equation:

$$\frac{k}{t} = \Psi = \frac{q}{\Delta h \times A} \tag{2}$$

The relationships between the air permittivity of CCLs and water content are shown in Fig. 11. Although the data are scattered considerably, it is obvious that the air permittivity values of desiccated CCLs are sensitive to the change of water content.

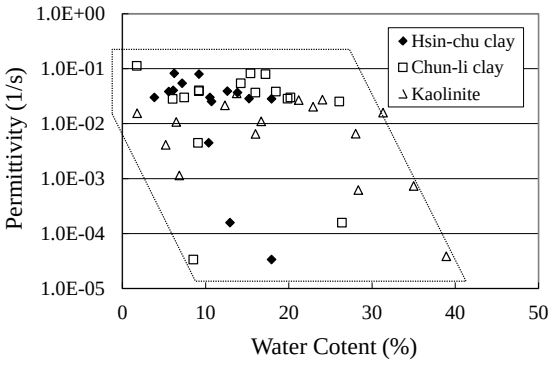

Fig. 11 Air permittivity of compacted clay liners.

Air Permeability Tests on GCLs

Since the results of air permeability tests of GCLs has been described in detail by Shan and Yao (2000), only a summary of the results is presented here. The relationships between air permeability and water content for GCL-A and GCL-B are shown in Fig. 12. For GCL-B specimens with water content higher than 190%, no flow of air was observed. On the other hand, it was unable to detect any flow of air for GCL-A specimens with water content higher than 170%. It can be clearly seen that air permeability increases as the water content decreases. The relationship between air permeability and water content of GCL-B is much clearer than that of GCL-A.

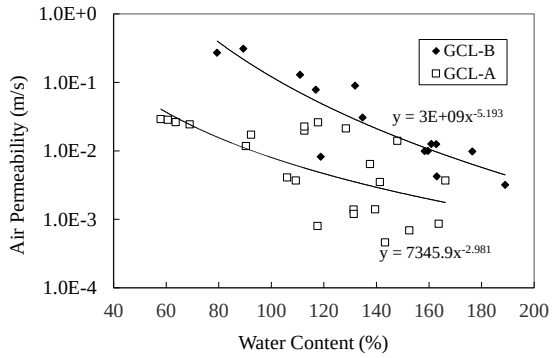

Fig. 12 Relationship between air permeability and water content of GCLs (Shan and Yao, 2000).

Cracks could be observed for GCL-B specimens with water content lower than about 140%. The bentonite in these specimens formed chunks of about 1 cm2 such that the GCL developed a network of wide-open cracks (Fig. 13). For specimens with very low water content, the cracks were as wide as 3 mm. A similar pattern of desiccation cracks of GCL-B specimens have been reported by Shan and Daniel (1991), Boardman (1993) and LaGatta et al. (1997). For GCL-B specimens with water content higher than about 140%, only barely visible hairline cracks in the bentonite was observed.

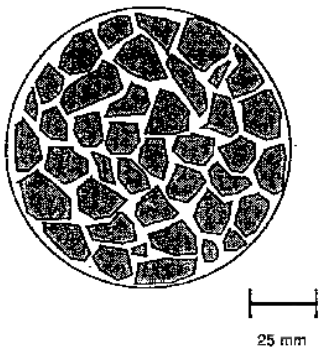

Fig. 13 Crack pattern of GCL-B specimens.

On the other hand, there was no network of large cracks found in the desiccated GCL-A specimens. Instead of forming large chunks, the bentonite in the GCL-A specimens shrank to form small granules as when it was manufactured. The needlepunched fibers seemed to prevent the bentonite from forming chunks during the drying process. As a result, the air permeability of desiccated GCL-A specimens was much lower than that of GCL-B specimens.

The relationships between the air permittivity of GCLs and water content are shown in Fig. 14. The air permittivity values of desiccated GCL-B are much higher than those of desiccated GCL-A for water content ranging from 50 - 150%. Beyond 150%, the air permittivity of both GCLs is very low.

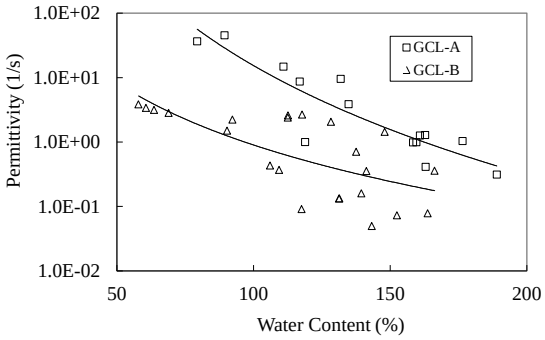

Fig. 14 Air permittivity of GCLs.

The air permittivity of 3 CCLs and 2 GCLs are compared in Fig. 15. The air permittivity of desiccated CCLs is much lower than that of desiccated GCLs. This means that desiccated GCLs will allow air to pass through more easily.

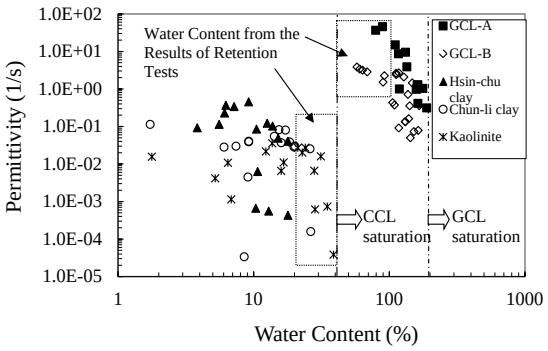

Fig. 15 Air permittivity of clay liners.

PRACTICAL IMPLICATIONS

The emission rate of the landfill gas can be estimated for a landfill under specific conditions. The rate of convective flow of landfill gas through clay liners can be computed with Darcy's law. In order to compare the flux through CCLs and GCLs, the following field condition is assumed. The head difference across the barrier layer is assumed to be 1.0 mm H_2O. The thickness of CCLs and GCLs are assumed to be 600 mm and 6 mm, respectively. The flux was computed with air permeability of CCLs and GCLs corresponding to three different suction levels, which are 30 mb, 60 mb, and 80 mb, respectively.

An appropriate reference suction value is the one that corresponds to the field capacity of the cover soil. Field capacity of a soil is usually defined as the water content of the soil after 24 hours of gravitational drainage. Some soil scientists have

proposed to take the water content of a soil under a suction of 30 kPa (0.3 bar or 300 mb) to be the field capacity. Another relevant reference suction value is the wilting point of the plants is 1500 kPa (15 bar), beyond which the plants are not able to absorb water from the soil.

Table 7 is a list of the rate of convective flow through the desiccated clay liners per unit area. These results are also graphed in Fig. 16. It is clear that the gas flux through GCLs is much higher than the flux through CCLs. It is not only resulted from the higher air permeability of GCLs but also because of the fact that CCLs are thicker than GCLs. The thinness of GCLs caused the hydraulic gradient to be approximately 100 times higher than that across CCLs.

Table 7 Convective flux through clay liners ($m^3/m^2/day$).

Suction (mb)	30	60	80
Hsin-chu clay	1.91×10^{-2}	2.02×10^{-2}	3.26×10^{-2}
Chung-li clay	2.91×10^{-2}	2.95×10^{-2}	2.98×10^{-2}
Kaolinite	7.55×10^{-3}	7.83×10^{-3}	8.89×10^{-3}
GCL-A	7.32×10^{1}	3.24×10^{2}	7.88×10^{2}
GCL-B	1.78×10^{3}	9.87×10^{3}	7.79×10^{4}

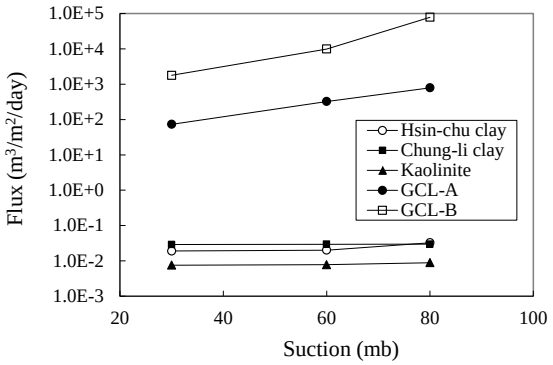

Fig. 16 Gas flux through clay liners.

CONCLUSIONS

The air permeability of both CCLs and GCLs were measured in this study. The compacted clay liners, in spite of being infamous for cracking upon desiccation, have much lower air permeability than GCLs do. In addition, the air permittivity of CCLs is also lower than that of GCLs. Although GCLs have been proved to be effective hydraulic barriers, their air permeability increases rapidly once they start to lose pore water. The results of water absorption tests by Daniel et al. (1993) and water retention tests by Yao (1998) indicate that GCLs will not maintain fully hydrated when they are in contact with soils. Therefore, GCLs are not as reliable in limiting gas emission out from the landfills as they are in preventing water infiltration into the landfills.

Both advection and diffusion should be taken into account when estimating the gas flux through the clay liners in a landfill cover system. For desiccated clay liners with lower water contents, advection dominates the gas transport. For clay liners with high water contents, only a very small amount of gas would diffuse through the material. It is thus important to maintain the clays in a near saturation state in order to limit the gas migration.

With regards to the concern on the emission of landfill gas, the design of final cover system of MSW landfills must take the high air permeability of desiccated clay liners into account. It is suggested that for landfills that are expected to generate large amount of landfill gas, geomembranes may be a better choice than clay liners as the hydraulic barrier for the final covers.

ACKNOWLEDGEMENTS

The authors would like to express their sincere appreciation toward Mr. Kevin Wu of Newmark Engineering Products Co., Ltd. for kindly providing GCL samples for this research.

REFERENCES

Aubertin, M. Aachib, M. and Cazaux, D. (2000). Evaluation of diffusive gas flux through covers with a GCL Geotextiles and Geomembranes 18 (2–4), 215–234.

Boardman, B. T. (1993). The potential use of geosynthetic clay liners as final covers in arid regions. MS thesis, University of Texas, Austin, Texas, U.S.A.

Bouazza, A. and Vangpaisal, T. (2000). Gas advective flux through partially saturated geosynthetic clay liners. Advances in Transportation and Geoenvironmental Systems Using Geosynthetics, American Society of Civil Engineering, Geotechnical Speciality Publication No. 103:54–67.

Clem, J. (1992). GCLs used successfully in hazardous waste containment. Geotech. Fabrics Rep., 10(3):4-7

Daniel, D. E. (1991). Clay liners and covers for waste disposal facilities, unpublished short course class notes. University of Texas at Austin, Austin, Texas, USA

Daniel, D. E. and Benson, C. H. (1990). Water content – Density criteria for compacted soil liners.

J. Geotech. and Geoen. Engrg., ASCE, 116(12):1811-1830

Daniel, D. E. and Koerner, R. M. (1991). Landfill liners from top to bottom. Civ. Engrg., ASCE, 61(12):46-49

Daniel, D. E. and Koerner, R. M. (1993). Cover systems. Geotechnical practice for waste disposal, D. E. Daniel, ed., Chapman and Hall, Ltd., London, England, 455-496

Daniel, D. E., and Richardson, G. N. (1995). The role of geomembranes and geosynthetic clay liners in landfill covers. Geotech. Fabrics Rep., 13(1):44-49

Daniel, D. E. Shan, H.-Y., and Anderson, J. (1993). Effects of partial wetting on strength and hydrocarbon permeability of a geosynthetic clay liner. Proc., Geosynthetics '93, Vancouver, British Columbia, Canada, 1483-1496

Day, R. W. (1998). Discussion of 'Infiltration tests on fractured compacted clay,' by McBrayer et al. J. Geotech. and Geoen. Engrg., ASCE, 124(11):1149-1152

Didier, G., Bouazza, A., Cazaux, D., 2000. Gas permeability of geosynthetic clay liners. Geotextiles and Geomembranes 18 (2–4):235–250.

Figueroa, R. A. and Stegmann, R. (1991). Gas migration through natural liners. Proc., Sardinia '91, 3th International Landfill Symposium, S. Margherita di Pula, Cagliari, Italy, 167-177

Geoservices, Inc. (1989). Report of moisture retention tests, Claymax CR, Report to James Clem Corp., Norcross, Georgia, 14 p.

Koerner, R. M. and Daniel, D. E. (1992). Better cover-ups. Civ. Engrg., ASCE, 62(5):55-57

Kraus, J. F., Benson, C. H., Erickson, A. E. and Chamberlain, E. J. (1997). Freeze-thaw cycling and hydraulic conductivity of bentonitic barriers. J. Geotech. and Geoenv. Engrg., ASCE, 123(3), 229-238

LaGatta, M. D., Boardman, B. T., Cooley, B. H. and Daniel, D. E. (1997). Geosynthetic clay liners subjected to differential settlement. J. Geotech. and Geoenv. Engrg., ASCE, 123(5):402-410

Manassero, M., Benson, C. and Bouazza, A., (2000). Solid waste containment systems. Proceedings International Conference On Geological and Geotechnical Engineering, Vol. 1, Melbourne, Australia, 520–642.

Matyas, E.L. (1967). Air and water permeability of compacted soils. Permeability and Capillary of Soils, ASTM STP 417. ASTM, Philadelphia, 160–175.

McBrayer, M. C., Mauldon, M., Drumm, E. C. and Wilson, G. V. (1997). Infiltration tests on fractured compacted clay. J. Geotech. and Geoenv. Engrg., ASCE, 123(5):469-473

Schubert, W. R. (1987). Bentonite matting in composite lining systems. Proc., Geotech. Pract. For Waste Disposal '87, R. D. Woods, ed., ASCE, New York, N.Y., 784-796

Shan, H.-Y. and Daniel, D. E. (1991). Results of laboratory tests on a geotextile/bentonite liner material. Proc., Geosynthetics '91, Industrial Fabrics Association, St. Paul, MN, 517-535

Shan, H.-Y. and Yao, J.-T. (2000). Measurement of Air Permeability of Geosynthetic Clay Liners. Geotextiles and Geomembranes (18):251-261

Tchobanoglous, G., Theisen, H. and Vigil, S. A. (1993). Integrated solid waste management. McGraw-Hill, Inc., 978 p.

Trauger, R. (1991). Geosynthetic clay liner installed in a new municipal solid waste landfill. Geotech. Fabrics Rep., 9(8):6-17

Trauger, R. (1992). Geosynthetic clay liners: An overview. Pollution Engrg., (May 15), 44-47

Trauger, R. J. and Lucas, H. L. (1995). Determining the flow rate of landfill gas constituents through a geosynthetic clay liner. Proc., Geosynthetics '95, Nashville, Tennessee, USA, 1085-1096

Vangpaisal, T. and Bouazza, A. (2001). Gas permeability of three needle punched geosynthetic clay liners. Proceedings of the Second ANZ Conference on Environmental Geotechnics, Newcastle, Australia, 373–378.

Vangpaisal, T. and Bouazza, A. (2003). Gas permeability of partially hydrated geosynthetic clay liners. Journal of Geotechnical and Geoenvironmental Engineering, ASCE, Vol. 130(8):93 – 102

Woodward, B. L. and Well, L. W. (1995). Alternative cover for saturated, low-strength waste. Proc., Geosynthetics '95, Industrial Fabrics Association International, St. Paul, Minn., 551-562

國科會補助專題研究計畫項下出席國際學術會議心得報告

日期：102 年 8 月 31 日

計畫編號	NSC 101-2221-E-009 -135 -		
計畫名稱	LNAPL 多相抽除法對 BTEX 移除效能提升之探討		
出國人員姓名	單信瑜	服務機構及職稱	國立交通大學土木工程系副教授
會議時間	101 年 12 月 13 日至 101 年 12 月 16 日	會議地點	泰國　曼谷 Bangkok, Thailand
會議名稱	(中文)　GEOSYNTHETICS ASIA 2012-第五屆亞洲地區地工合成材料研討會 (英文) GEOSYNTHETICS ASIA 2012 - 5th Asian Regional Conference on Geosynthetics		
發表論文題目	(中文)夯實黏土與地工皂土毯之透氣性 (英文) AIR PERMEABILITY OF COMPACTED CLAYS AND GEOSYTHETIC CLAY LINERS		

一、參加會議經過

本次研討會在泰國曼谷舉行，是每兩年一次，亞洲國家地工合成材料界定期的大型國際研討會。由本次研討會的狀況來看，亞洲地區在金融風暴與金融海嘯的影響後似乎並未完全恢復，且泰國本身歷經曼谷的水災也受創嚴重，所以研討會的時間曾經數度延期。因此，相較於過去的盛況，今年台灣與會者比往年少了許多。

本人於 2012.12.14 下午進行簡報發表論文，與各國的專家分享掩埋場覆蓋系統使用地工皂土毯或夯實黏土在透氣性上的表現。因為一般廢棄物掩埋場若掩埋生垃圾（台灣在推動垃圾焚化之前，以及目前東南亞國家大多數的狀況）會產生甲烷氣，不僅是溫室氣體，且若氣溫過高或有意外（保特瓶、廢玻璃等具凸透鏡效果的物品聚焦）易引發火災或爆炸。因此透氣性愈低愈好，且應配合排氣系統控制。因此，這一議題也在會議中和各國代表進行討論。

本次大會的專題演講如下：

Keynote speech

- Embankments of soft ground and ground improvement , J. Chu
- Geosynthetics for riverbank and coastal protection in Asia , C. Lawson
- Geosynthetics for environmental protection – compatibility and integrity, T. Katsumi
- Geosynthetics innovation for sustainable engineering, H. Y. Jeon

本次大會期間，國際地工合成材料學會的相關代表，歐美各國地工合成材料的產學界代表，也都紛紛與會。在國內代表部分，暨南大學的劉家男教授、台灣科技大學的楊國鑫教授、屏東科技大學的謝啟萬教授、海洋大學的林三賢教授也都參與，廠商部分包括盟鑫企業、惠光企業等廠商代表也都與會。此外，所有台灣代表也都與國際地工合成材料協會的理事長 Prof. Zongberg 進行午餐會談，商談有關台灣分會的強化方向。

大會會場

研討會會場外

與台灣參展廠商盟鑫公司工程師討論

研討會廠商展覽會場

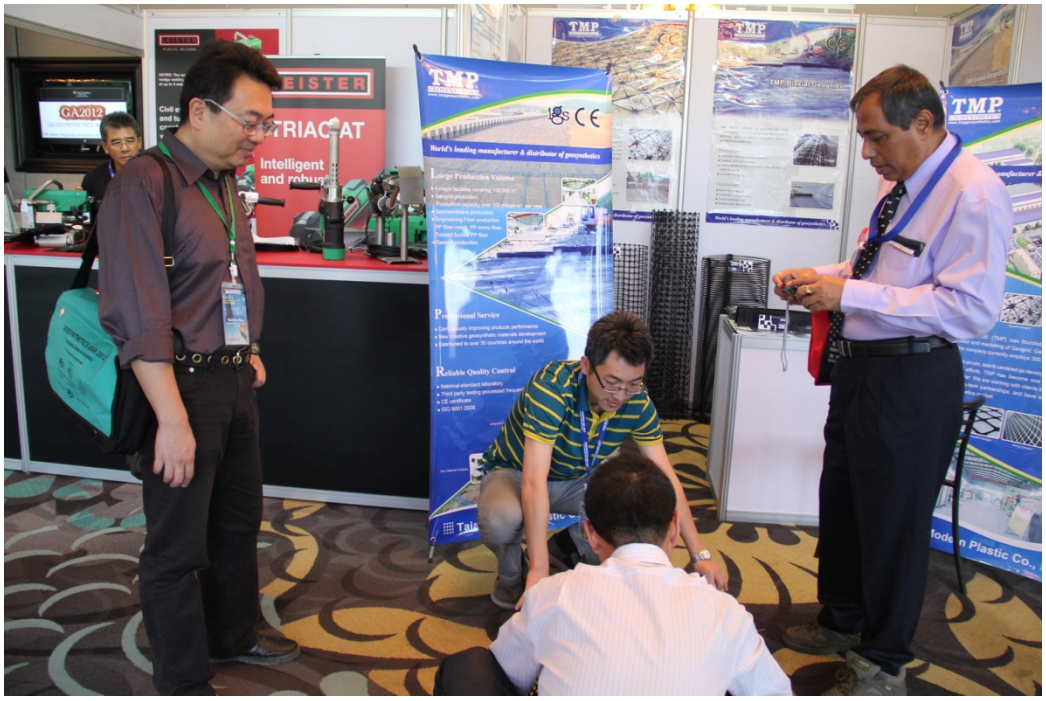

廠商展示該公司生產的 Geoweb

印度廠商介紹椰纖防沖蝕毯

二、與會心得

本次研討會各國人士的參與狀況仍然頗為踴躍。由研討會與展覽的參與者來看中國與韓國的與會者在今年與過去近幾年來一樣，仍是持續成長中。

在研討會的論文主題來看，在加勁相關議題部分，無論是加勁擋土牆、加勁邊坡、地盤改良、河海堤護岸、道路鋪面加勁等議題仍佔了主要的部分，有關地表加勁與防沖蝕的相關應用方面也維持一定的比例。但在和廢棄物處理或土壤地下水污染相關的部分，例如掩埋場的阻水材料、集排水材料，在污染場址圍堵用的垂直隔水牆或具電動勢能整治的材料的比例原本就較低，今年看來較過去更少。

地工合成材料歷經了這些年的快速發展，最近幾年的較少有重大的突破或創新。因此在研討會中可看出在材料的應用方式與試驗上的創新頗為有限，但在數值模擬等相關研究上有較過去更多的成果。

另一方面，地工合成材料在「永續」面向上的優勢也較以往更受到重視，因此與使用地工合成材料可促進永續性與節能減碳的相關工程案例介紹的數量也較往年顯著增加。

三、考察參觀活動(無是項活動者略)

參觀活動需自費參加，未報名。

四、建議

我國的地工合成材料產業歷經二十餘年的發展，歷史雖然不長，但是其間的變化甚鉅。此外，我國的產官學界所組成的中華地工合成材料協會也從成立到持續的運作。

然而，因林肯大郡事件之後，山坡地住宅社區的開發數量驟降；且山坡地開發高爾夫球場、遊樂園區的案件也逐年減少。曾經因為這些工程而急速成長的地工加勁材料市場在國內顯得停滯多年，即使少部分的大型公共工程與道路災修工程近年來有部分使用加勁擋土牆或加勁邊坡，但數量遠不如過去多。且在因近幾年實際上的公共建設經費減少，且其中「生態工法」的應用上也遇到一些困境，也導致了國內地工合成材料的應用與研究受到直接的影響。

五、攜回資料名稱及內容

1. 研討會論文集（紙本與光碟）

2. 展示廠商之相關資料

六、其他

LOCAL ORGANIZING COMMITTEE

Prof. Dennes T. Bergado	Thailand
Dr. Sompote Youwai	Thailand
Mr. Nuttapong Kovittayanun	Thailand
Dr. Suttisak Soralump	Thailand
Dr. Montri Dechasakulsom	Thailand
Dr. Panich Voottipruex	Thailand
Dr. Yip Poon Lai	Malaysia
Dr. Pham Van Long	Vietnam

INTERNATIONAL ADVISORY COMMITTEE

Prof. Guangxin Li	China
Prof. Rajagopal	India
Mr. Gouw Tjie Liong	Indonesia
Dr. Hiroshi Miki	Japan
Prof. Han Yong Jeon	Korea
Mr. Thomas Wintermar	Philippines
Dr. Dave Chang	West Pacific Region

TECHNICAL COMMITTEE

Prof. Dennes T. Bergado	Thailand/Chairman
Prof. Chungsik Yoo	Korea
Prof. Han Yong Jeon	Korea
Mr. John Cowland	Hong Kong
Prof. Jun Otani	Japan
Prof. Jiro Kuwano	Japan
Prof. Shui Long Shen	China
Prof. Xiao Wu Tang	China
Prof. San Shyan Lin	Taiwan
Dr. Ennio Palmeira	Brazil
Dr. Abdelmalek Bouazza	Australia
Mr. Mike Sadlier	Australia
Mr. Sam Allen	U.S.A.

VENUE

GA2012 will be held at Centara Grand at Central Plaza Ladprao Bangkok (CGLB), a newly renovated 5-star hotel superbly located near the elevated highway system, the underground Mass Rapid Transit and the BTS Skytrain. CGLB provides an easy access to Suvarnabhumi International Airport which takes just over 30 minutes. It also has a direct link to the Central Plaza shopping complex through a covered walkway.

REGISTRATION

The Registration Fees which covers the Conference Proceedings, Lunch and Coffee Breaks are as follows:

Participants	US$ 500
IGS Member	US$ 450
IGS Corporate Member (up to 5 each members)	US$ 450
Student Participants	US$ 250

IMPORTANT DATES

For Technical Papers:

Deadline for Abstract Submission	29 February 2012
Notification of Abstract Acceptance	30 April 2012
Deadline for Paper Submission	15 July 2012
Notification of Paper Acceptance	15 August 2012
Final Paper Submission	01 October 2012
Deadline for Author Registration	01 October 2012

For Student Papers:

Deadline for Abstract Submission	15 July 2012
Deadline for Paper Submission	31 July 2012
Notification of Paper Acceptance	15 September 2012
Final Paper Submission	01 October 2012
Deadline for Author Registration	01 October 2012

For Case Histories, Country Reports, Keynote and Theme Lectures:

Deadline for Paper Submission	31 August 2012
Final Paper Submission	01 October 2012
Deadline for Author Registration	01 October 2012

According to the International Geosynthetics Society regulations, participants may have only one paper as first authors (no limit for co-authoring papers). Chapters of IGS may submit up to 3 "Case Histories of Geosynthetics Engineering Practice" in addition to individual submission.

Contact Information:

GA2012 Secretariat
c/o Asian Center for Soil Improvement and Geosynthetics
Asian Institute of Technology, Bangkok, Thailand
E-mail: geosyntheticsasia2012@gmail.com

Conference Chairman: Prof. Dennes T Bergado
E-mail: bergado@ait.ac.th

website: http://geosynthetics-asia2012.com/

GA2012

GEOSYNTHETICS ASIA 2012

5th Asian Regional Conference on Geosynthetics
13 to 16 December 2012
Bangkok, Thailand

BULLETIN NO. 7

" Geosynthetics for Sustainable Adaptation to Climate Change"

Organized by:

International Geosynthetics Society—Thailand Chapter

Asian Center for Soil Improvement and Geosynthetics

Suranaree University of Technology

Under the auspices of:

International Geosynthetics Society

GA2012

5th Asian Regional Conference on Geosynthetics

- Geosynthetics for Sustainable Adaptation to Climate Change -

Conference Program
13-16 December 2012, Bangkok, Thailand

International Geosynthetics Society Thailand Chapter

Asian Center for Soil Improvement and Geosynthetics

Suranaree University of Technology

Under the auspices of:

International Geosynthetics Society

口頭發表場次表

Friday, 14th December 2012

08:30 – 09:15	Geosynthetics for environmental protection – compatibility and integrity – *Keynote Lecture 3 - T. Katsumi* *Chair- P. H. Giao* *Co-Chair- W. Kongkitkul*
09:15 – 09:45	Award Ceremony
09:45 – 10:15	Coffee Break and Trade Expo
10:15 – 11:00	Geosynthetics innovation for sustainable engineering *Keynote Lecture 4 - H. Y. Jeon* *Chair- S. Chandra* *Co- Chair- S. Touwai*
	Technical Committee on Barriers Session *Chair- K. P. Von Maubeuge* *Co-Chair- N. Touze-Foltz*
11:00 – 11:10	GCLS to mitigate natural contamination from excavated rocks *T. Katsumi*
11:10 – 11:20	A literature review on lifetime prediction of this HDPE geomembranes in the exposed environment *R. Denis*
11:20 – 11:30	Hydraulic performance of geosynthetic clay liners (GCLS) compared with compacted clay liners (CCLS) in landfill lining systems *K. P. von Maubeuge*
11:30 – 11:40	Peel and shear test comparison and geosynthetic clay liner shear strength correlation *K. P. von Maubeuge*
11:40 – 11:50	Flow rate in composite liners including GCLS and bituminous geomembranes *H. Bannour*
11:50 – 12:00	Geotextile barriers in the tailing dump inwash technology in permafrost region *A. B. Lolaev*
12:00 – 13:00	Lunch at Rooms: Lardprao Suite and Krungthep 2
	Technical Committee on Reinforcement Session *Chair- Y. Miyata* *Co-Chair- G. Brau*
13:00 – 13:10	Behavior of geosynthetics reinforced walls in back-to-back configuration *C. S. Yoo*
13:10 – 13:20	EBGEO2010 – experience with German design procedures for geosynthetics reinforced structures *G. Bräu*
13:20 – 13:30	Real-time monitoring for geosynthetics reinforced systems *T. Abdoun*
13:30 – 13:40	A new type reinforced soil structure with inserting pile foundation *T. Hara*
13:40 – 13:50	Load transfer mechanism of geocells *A. Emersleben*
13:50 – 14:00	Effect of geogrid type on performance of reinforced dense-graded aggregate base *R. Ghabchi*
14:00 – 14:30	Coffee Break and Trade Expo

	Ballroom B	Ballroom C
	Theme Session 3-Barrier/ Environmental *Chair- S. Soralump* *Co-Chair- A. Ritirong*	*Theme Session 4-Natural Fibers/Innovations* *Chair- P. Voottipruex* *Co-Chair- P. Jamsawang*
14:30 – 15:00	Geomembranes in mining works ~~*Theme Lecture 3 – A. Bouazza*~~	Sustainable infrastructure development including limited life geosynthetics *Theme Lecture 4 - K. Rajagopal*
15:00 – 15:10	Air permeability of compacted clays and geosynthetic clay liners ***H. Y. Shan***	Experimental study on natural bamboo geogrid encased stone column ***J.N. Mandal***
~~15:10 – 15:20~~	~~The influence of bag's shape and~~ internal friction angle of sand on ultimate capacity of sand-bag by using analytical and numerical analysis ***A. Haddad***	Application of fibers from Sabai grass in construction of subbase of roads in conjunction with sands ***J. Maity***
15:20 – 15:30	Ground improvement with geotextile reinforcement: case studies – embankment over soft clay in Australia and sludge pond capping in China ***W.C. Loh***	Preponderance of jute as geotextiles ***T. Sanyal***
15:30 – 15:40	Centrifuge model tests on the connecting form between cut off wall and composite geomembrane of cofferdam ***B. Li***	Study on impact absorbency of soil mixed with crushed EPS waste – relation to the deformation characteristics of soil – ***T. Kimata***
15:40 – 15:50	A feasibility study for the drainage and protection of GMC (Geo Multicell Composite) as a leachate collection system in landfill ***J. H. Kim***	Deformation and strength characteristics of lightweight geomaterial mixed with EPS beads for subgrade ***K. Yamanaka***
15:50 – 16:00	Hanging bag test of sludge filter through geotextiles ***Y. C. Wu***	Experimental study on one-dimension compression and creep characteristics of EPS in the application for stabilizing slope of expansion soil canal ***W. Zou***
16:00 – 16:10	A study on using waterproof asphalt to make frost heave-resistant drainage ditches ***T. Adachi***	Experimental study on the thermal conductivity of light soil mixed with EPS particles ***G. Liu***
16:10 – 16:20	The study on swelling index of sodium bentonite under different conditions ***P. Wu***	Eco-friendly engineering performance evaluation of PLA geosynthetics ***H. Y. Jeon***

AIR PERMEABILITY OF COMPACTED CLAYS AND GEOSYTHETIC CLAY LINERS

Hsin-Yu Shan [1], Jenn-Tien Yao [2]
[1] Department of Civil Engineering, National Chiao Tung University, Taiwan; Tel: +886-35131562; Fax: +886-35716257; Email: hyshan@mail.nctu.edu.tw,
[2] Fareastern General Construction, Inc., Taiwan; Tel: +886936292783; Email: ponyao@mail.fegc.com.tw

ABSTRACT

Two of most important functions of a landfill cover are to minimize the infiltration of water and to control the emission of landfill gas. Compacted clay liner (CCL), geosynthetic clay liner (GCL), and geomembrane (GM) are the three major types of hydraulic barrier materials used in the bottom lining systems as well as cover systems of landfills. However, it is well recognized that clay liners crack upon desiccation. The cracked liner may enhance the capacity to conduct fluid, which not only increase the infiltration of the downward moving water but also the emission of upward moving gas. Laboratory air permeability tests were conducted to quantify the rate of air passing through desiccated clay liner specimens. In addition, the equilibrium water content of clay liners in the field condition is also studied. The results show that desiccated clay liners may allow considerable amount of landfill gas to pass through. In addition, the air permeability of desiccated GCLs are much higher than that of desiccated CCLs. Accordingly, it is suggested that geomembranes should be used to contain landfill gas for landfills located in areas where landfill gas emission are to be controlled effectively.

Keywords: landfill, clay liner, air permeability, landfill gas emission

INTRODUCTION

In recent years, landfill gas emission has raised considerable concerns since methane is a major greenhouse gas. As a result, for closed landfills, the effectiveness of the cover system to control the emission rate of methane and non-methane organic compounds (NMOCs) needs to be assured. Gas passes through the landfill cover system by means of advection and molecular diffusion. In MSW landfills where large amount of gas is produced, the internal pressure is usually greater than atmospheric pressure such that landfill gas will be released not only by diffusion but also by pressure-driven advection. In the meantime, the natural fluctuation of atmospheric pressure can also cause gas to flow into or out of the landfill. Furthermore, a change in leachate/water table or difference of temperature across the cover system may also lead to gas migration. In many cases, the temperature within the landfill reaches higher than 40°C due to the heat generated by the anaerobic degradation process (Tchobanoglous et al. 1993).

Gas movement by diffusion is driven by gradient of concentration. When a gas is more concentrated in one region of a mixture more than another, it will diffuse into the less concentrated region. Thus the molecules move in response to a partial pressure gradient or concentration gradient of the gas. The present paper will focus only on advective transport.

Figueroa and Stegmann (1991) performed several field tests on a 0.6 m-thick soil cover (SC-SM) at a German landfill. They found that the landfill gas flow rates ranged from 5.2×10^{-6} to 9.6×10^{-5} $m^3/m^2/s$. They suggested that the dominant gas transport mechanism was advection.

In most of the modern landfills, compacted clay liner (CCL), geosynthetic clay liner (GCL), and geomembrane (GM) are the three major types of hydraulic barrier materials used in the bottom lining systems and cover systems.

Many landfills have used compacted clays as hydraulic barrier in the cover system since the hydraulic conductivity of well-constructed CCL can be as low as 1×10^{-10} m/s and can meet the regulatory requirements. However, the major disadvantage of compacted clay liner is that they will crack as a result of desiccation, freeze-thaw cycles, and differential settlement (Koerner and Daniel 1992, Daniel and Koerner 1993). For clay minerals with high swelling potential, the cracks may heal upon rehydration. Kraus et al. (1997), McBrayer et al. (1997), and Day (1998) have looked into the phenomenon of crack-healing of compacted clay. Furthermore, Day (1998) suggested that an important factor in the healing of cracks upon wetting is the type of clay mineral. He stated that for montmorillonite the desiccation cracks are completely healed upon wetting. The hydraulic conductivity of cracked Otay Mesa natural clay specimen decreased from 7×10^{-7} m/s to 3×10^{-10} m/s as a result of healing of cracks.

Geosynthetic clay liners have not only been used in bottom liners for landfills and surface

impoundments (Schubert 1987; Daniel and Koerner 1991; Trauger 1991, 1992; Clem 1992), but also in final covers for landfills and remediation projects as well (Koerner and Daniel 1992, Daniel and Richardson 1995; Woodward and Well 1995). The main advantages and disadvantages of GCLs have been discussed by Boardman (1993) and Manassero et al. (2000) amongst many others.

Although GCLs are usually installed to limit advection of liquids (e.g., water through a cover system) they may also serve an important role in covers as a gas barrier. Theoretically, hydrated GCLs as well as wet compacted soils should hardly allow any gas to pass through (Daniel, 1991). Nevertheless, Trauger and Lucas (1995) did measure the rate of methane gas migrating through GCLs via diffusion. Their results show that the rate of gas transport through GCL was very low as long as its water content was greater than 90%. The permeance is about 2 x 10^{-6} m/s for GCL sample with a water content of around 50% and drops below 1 x 10^{-9} m/s when water content reached above 90%. This suggests that the gas permeability of GCLs is dependent on the water content.

GCLs are known to have a phenomenal ability to retain moisture such that they might have the potential to be effective barrier to gas migration. Research on GCLs buried in sands showed that they were able to absorb water from the environment very quickly why buried dry or hardly lose any water when buried saturated (Geoservice, 1989; Daniel et al., 1993).

With GCLs being increasingly used as part of the capping, their gas performance has come under a growing scrutiny. Recent work has shown that the gas permeability of GCLs is affected by the manufacturing process and the form of bentonite (Didier et al., 2000; Bouazza and Vangpaisal, 2000; Shan and Yao, 2000; Aubertin et al. 2000; Vangpaisal and Bouazza, 2001, 2003).

This paper presents a test method developed speci.cally to assess the gas permeability of GCLs. It is based on the method developed by Matyas (1967) for the measurement of air permeability in soils. The testing apparatus has been designed to accommodate the GCL sample and gas. Flowmeters are used to monitor gas outflow from the device. The test method offers the possibility of carrying out gas permeability tests at different pressure gradients and confining stresses.

EXPERIMENTAL PROGRAM

The air permeability of soil depends on factors such as the size and number of cracks, the air porosity (n_a), and the degree of saturation. Many of these factors are dependent on each other or on some other factors. For example, the degree of saturation depends on both the water content and the void ratio. Among these factors, the air permeability of soils is most sensitive to the variation of degree of saturation. On the other hand, the void ratio of a clay liner in the cover system will be almost constant, since effective stress is kept unchanged throughout the service period. Therefore, the degree of saturation solely depends on water content. Furthermore, the cracking of clay liners is also closely related to the water content. Therefore, in a cover system, the water content is the single most important factor that affects its air permeability of a clay liner. As a result, this research focused on determining the effect of water contents on the air permeability of the clay liners.

Materials

The three clays selected to represent the compacted liners were kaolinite, Hsin-chu clay, and Chung-li clay. The properties of the clays are listed in Table 1.

Table 1 Properties of soils samples.

Soil	Finer than #200 sieve (%)	LL*	PL*	PI*	G_s	USCS
Hsin-chu clay	48.88	25.4	21.1	4.3	2.58	SM-SC
Chung-li clay	92.51	58.5	22	36.5	2.65	CH
Kaolinite	100	56.5	41.1	15.4	2.71	MH

Note:*Portion Finer than #40 Sieve s

The CCL samples were compacted with 48% of the energy produced by standard Proctor compaction test. The results of the compaction tests are listed in Table 2 and the compaction curves are shown in Fig. 1. The shrinkage limits of the bentonite in the clays were determined according to standard test method ASTM D427-92 and are listed in Table 3. The results of hydraulic conductivity of the CCL specimens are listed in Table 4.

Table 2 Results of compaction tests.

Soil	$\gamma_{d,\,max}$ (g/cm^3)	Optimum water content (%)
Hsin-chu clay	1.72	18
Chung-li clay	1.48	27
Kaolinite	1.27	36

Note: Specimens were compacted with 48% of Standard Proctor compaction energy.

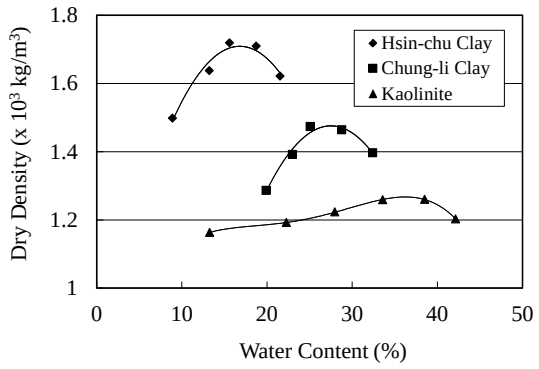

Fig. 1 Compaction curves of clays tested.

Table 3 Shrinkage Limit of Soils.

Soil	Shrinkage limit (%)	Volume change (%)
Hsin-chu Clay	16.7	15.61
Chung-li Clay	19.6	39.88
Kaolinite	40.5	30.64

Table 4 Results of fixed-wall hydraulic conductivity tests.

Soil	k (m/s)
Hsin-chu Clay	4.6×10^{-9}
Chung-li Clay	1.2×10^{-9}
Kaolinite	2.8×10^{-9}

Note: Hydraulic gradient = 100.

The two GCLs tested in this study were a needle-punched GCL and a stitch-bond GCL, which will be designated as GCL-A and GCL-B, respectively. GCL-A is comprised of a nonwoven needlepunched geotextile that is needle punched again through a layer of bentonite into a woven slit-film geotextile. The bentonite content is 3.6 kg/m^2. The water content of the bentonite in dry GCL-A is about 10 - 12%. In GCL-B, 3.6 kg/m^2 of bentonite is sandwiched between woven geotextile on the top and open weave geotextile at the bottom.

The shrinkage limits of the bentonite in the GCLs are listed in Table 5. It is interesting to note that the shrinkage limits of the bentonite are very low comparing to the high water content of saturated bentonite.

Table 5 Results of shrinkage limit tests on bentonite in the GCLs.

GCL	**Shrinkage limit (%)**	**Volume change (%)**
GCL-A	**35.2**	**87.86**
GCL-B	**29.9**	**88.15**

Water Retention Test

Clay liner specimens were placed under 0.5 m of moist sand and loosely compacted moist clay in two 86-liter plastic buckets separately. The specimens had been allowed to absorb water under dead weights that imposed a vertical stress that is equivalent to 0.5 m of soil before they were put in the buckets. The test was performed over a 90-day period spanning from March to May. The monthly average temperatures were 17.2°C, 21.1°C, and 24.6°C, respectively. The average humidity during the test period was about 85%. The suction in the cover soils was monitored with tensiometers.

The soil water characteristics of the clay liner samples were determined with a 15-bar pressure cell. The main drainage curves (MDC) of the compacted clay specimens are shown in Fig. 2. The specimens were soaked to enhance saturation before the test. On the other hand, the specimens of water retention tests were placed in the surrounding soils immediately after they had been cut from the compacted samples. As a result, the water contents of the retention test specimens were a little less than those indicated by the MDC.

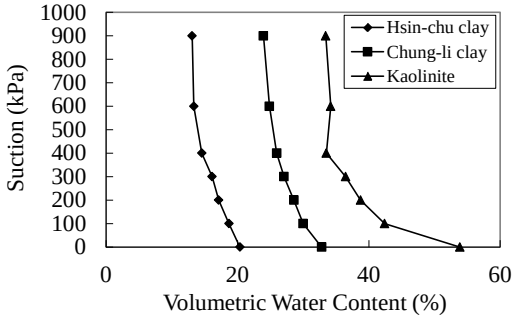

Fig. 2 Soil water characteristic curves of compacted clay samples.

Air Permeability Test

The diameter and the height of the CCL specimens were 101.6 mm and 19.5 mm, respectively. The clays were compacted at a water content 2% wet of optimum with 48% of standard Proctor compaction energy. In order for the cracks to develop more easily, it was decided to use shorter CCL specimens. Therefore, the specimens were compacted in a compaction mold of reduced size. The compacted samples were trimmed and then retrieved from the compaction mold.

The GCL specimens were cut from the rolls supplied by the manufacturer to a diameter of 114.5 mm. The specimen was placed in an acrylic mold with an inner diameter of 114.5 mm. The specimen was then hydrated with tap water for 1 day.

Both CCL and GCL specimens were placed

inside an oven and heated under a temperature of around 35°C for a given period of time. During the desiccation period, a dead load weighing 4 kg was put on top of each specimen to provide a normal stress equivalent to that created by 300 mm of topsoil. In addition, the CCL specimens were put on top of a sheet of sand paper to prevent them from shrinking as a whole so that cracks could develop. This process was repeated for different drying times to obtain specimens with various water contents.

The air permeability tests of CCL specimens were performed with flexible-wall permeameters (Fig. 3). During the tests, a low cell pressure of 3.5 kPa (0.5 psi) was applied to ensure good contact between the membrane and the specimen.

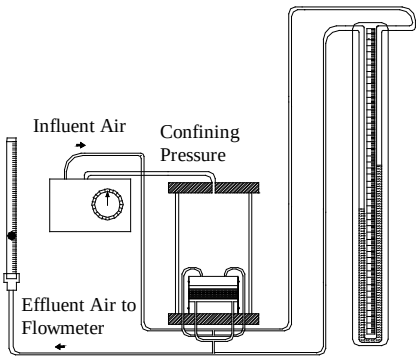

Fig. 3 Schematic diagram of the compacted clay air permeability testing system.

Fig. 4 shows the schematic diagram air permeameter for testing the GCL specimens. GCL specimens were clamped between two ring-shape holders. Bentonite paste was placed along the edges of the specimens to prevent air leakage.

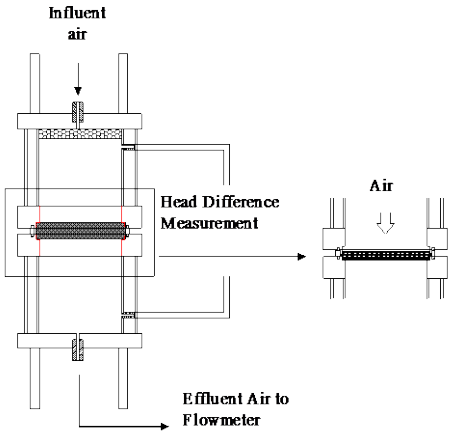

Fig. 4 Schematic diagram of the permeameter for measuring air permeability of GCL (Shan and Yao 2000).

For testing of both types of materials, the flow rate of air was adjusted by regulating influent air pressure with the pressure control panel (Fig. 5). Very low influent air pressure was used for the tests (less than 2 kPa). The range of flow rate was as high as 27 l/min for the more permeable specimens under larger gradients and as low as 0.5 l/min for less permeable specimens under smaller gradients. The head loss across the specimen was measured by U-tube manometer. For each specimen, head differences corresponding to 5 different flow rates were measured. The linear relationship between flow rate and gradient justified that the gas flow was in the laminar range. The test results of one of the compacted Chung-li clay specimen are shown in Fig. 6 as an example. After each test, the water content and the dimensions of specimen were measured.

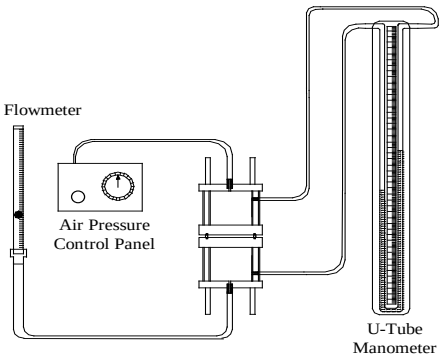

Fig. 5 Schematic diagram of the gcl air permeability testing system (Shan and Yao 2000).

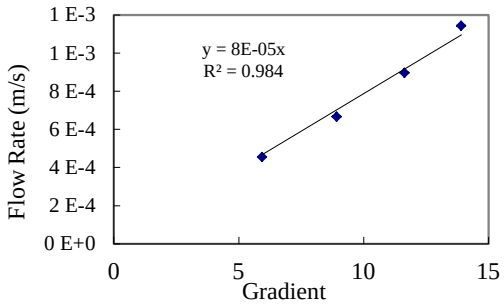

Fig. 6 Relationship between flow rate and gradient of air permeability tests.

The air permeability of the specimens was computed with the following equation:

$$k = \frac{q / A}{\left(\frac{\Delta h_{total} - \Delta h_{equipment}}{t} \right)} \quad (1)$$

where Δh_{total} is the total head loss measured (mm); $\Delta h_{equipment}$ is the head loss of system without specimen in it (mm); k is the air permeability (mm/s).

The compressibility of air has been taken into account when computing the flow rates that passed through the specimens from the values measured with the flowmeter.

RESULTS AND DISCUSSION

Water Retention Tests

Results of the water retention tests show that the hydrated GCLs did not have a strong ability to retain water. The variations of the water content of GCL specimens with time are shown in Fig. 7. The final water content of GCL-A and GCL-B buried in sand are 48% and 53%, respectively. The final water content of GCL-A and GCL-B buried in clay are 27% and 28% which are lower than the shrinkage limit of bentonite. The water contents of the specimens at the end of the tests were much lower than those reported by Geoservice (1989). On the other hand, the final water contents of the specimens are comparable to the results of absorption tests performed by Daniel et al. (1993).

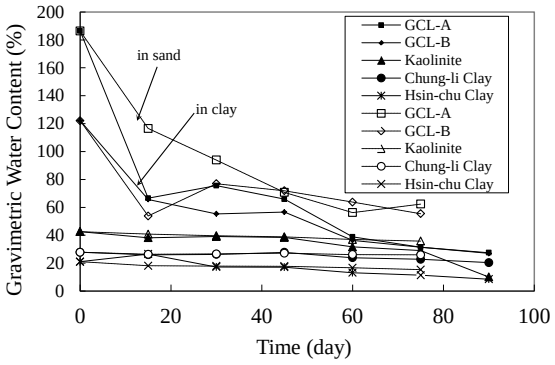

Fig. 7 Variation of water content of CCL and GCL specimens with time.

The CCL specimens also lost considerable amount of water during the test period. The difference between final water contents of specimens buried in sand and clay is most significant for kaolinite. On the other hand, only a small difference in water content was measured for Chung-li clay. In addition, the final water contents of kaolinite and Hsin-chu clay were all lower than their shrinkage limits. By comparing the results with the index properties, it can be concluded that clays with higher plastic limit are capable of retaining more water.

Air Permeability Tests on CCLs

The relationship between air permeability and water content of CCLs are depicted in Fig. 8(a), Fig. 9 (a), and Fig. 10 (a). The air permeability of the compacted clay specimens shows a slight increase as the water content decreases. The trend is most obvious for kaolinite.

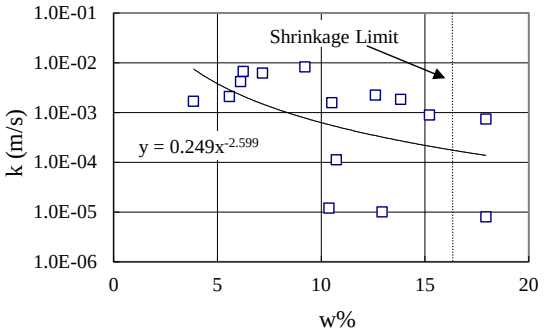

(a) Relationship between air permeability and water content

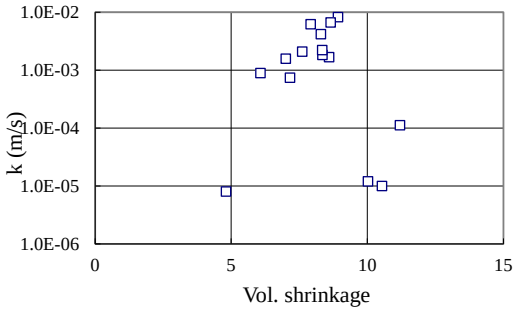

(b) Relationship between air permeability and volume change

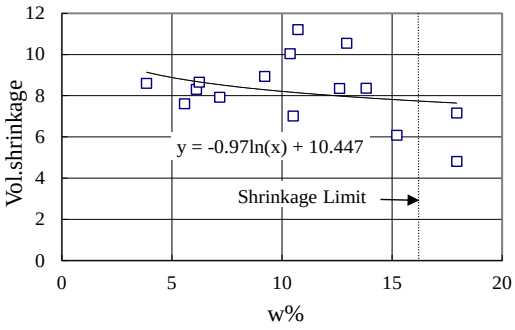

(c) Relationship between volume change and water content

Fig. 8 Relationship between air permeability, water content, and shrinkage of compacted hsin-chu clay.

Among three CCLs, kaolinite has the lowest air permeability while Hsin-chu clay has the highest. It is interesting to note that the hydraulic conductivity of Hsin-chu clay is also the highest among the three clays (Table 4).

The increase of air permeability with decreasing water content did not seem to be solely related with the increased number of cracks. The cracks developed before the water content of the specimens fell below the shrinkage limit. The loss of water of clay particles along the cracks might actually widen the pathway for air.

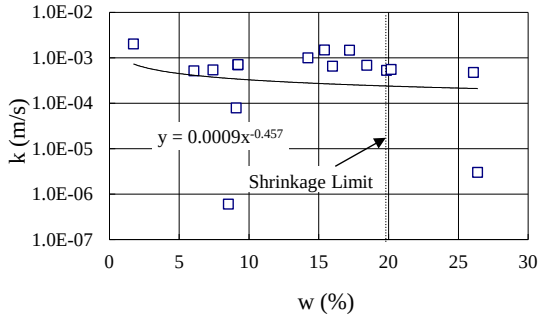

(a) Relationship between air permeability and water content

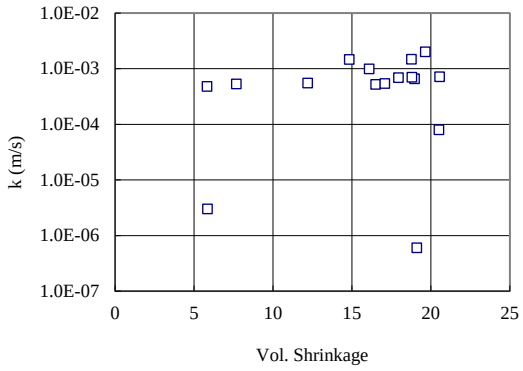

(b) Relationship between air permeability and volume change

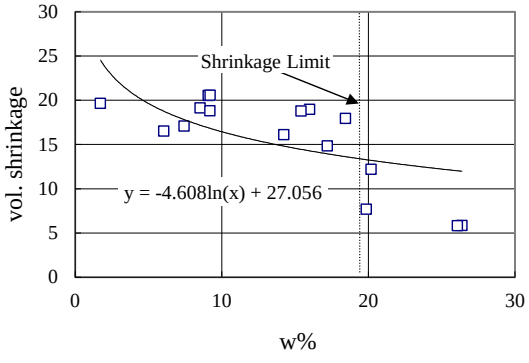

(c) Relationship between volume change and water content

Fig. 9 Relationship between air permeability, water content, and shrinkage of compacted chung-li clay.

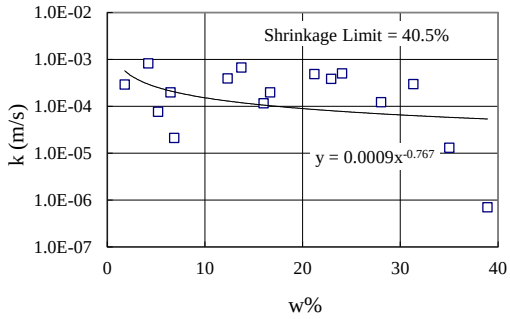

(a) Relationship between air permeability and water content

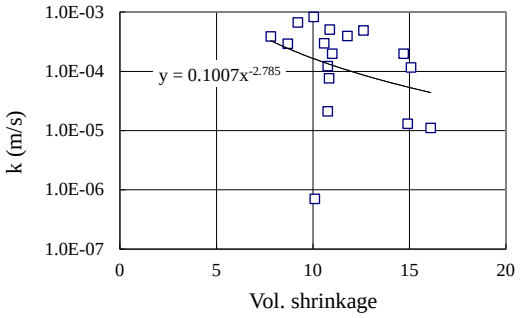

(b) Relationship between air permeability and volume change

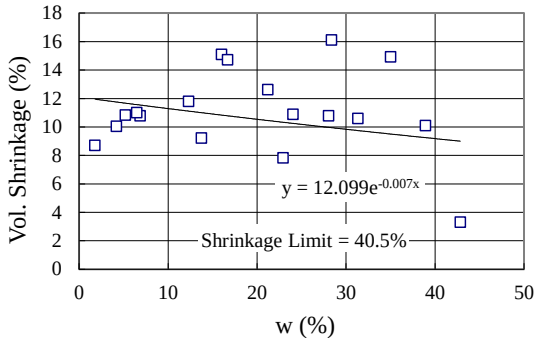

(c) Relationship between volume change and water content

Fig. 10 relationship between air permeability, water content, and shrinkage of compacted kaolinite.

The relationship between the air permeability and shrinkage of the clay specimens are shown in Figs. 8 (b), Fig. 9 (b), and Fig. 10 (b). Only the air permeability of compacted kaolinite decreased at the same time when it shrank (Fig. 10(b)). For Hsin-chu clay and Chung-li clay, there did not seem to be any relationship between air permeability and shrinkage (Figs. 8 (b) and 9 (b)). Again, the reason is that the air permeability of the CCLs is related to the widening of the cracks rather than the reduction of

the total volume.

It is interesting to note that the optimum water content of Hsin-chu clay and Chung-li clay are higher than the shrinkage limits whereas the optimum water content of kaolinite is lower than the shrinkage limit. As a result, the volume change of kaolinite specimens was only about 1/3 of the volume change determined from shrinkage limit test, while this ratio was about 1/2 for the other two clays. In addition, kaolinite has more fine particles and lowest plastic index value. These factors may contribute to the low air permeability of desiccated kaolinite.

On the other hand, the content of fines of Hsin-chu clay is slightly below 50% such that the sand particles may be in contact with each other. Therefore, as the water content decreases, the clay in between the sand particles shrank and pathways of air formed. As a result, Hsin-chu clay had higher air permeability than the other two types of CCLs.

Theoretically, the volume of the clays does not change after the water content dropped below the shrinkage limit. However, as shown in Figs. 8 (c) and 9 (c), for Hsin-chu clay and Chung-li clay, the specimens still experienced noticeable volume change when dried to a water content below the shrinkage limit. In addition, visual observation showed that as the water content decreased, the number of cracks remained approximately the same. The water left in the desiccated specimens either occupied the smallest pores or adhered to the surface of the clay particles. Further decrease of water content made the pathways become wider and allowed faster flow of air. As a result, the air permeability of Hsin-chu clay and kaolinite increased slightly as the water content decreased below the shrinkage limit (Figs. 8 (a) and 10 (a)).

On the contrary, for Chung-li clay, which has more than 90% of clay-size particles and the highest plastic index value, the air permeability remained almost unchanged when dried beyond the shrinkage limit (Fig. 9 (a)). It is noted that the desiccated Chung-li clay specimens shrank considerably with decreasing water content although the water content is lower than the shrinkage limit (Fig. 9 (c)). However, it is possible that compacted Chung-li clay liner may have much larger cracks than the other two clays in the field such that air will flow through it more easily.

The air permeability of the CCL specimens with water content drier than their shrinkage limits are listed in Table 6. Desiccated Kaolinite has the lowest air permeability, followed by Chung-li clay and then Hsin-chu clay. Daniel and Benson (1990) have concluded that compacted sandy clay (SC) is best suitable for hydraulic barrier because it has low permeability, high shear strength, and low shrinkage potential. However, the Hsin-chu clay (SM-SC), which consists of about 50% of sand has the highest air permeability. The most possible reason is that air not only passed through the cracks but also through the primary pores more easily than the other two clays. Although the structure formed by sand particles in contact with each other made the soil have low shrinkage potential, it also had larger pathways for air to go through when the clay shrank. The pathways were developed as the clay particles between the sand particles shrank such that additional pore space became available for transmitting air. Shrinkage of this scale is difficult to be measured or even be observed by visual inspection.

Table 6 Average air permeability of compacted soils drier than shrinkage limit.

Soil	k_a (m/s)
Hsin-chu Clay	2.8×10^{-3}
Chung-li Clay	8.2×10^{-4}
Kaolinite	2.7×10^{-4}

The ability of CCLs to transmit air can also be expressed as the permittivity to air in order to allow for comparison between barrier materials with different thickness. The permittivity is computed with the following equation:

$$\frac{k}{t} = \Psi = \frac{q}{\Delta h \times A} \tag{2}$$

The relationships between the air permittivity of CCLs and water content are shown in Fig. 11. Although the data are scattered considerably, it is obvious that the air permittivity values of desiccated CCLs are sensitive to the change of water content.

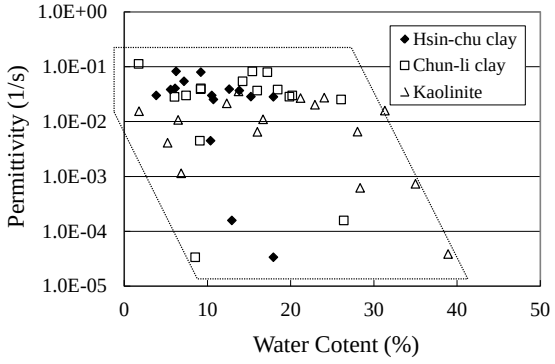

Fig. 11 Air permittivity of compacted clay liners.

Air Permeability Tests on GCLs

Since the results of air permeability tests of GCLs has been described in detail by Shan and Yao (2000), only a summary of the results is presented

here. The relationships between air permeability and water content for GCL-A and GCL-B are shown in Fig. 12. For GCL-B specimens with water content higher than 190%, no flow of air was observed. On the other hand, it was unable to detect any flow of air for GCL-A specimens with water content higher than 170%. It can be clearly seen that air permeability increases as the water content decreases. The relationship between air permeability and water content of GCL-B is much clearer than that of GCL-A.

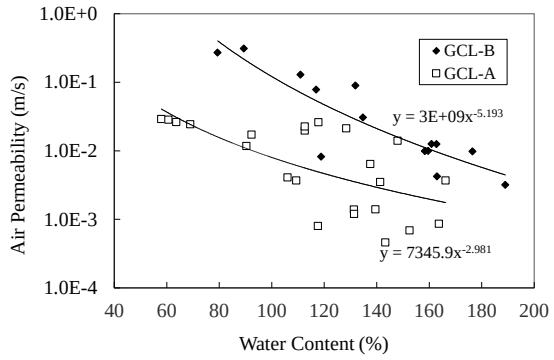

Fig. 12 Relationship between air permeability and water content of GCLs (Shan and Yao, 2000).

Cracks could be observed for GCL-B specimens with water content lower than about 140%. The bentonite in these specimens formed chunks of about 1 cm2 such that the GCL developed a network of wide-open cracks (Fig. 13). For specimens with very low water content, the cracks were as wide as 3 mm. A similar pattern of desiccation cracks of GCL-B specimens have been reported by Shan and Daniel (1991), Boardman (1993) and LaGatta et al. (1997). For GCL-B specimens with water content higher than about 140%, only barely visible hairline cracks in the bentonite was observed.

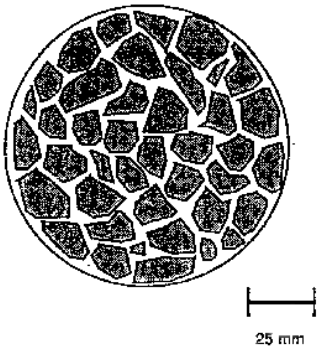

Fig. 13 Crack pattern of GCL-B specimens.

On the other hand, there was no network of large cracks found in the desiccated GCL-A specimens. Instead of forming large chunks, the bentonite in the GCL-A specimens shrank to form small granules as when it was manufactured. The needlepunched fibers seemed to prevent the bentonite from forming chunks during the drying process. As a result, the air permeability of desiccated GCL-A specimens was much lower than that of GCL-B specimens.

The relationships between the air permittivity of GCLs and water content are shown in Fig. 14. The air permittivity values of desiccated GCL-B are much higher than those of desiccated GCL-A for water content ranging from 50 - 150%. Beyond 150%, the air permittivity of both GCLs is very low.

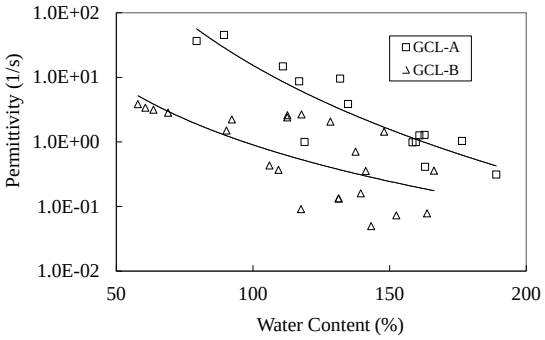

Fig. 14 Air permittivity of GCLs.

The air permittivity of 3 CCLs and 2 GCLs are compared in Fig. 15. The air permittivity of desiccated CCLs is much lower than that of desiccated GCLs. This means that desiccated GCLs will allow air to pass through more easily.

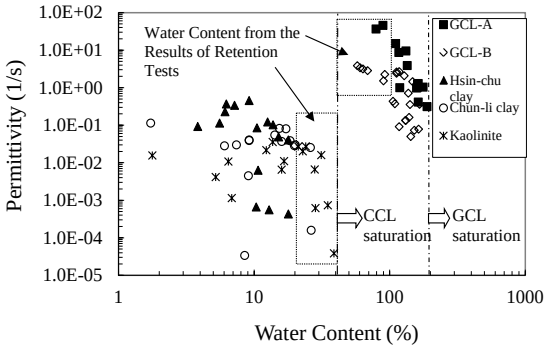

Fig. 15 Air permittivity of clay liners.

PRACTICAL IMPLICATIONS

The emission rate of the landfill gas can be estimated for a landfill under specific conditions. The rate of convective flow of landfill gas through clay liners can be computed with Darcy's law. In order to compare the flux through CCLs and GCLs, the following field condition is assumed. The head difference across the barrier layer is assumed to be

1.0 mm H_2O. The thickness of CCLs and GCLs are assumed to be 600 mm and 6 mm, respectively. The flux was computed with air permeability of CCLs and GCLs corresponding to three different suction levels, which are 30 mb, 60 mb, and 80 mb, respectively.

An appropriate reference suction value is the one that corresponds to the field capacity of the cover soil. Field capacity of a soil is usually defined as the water content of the soil after 24 hours of gravitational drainage. Some soil scientists have proposed to take the water content of a soil under a suction of 30 kPa (0.3 bar or 300 mb) to be the field capacity. Another relevant reference suction value is the wilting point of the plants is 1500 kPa (15 bar), beyond which the plants are not able to absorb water from the soil.

Table 7 is a list of the rate of convective flow through the desiccated clay liners per unit area. These results are also graphed in Fig. 16. It is clear that the gas flux through GCLs is much higher than the flux through CCLs. It is not only resulted from the higher air permeability of GCLs but also because of the fact that CCLs are thicker than GCLs. The thinness of GCLs caused the hydraulic gradient to be approximately 100 times higher than that across CCLs.

Table 7 Convective flux through clay liners ($m^3/m^2/day$).

Suction (mb)	**30**	**60**	**80**
Hsin-chu clay	**1.91×10^{-2}**	**2.02×10^{-2}**	**3.26×10^{-2}**
Chung-li clay	**2.91×10^{-2}**	**2.95×10^{-2}**	**2.98×10^{-2}**
Kaolinite	**7.55×10^{-3}**	**7.83×10^{-3}**	**8.89×10^{-3}**
GCL-A	**7.32×10^{1}**	**3.24×10^{2}**	**7.88×10^{2}**
GCL-B	**1.78×10^{3}**	**9.87×10^{3}**	**7.79×10^{4}**

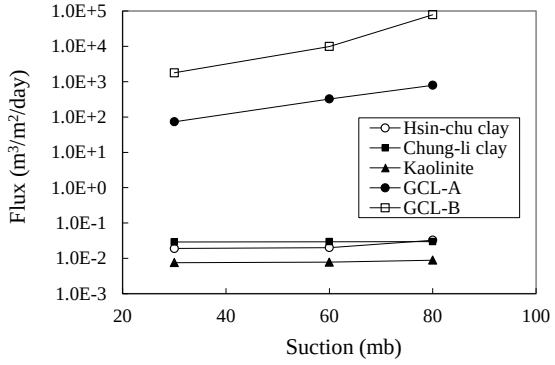

Fig. 16 Gas flux through clay liners.

CONCLUSIONS

The air permeability of both CCLs and GCLs were measured in this study. The compacted clay liners, in spite of being infamous for cracking upon desiccation, have much lower air permeability than GCLs do. In addition, the air permittivity of CCLs is also lower than that of GCLs. Although GCLs have been proved to be effective hydraulic barriers, their air permeability increases rapidly once they start to lose pore water. The results of water absorption tests by Daniel et al. (1993) and water retention tests by Yao (1998) indicate that GCLs will not maintain fully hydrated when they are in contact with soils. Therefore, GCLs are not as reliable in limiting gas emission out from the landfills as they are in preventing water infiltration into the landfills.

Both advection and diffusion should be taken into account when estimating the gas flux through the clay liners in a landfill cover system. For desiccated clay liners with lower water contents, advection dominates the gas transport. For clay liners with high water contents, only a very small amount of gas would diffuse through the material. It is thus important to maintain the clays in a near saturation state in order to limit the gas migration.

With regards to the concern on the emission of landfill gas, the design of final cover system of MSW landfills must take the high air permeability of desiccated clay liners into account. It is suggested that for landfills that are expected to generate large amount of landfill gas, geomembranes may be a better choice than clay liners as the hydraulic barrier for the final covers.

ACKNOWLEDGEMENTS

The authors would like to express their sincere appreciation toward Mr. Kevin Wu of Newmark Engineering Products Co., Ltd. for kindly providing GCL samples for this research.

REFERENCES

Aubertin, M. Aachib, M. and Cazaux, D. (2000). Evaluation of diffusive gas flux through covers with a GCL Geotextiles and Geomembranes 18 (2–4), 215–234.

Boardman, B. T. (1993). The potential use of geosynthetic clay liners as final covers in arid regions. MS thesis, University of Texas, Austin, Texas, U.S.A.

Bouazza, A. and Vangpaisal, T. (2000). Gas advective flux through partially saturated geosynthetic clay liners. Advances in Transportation and Geoenvironmental Systems Using Geosynthetics, American Society of Civil Engineering, Geotechnical Speciality Publication No. 103:54–67.

Clem, J. (1992). GCLs used successfully in hazardous waste containment. Geotech. Fabrics Rep., 10(3):4-7

Daniel, D. E. (1991). Clay liners and covers for waste disposal facilities, unpublished short course class notes. University of Texas at Austin, Austin, Texas, USA

Daniel, D. E. and Benson, C. H. (1990). Water content – Density criteria for compacted soil liners. J. Geotech. and Geoen. Engrg., ASCE, 116(12):1811-1830

Daniel, D. E. and Koerner, R. M. (1991). Landfill liners from top to bottom. Civ. Engrg., ASCE, 61(12):46-49

Daniel, D. E. and Koerner, R. M. (1993). Cover systems. Geotechnical practice for waste disposal, D. E. Daniel, ed., Chapman and Hall, Ltd., London, England, 455-496

Daniel, D. E., and Richardson, G. N. (1995). The role of geomembranes and geosynthetic clay liners in landfill covers. Geotech. Fabrics Rep., 13(1):44-49

Daniel, D. E. Shan, H.-Y., and Anderson, J. (1993). Effects of partial wetting on strength and hydrocarbon permeability of a geosynthetic clay liner. Proc., Geosynthetics '93, Vancouver, British Columbia, Canada, 1483-1496

Day, R. W. (1998). Discussion of 'Infiltration tests on fractured compacted clay,' by McBrayer et al. J. Geotech. and Geoen. Engrg., ASCE, 124(11):1149-1152

Didier, G., Bouazza, A., Cazaux, D., 2000. Gas permeability of geosynthetic clay liners. Geotextiles and Geomembranes 18 (2–4):235–250.

Figueroa, R. A. and Stegmann, R. (1991). Gas migration through natural liners. Proc., Sardinia '91, 3th International Landfill Symposium, S. Margherita di Pula, Cagliari, Italy, 167-177

Geoservices, Inc. (1989). Report of moisture retention tests, Claymax CR, Report to James Clem Corp., Norcross, Georgia, 14 p.

Koerner, R. M. and Daniel, D. E. (1992). Better cover-ups. Civ. Engrg., ASCE, 62(5):55-57

Kraus, J. F., Benson, C. H., Erickson, A. E. and Chamberlain, E. J. (1997). Freeze-thaw cycling and hydraulic conductivity of bentonitic barriers. J. Geotech. and Geoenv. Engrg., ASCE, 123(3), 229-238

LaGatta, M. D., Boardman, B. T., Cooley, B. H. and Daniel, D. E. (1997). Geosynthetic clay liners subjected to differential settlement. J. Geotech. and Geoenv. Engrg., ASCE, 123(5):402-410

Manassero, M., Benson, C. and Bouazza, A., (2000). Solid waste containment systems. Proceedings International Conference On Geological and Geotechnical Engineering, Vol. 1, Melbourne, Australia, 520–642.

Matyas, E.L. (1967). Air and water permeability of compacted soils. Permeability and Capillary of Soils, ASTM STP 417. ASTM, Philadelphia, 160–175.

McBrayer, M. C., Mauldon, M., Drumm, E. C. and Wilson, G. V. (1997). Infiltration tests on fractured compacted clay. J. Geotech. and Geoenv. Engrg., ASCE, 123(5):469-473

Schubert, W. R. (1987). Bentonite matting in composite lining systems. Proc., Geotech. Pract. For Waste Disposal '87, R. D. Woods, ed., ASCE, New York, N.Y., 784-796

Shan, H.-Y. and Daniel, D. E. (1991). Results of laboratory tests on a geotextile/bentonite liner material. Proc., Geosynthetics '91, Industrial Fabrics Association, St. Paul, MN, 517-535

Shan, H.-Y. and Yao, J.-T. (2000). Measurement of Air Permeability of Geosynthetic Clay Liners. Geotextiles and Geomembranes (18):251-261

Tchobanoglous, G., Theisen, H. and Vigil, S. A. (1993). Integrated solid waste management. McGraw-Hill, Inc., 978 p.

Trauger, R. (1991). Geosynthetic clay liner installed in a new municipal solid waste landfill. Geotech. Fabrics Rep., 9(8):6-17

Trauger, R. (1992). Geosynthetic clay liners: An overview. Pollution Engrg., (May 15), 44-47

Trauger, R. J. and Lucas, H. L. (1995). Determining the flow rate of landfill gas constituents through a geosynthetic clay liner. Proc., Geosynthetics '95, Nashville, Tennessee, USA, 1085-1096

Vangpaisal, T. and Bouazza, A. (2001). Gas permeability of three needle punched geosynthetic clay liners. Proceedings of the Second ANZ Conference on Environmental Geotechnics, Newcastle, Australia, 373–378.

Vangpaisal, T. and Bouazza, A. (2003). Gas permeability of partially hydrated geosynthetic

clay liners. Journal of Geotechnical and Geoenvironmental Engineering, ASCE, Vol. 130(8):93 – 102

Woodward, B. L. and Well, L. W. (1995). Alternative cover for saturated, low-strength waste. Proc., Geosynthetics ’95, Industrial Fabrics Association International, St. Paul, Minn., 551-562

國科會補助計畫衍生研發成果推廣資料表

日期:2013/08/31

國科會補助計畫	計畫名稱: LNAPL多相抽除法對BTEX移除效能提升之探討
	計畫主持人: 單信瑜
	計畫編號: 101-2221-E-009-135- 學門領域: 大地工程

無研發成果推廣資料

101 年度專題研究計畫研究成果彙整表

計畫主持人：單信瑜	計畫編號：101-2221-E-009-135-
計畫名稱：LNAPL 多相抽除法對 BTEX 移除效能提升之探討	

成果項目			量化			單位	備註（質化說明：如數個計畫共同成果、成果列為該期刊之封面故事...等）
			實際已達成數（被接受或已發表）	預期總達成數(含實際已達成數)	本計畫實際貢獻百分比		
國內	論文著作	期刊論文	50	50	100%	篇	汽油污染場址 MPE 整治下各相中污染物之變化評估
		研究報告/技術報告	100	0	100%		
		研討會論文	50	50	100%		汽油污染場址多相整治效果評估之數值模擬
		專書	0	0	100%		
	專利	申請中件數	0	0	100%	件	
		已獲得件數	0	0	100%		
	技術移轉	件數	0	0	100%	件	
		權利金	0	0	100%	千元	
	參與計畫人力（本國籍）	碩士生	3	3	100%	人次	
		博士生	0	0	100%		
		博士後研究員	0	0	100%		
		專任助理	0	0	100%		
國外	論文著作	期刊論文	50	50	100%	篇	撰寫中的論文：Assessment of effectiveness of MPE based on simulation of multi-species VOC transport
		研究報告/技術報告	0	0	100%		
		研討會論文	50	50	100%		撰寫中的論文：Simulation of free-product recovery at gasoline contamination site with TMVOC
		專書	0	0	100%	章/本	
	專利	申請中件數	0	0	100%	件	
		已獲得件數	0	0	100%		
	技術移轉	件數	0	0	100%	件	

		權利金	0	0	100%	千元	
	參與計畫人力（外國籍）	碩士生	0	0	100%	人次	第一位參與本計畫的江姓碩士班學生以順利畢業，且利用過程中習得的能力，在國內某大顧問公司土壤與地下水污染部門任職。吳姓碩士生，以順利取得碩士學位，研究題目也與本計畫密切相關，也是以TMVOC 模擬污染。第三位曹姓碩士生，仍在進修碩士學位中。
		博士生	0	0	100%		
		博士後研究員	0	0	100%		
		專任助理	0	0	100%		
其他成果 (無法以量化表達之成果如辦理學術活動、獲得獎項、重要國際合作、研究成果國際影響力及其他協助產業技術發展之具體效益事項等，請以文字敘述填列。)		本研究之成果已由主持人在國內相關的教育訓練，包括環保署環訓所辦理的加油站地下儲槽與管線監測訓練班、台中港加工出口區辦理的土壤與地下水污染講習會、南投縣政府的土壤與地下水監測計畫講習會等相關教育訓練中，向與會者進行報告。且在參與環保署土壤與地下水整治基金會、各縣市環保局的相關計畫審查會議中，提出與環保署官員和計畫執行單位討論。且在台灣中油、縣市政府的污染整治計畫案審查會議中，與相關單位進行討論。對於利用 MPE 的效果向各單位進行討論，許多場址已實際上用 MPE 進行抽油，但往往效果不佳，本計畫之成果，也可以說明為何其然。並說明未來各單位應否與如何利用數值模式先期模擬，可先期研判 MPE 之效果。					

	成果項目	量化	名稱或內容性質簡述
科教處計畫加填項目	測驗工具(含質性與量性)	0	
	課程/模組	0	
	電腦及網路系統或工具	0	
	教材	0	
	舉辦之活動/競賽	0	
	研討會/工作坊	0	
	電子報、網站	0	
	計畫成果推廣之參與（閱聽）人數	0	

國科會補助專題研究計畫成果報告自評表

請就研究內容與原計畫相符程度、達成預期目標情況、研究成果之學術或應用價值（簡要敘述成果所代表之意義、價值、影響或進一步發展之可能性）、是否適合在學術期刊發表或申請專利、主要發現或其他有關價值等，作一綜合評估。

1. 請就研究內容與原計畫相符程度、達成預期目標情況作一綜合評估

■達成目標

□未達成目標（請說明，以 100 字為限）

□實驗失敗

□因故實驗中斷

□其他原因

說明：

2. 研究成果在學術期刊發表或申請專利等情形：

論文：□已發表 □未發表之文稿 ■撰寫中 □無

專利：□已獲得 □申請中 ■無

技轉：□已技轉 □洽談中 ■無

其他：（以 100 字為限）

本研究成果已在撰寫論文中，預計發表於國際期刊與國際研討會。

3. 請依學術成就、技術創新、社會影響等方面，評估研究成果之學術或應用價值（簡要敘述成果所代表之意義、價值、影響或進一步發展之可能性）（以 500 字為限）

本研究係利用 TMVOC 多 VOC 物種、多相傳輸模擬軟體，模擬汽油污染場址利用多相抽取 MPE 整治的結果。本研究克服 TMVOC 在油品抽取設定上的困難，成功地模擬多相抽取的狀況。以此程式模擬，不僅可計算出抽出油品的量、殘留在現地的油品分布，且同時可計算出在非飽和層中 VOC 濃度的變化與地下水中 VOC 溶解象濃度的變化。對於油品污染場址整治來說，是第一次可以完整的「單獨一個」「多物種 VOC」模擬模式評估整治的效益。對於國內外許多的大型煉油廠、轉運站、油庫與加油站的浮油回收整治評估來說，有極重要的意義。